Energy Research and Development Division
FINAL PROJECT REPORT

ENVIRONMENTAL IMPACT ASSESSMENT TOOL FOR WAVE ENERGY CONVERSION

Prepared for: California Energy Commission
Prepared by: Asfaw Beyene, San Diego State University

SAN DIEGO STATE UNIVERSITY

MARCH 2015
CEC-500-2016-007

PREPARED BY*:*

Primary Authors:

Asfaw Beyene, Department of Mechanical, Engineering, San Diego State University

James H. Wilson, Jove Sciences, Inc.

Temesgen Garoma, Department of Civil and Environmental Engineering, San Diego State University

Brian Stiber, Department of Mechanical, Engineering, San Diego State University

Contract Number: **500-11-033**

Prepared for:

California Energy Commission

Joe O'Hagan
Lillian Mirviss
Contract Managers

Aleecia Gutierrez
Office Manager
Energy Generation Research Office

Laurie ten Hope
Deputy Director
ENERGY RESEARCH AND DEVELOPMENT DIVISION

Robert Oglesby
Executive Director

ACKNOWLEDGEMENTS

The support of the California Energy Commission's research program is gratefully acknowledged. The authors express their gratitude to the California Institute for Energy and Environment for providing technical support and reviews and guidance during the development of this project.

PREFACE

The California Energy Commission Energy Research and Development Division supports public interest energy research and development that will help improve the quality of life in California by bringing environmentally safe, affordable, and reliable energy services and products to the marketplace.

The Energy Research and Development Division conducts public interest research, development, and demonstration (RD&D) projects to benefit California.

The Energy Research and Development Division strives to conduct the most promising public interest energy research by partnering with RD&D entities, including individuals, businesses, utilities, and public or private research institutions.

Energy Research and Development Division funding efforts are focused on the following RD&D program areas:

- Buildings End-Use Energy Efficiency
- Energy Innovations Small Grants
- Energy-Related Environmental Research
- Energy Systems Integration
- Environmentally Preferred Advanced Generation
- Industrial/Agricultural/Water End-Use Energy Efficiency
- Renewable Energy Technologies
- Transportation

Environmental Impact Assessment Tool for Wave Energy Conversion is a final report for the Exploratory Studies of Potential Environmental Issues with Alternative Energy Development for California (contract number 500-11-033) conducted by San Diego State University. The information from this project contributes to Energy Research and Development Division's Energy-Related Environmental Research Program.

For more information about the Energy Research and Development Division, please visit the Energy Commission's website at www.energy.ca.gov/research/ or contact the Energy Commission at 916-327-1551.

ABSTRACT

This report describes a wave energy conversion (WEC) environmental impact assessment tool used to assess potential physical and biological effects from wave energy development along the California coast. The researchers compiled applicable literature on wave energy; reviewed and summarized the current assessment tools and their performance ranges; and assessed the Wave Energy Environmental Assessment Tool. To develop this tool, the researchers categorized anticipated adverse environmental effects including changes in wave conditions, mechanical intrusions, and disturbances and interferences with the sea environment such as toxicity from wave energy structures.

The researchers reviewed a number of wave and sediment modeling tools focusing on Simulating Waves Nearshore (SWAN) software and the Coupled-Ocean-Atmosphere-Wave-Sediment Transport Model, which enabled two-way coupling between the Regional Ocean Modeling System and SWAN software with variables transferred between the two models. The researchers first used the Coupled-Ocean-Atmosphere-Wave-Sediment Transport Model to simulate the domain in the absence of wave energy conversions. The researchers then altered the SWAN wave model portion of the software to simulate a reduction in wave energy due to wave energy conversions. This altered wave model was coupled with the ocean and sediment model using the Coupled-Ocean-Atmosphere-Wave-Sediment Transport Model to assess the effects of wave energy conversions on sediment conditions. As part of the proposed tool, a new Wave Height and Energy Automation Tool was provided to simplify wave energy conversions field data entry and consequently assess their performance and environmental impact.

Keywords: California Energy Commission, wave energy conversion, environmental assessment tool, Simulating Waves Nearshore (SWAN) software, Coupled-Ocean-Atmosphere-Wave-Sediment Transport Model (COAWST).

Please use the following citation for this report:

Beyene Asfaw (San Diego State University), Wilson James (Jove Sciences), Garoma Temesgen (San Diego State University), Stiber Brian (San Diego State University). 2015. ***Environmental Impact Assessment Tool for Wave Energy Conversion.*** California Energy Commission. Publication number: CEC-500-2016-007.

TABLE OF CONTENTS

LIST OF FIGURES

LIST OF TABLES

EXECUTIVE SUMMARY

Introduction

There is growing interest in harnessing the significant energy potential found in ocean waves on the California's coast to help the state meet its greenhouse gas reduction and renewable energy promotion goals. Although in 2011 the Department of Energy estimated that wave energy generated off California's coastline could generate enough energy to power 14 million homes, to date no wave energy devices have been deployed in California waters.

This interest in developing wave energy is met by concerns regarding the potential adverse effects of wave energy conversion technologies on marine and coastal environment. This report describes a wave energy conversion (WEC) environmental impact assessment tool that can be used to assess potential physical and biological effects from wave energy development along the California coast.

Potential physical effects from deploying WECs may include changes introduced as a result of alteration of near shore wave-driven processes. Biological effects may include behavioral changes in aquatic or avian species mainly from noise or electro-magnetic fields. This Wave Energy Environmental Assessment Tool specifically addresses:

1. Changes in wave conditions (height, direction, frequency) imposing alterations in sediment transport and deposition, requiring wave and sediment movement modelling;

2. WEC devices and structure intrusions altering animal movements and migrations, including risks of entanglement or strike by moving parts;

3. Disturbances including noise during facility construction and operation as well as electromagnetic fields (EMF); and

4. Interferences with sea environment including toxicity of paints, lubricants, and antifouling coatings of WEC structures.

Difficulties in modeling seashore phenomena and in predicting the risks of WECs to the environment, combined with the large number of conceptual WEC designs made developing a compact tool for impact analyses challenging. Furthermore, the WEC devices can be floating, placed in mid-depth water, or mounted at seabed, with single or clustered configurations, imposing varying levels of effects unique to each sea state and device type. WEC location, wave characteristics, habitats, bathymetry (water depth) and biodiversity also had an impact on the accuracy of the environmental impact study tool's predictions. These impacts were time-dependent and could be long-lasting.

Project Process and Results

There are existing wave, hydrodynamic and sediment modeling tools to assess certain environmental aspects of WEC siting and operation. The researchers compiled applicable literature on wave energy and associated effects; reviewed and summarized currently available

assessment tools and their performance ranges; and developed and assessed the Wave Energy Environmental Assessment Tool.

Studying the conversion of wave energy and its effects on the environment involves the use of several different types of computational models, each having a particular physical basis. Wave models describe the wind-induced creation and propagation of waves over domains of interest. Hydrodynamic models are used to study the interaction of *WEC*s with the wave resource at the fluid-structure interface. Ocean models describe circulation and currents on various scales, as well as variations in temperature, salinity and density. Sediment models show the evolution of suspended and settled sediment matter, including seabed morphology. Other related geophysical models include ocean ice models, ocean biological and chemical and atmospheric models.

Although the capability of specialized tools designed to address WEC impacts on the environment are unsatisfactory, software developed for other purposes, such as studying the interaction of waves with vessels and offshore structures, can be conveniently used. Therefore, the Wave Energy Environmental Assessment Tool, developed through this study, consists of a number of coupled models.

In order to demonstrate the efficacy of the proposed tool including demonstration of the effects of *WEC*s on sediment transport processes, the researchers include case studies using the model for potential WEC development off the coast of Central California.

Project Results

The case studies show that the coupled model can successfully model wave height changes and sediment movement with and without deployment of WECs. The two case studies indicated that, for the two sites considered, the effect of a wave farm on the suspended sediment environment is very small.

Project Benefits

California has significant wave energy resources along its coastline. As the state strives to meet its greenhouse gas emission reduction and renewable energy goals, this resource could become increasingly important. With the Wave Energy Environmental Assessment Tool, a consistent approach can be taken to determine the environmental effects of this technology across different wave energy conversion technologies, siting and ocean conditions.

CHAPTER 1:
Background

According to a 2003 U.S. Department of Energy (DOE) report to Congress, there are over 100 conceptual and semi-operational designs for wave energy conversion (WEC). And yet there have been few environmental impact studies of wave energy converters. In part because a comprehensive tool that attempts to address a broadly formulated WEC impact evaluation covering biodiversity, sediment transport, etc., doesn't exist. Attempts to evaluate such impacts are often restricted to predictive assessments – without verification or validation of the model claims. Scattered and fragmented as they are, these predictive studies have however been instrumental in identifying common elements of risks en route to an attempt of designing this comprehensive tool.

Adverse environmental effects of WECs which may influence concentration, migration, and reproduction of sea and benthic habitat as well as the shore environment can be categorized in four groups as related to:

a) Changes in wave conditions (height, direction, frequency) which will then impose alterations in sediment transport and deposition, requiring wave and sediment transport model,

b) Mechanical intrusions of WEC devices and structures altering animal movements and migrations, including risks of entanglement or strike by moving parts.

c) Disturbances including noise during construction and operation as well as electromagnetic fields (EMF),

d) Interferences with sea environment: toxicity of paints, lubricants, antifouling coatings of WEC structures, etc.

The difficulty in modeling many of these risk factors, combined with large number of conceptual WEC designs to which the risks may apply make impact analyses of WEC systems very complex. The WEC devices can be floating, placed in mid-water, or seabed mounted, each with a variety of configurations imposing varying levels of risks and consequences unique to each device type (Frid et al. 2012). Furthermore, any of these design choices can be singular or clustered. The accuracy of scaled observations and modeling of clustered commercial farms further complicate the environmental tool design. The site of WEC location, wave characteristics, bathymetry and biodiversity will also have impacts on the predictability and reversibility of the effects, i.e. recovery from the damage. These impacts also depend on life time of the structure, which, given the analogy of oil platforms, can be up to 100 years.

Recapping, there are some environmental studies of WECs but for narrowly targeted scenarios. To date there is no comprehensive assessment tool to conduct such studies, and even if made available, the tool should be considered to be an important but imperfect start because of inherent complexities resulting from design variations of WEC devices and operating conditions.

CHAPTER 2:
Literature Review

2.1 Wave Modeling

The literature on wave energy has grown significantly in recent years, but studies on the impact of WECs on the environment have not followed suit. On the wave energy resource assessment side, while the North America's west coast is fairly well-mapped, the East coast is lagging behind. Complete long-term field data-based analyses of WEC devices, conversion efficiencies, performance, etc., are virtually non-existent other than those claimed by few vendors. The diversity of mechanisms proposed with little field data, combined with multiple design failures of the last few decades and lack of strong public interest in WECs at least so far, have left the development of WECs lagging far behind that of other forms of renewable energy. The authors have made a modest contribution to the resource analysis as well as aspects of energy conversion, for US west coast in particular, (Beyene et al. 2003; 2005; 2006(a); 2006(b); 2007; 2008; 2009; and Wilson et al, 2007). The studies are based on more than 50 years of statistical wave data. Statistical data is useful when evaluating the mean or average annual resource potential as well as when assessing the impact of exceptional, large and rogue waves on WEC structures. Most, if not all the structural damages of WECs so far have been caused by rare but powerful waves.

The prevalence of large waves that can undermine WEC structures can best be identified from such long-term data, and when likely, should be incorporated into the design process to build a robust system. This is particularly important in that Graham and Diaz (2001) documented that the storms in the North Pacific grew in number and intensity in the period from 1948 to 2001.

Another important consideration to WEC potential is their impact on bottom friction and consequent contribution to sediment transport. Bottom friction loss (BFL) is addressed by Hwang et al., (1989) and further discussed in the California Wave Resource Study by Beyene and Wilson, (2003). This resource study also includes assessment of regulatory and environmental permitting issues. The Coastal Data Information Program (CDIP) and other historical wave buoy data off the coast of California substantiate conclusions made in that report that significant wave heights decreased significantly with shallow depths shoreward long before the depth was one wave length or less, when the circular wave motion would be expected to "touch" the ocean bottom. Finally, unpublished work of Zettermann and Wilson (2009) addresses the wave abatement from seaward to the shore caused by inserting various wave energy converters (WECs) into the ocean wave environment.

Although most existing publications on WECs are primarily on wave modeling with some component analysis, there are some activities to at least recognize, if not partly address WEC impacts on the environment. A workshop on "Ecological Effects of Wave Energy Development in the Pacific Northwest" was organized with this in mind at the Hatfield Marine Science Center in Newport, Oregon, on October 11 - 12, 2007 (Boehlert et al. 2007) - to address ecological issues related to wave energy development. Apart from this and a few other works narrowly

targeting impact assessment of WECs as discussed below, studies of WECs in general are scattered covering singular or isolated impacts, and there is no comprehensive tool to conduct such studies.

As stated above, the mathematical modeling and statistical data analyses, as well as the limited lab tests have not propelled the technology to a healthy full scale operation. AquaBuoy deployed off the coast of Oregon its WEC technology in 2007. Unfortunately, the device sank due to an apparent malfunction. Also, a commercial size installation of several Pelamis WECs off the north coast of Portugal had technical difficulties that stopped progress on the project for years. It is critically important to have a fully operational WEC device to back-up and validate the models, and consequently make progress towards understanding the impact of WEC devices on the environment.

In California, although WEC technology and acceptance is improving in recent years, commercial WEC applications are still years off. In 2007, PG&E began examining the feasibility of using wave energy to produce power, and the Humboldt site was selected for a pilot project, Wave Connect, (Pacific Gas & Electric 2014). This project was terminated due to several concerns, including the long-term (> 20 years) commercial viability of WECs. There have been several other WEC projects proposed for the California coast recently (e.g., Morro Bay), but based on a personal communication between a California Energy Commission official and the PIs, there is no known current ocean-based project application in California, except one tidal energy project near San Francisco. This long-term economic concerns are contrary to previous studies (Beyene, 2003) which concluded that the wave energy resource at least north of Point Conception is ideal for WEC projects. The lack of WEC project applications in the West coast of the US, despite the availability of such high density resource, should be considered a weakness on the part of the renewable energy industry as a whole.

As mentioned above, almost all the literature on environmental impacts of WECs target disturbances of the devices on some aspects of wave condition; there are no comprehensive assessment tools proposed or reviewed. The published works of the targeted studies are summarized below.

Langhamer (2010) discuss colonization patterns and biofouling with emphasis on changes of the seabed and alterations due to new substrates. The authors suggest an artificial reef specifically catered for economically important or threatened species. This suggestion included incorporation of environmental studies in specific projects to conduct long-term studies on single or multiple arrays to get early insight into changes of sessile and motile organisms. The authors propose incorporating environmental studies to project design and implementation which promotes adaptive technology and also serve as a library of knowledge and experience for others.

Dolman et al (2010) argue that a comprehensive environmental study has to include the construction and maintenance related to the exploitation phases – transportation, drilling, bridging, and services over a lifetime of the project and post-exploitation. WEC devices may

come in various sizes and shapes, in single units or arrays, covering areas of marine habitation, with yet unknown consequences of encounter with a new technology.

Less direct is a study conducted by Grant et al (2008) on marine energy economy, based on a 3GW power plant. The paper concludes that there are substantial economic benefits of wave energy conversion, including legacy effects.

Efficacy of tools greatly depends on cyclic improvements based on shared feedback. A lesson could also be learned from oil platforms as well as wind and tidal energy industry development, cases where impact studies also lagged far behind exploitation.

2.1.1 Likely Technologies that Will be Adopted for *WEC*s in California

Wave energy devices can be categorized in several ways. One distinction is device location, classified as onshore, near-shore or off-shore, (Clément et al 2002). Near-shore and offshore devices can be further divided into floating or bottom mounted types. Devices which produce electricity can be classified by Power Take Off (*PTO*) system, examples such as water and air turbines, hydraulic generators, and linear electrical generators, (Falcão 2010).

*WEC*s can also be classified by their energy conversion scheme. One important class of devices is called terminator. These devices are oriented perpendicular to the direction of the waves, and either absorb or reflect all of the wave energy. One of the most studied and developed type of devices in this class is the Oscillating Water Column (OWC). A second important terminator scheme is used in overtopping devices, (Bedard et al 2010). Other classes of devices are point absorbers, and attenuators, which are sometimes grouped together as oscillating bodies.

2.1.1.1 Oscillating Water Column

OWCs were among the first *WEC* concepts to be researched and tested. These devices employ a chamber that encompasses the air-water interface. As waves raise and lower the level of the water column, air is pushed and pulled through the chamber. This air turns a turbine, typically a Wells turbine. This type of turbine rotates in the same direction regardless of air flow direction, eliminating the need for check valves to rectify the airflow. These devices can be fixed in an onshore location, attached to the ocean floor in a near-shore location, or floating either near-shore or offshore. Notable examples of OWCs include the LIMPET device (onshore) and the Mighty Whale (floating). OWCs can produce electricity at a cost in 2005 dollars of $0.08/kWh, with installation costs of approximately $840/kW, and a life cycle of less than 15 years (Price 2009).

2.1.1.2 Overtopping

Overtopping devices are another important group within the terminator class of devices. The working principle behind these devices is allowing the wave crests to flow over a partially submerged ramp into a reservoir higher than the water level outside the reservoir. This converts the kinetic energy of the wave into potential energy. The water then flows back through a low head hydroelectric turbine to produce electricity. These devices typically use reflector arms to concentrate the waves as they approach the ramp. A notable example of this technique in an onshore location is the *TAPCHAN* device developed in Norway, short for Tapered Channel (Falnes 1993). The *TAPCHAN* device has a generated electricity cost of about $0.09/kWh in 2005

dollars (Price 2009). Another example of a floating overtopping *WEC* is the Wave Dragon (Kofoed et al. 2006).

2.1.1.3 Point Absorbers

Point absorber devices comprise the most diverse set of operating designs. This class of devices is defined by its characteristic dimension, which is much smaller than the typical wavelength of incident waves. An advantage of this condition is that the device operates essentially independent of wave direction, unlike other *WEC* schemes. Point absorber technologies include floating devices, or buoys, in heaving motion, as well as two-body bottom mounted devices with the floating body driven by pressure differentials. *PTO* systems for these devices include hydraulic motors and linear electrical generators. Among the many examples of devices using this technology are the floating PowerBuoy, (Budal et al 1982) and the bottom mounted Archimedes Wave Swing, (Valério et al 2007). Vantorre et al (2002) have estimated the typical efficiency of a point absorber at 62%.

2.1.1.4 Attenuators

Attenuator devices are associated with characteristic dimensions which are larger than typical incident wavelengths. These devices are aligned approximately parallel with the wave direction and consist of multiple floating articulated bodies. The relative motion of the bodies drives a hydraulic pump at the hinge points, which can be used to drive a turbine to produce electricity. Of the devices of this class, the Pelamis device, (Henderson 2006) is among the most- commercially developed *WEC*s, and the hinged barge McCabe Wave Pump has been proposed for use with a desalination plant, (Davies 2005). The power conversion efficiency of the Pelamis was studied for six distinct wave climate zones, including the West coast of the US. Average capture width for this climate zone was found to be 7m for an incident width of 8.5m, or an efficiency of 80% (Dalton et al 2010). The cost of electricity from the Pelamis device is about $0.096/kWh (2005), and typical average outputs are 25-40% of the rated capacity, (Price 2009).

2.1.1.5 Other Devices

One other notable device is the Oyster. This bottom mounted device exploits the surging motion of the incident waves using a flap to drive a hydraulic pump, and is capable of generating electricity at a cost of $0.08/kWh in 2005 dollars (Price 2009).

Given the large number of conceptual conversion devices patented as well as posted in open forums, a preferred *WEC* technology of California will likely be market-tested, with design iterations to allow survivability and better performance in harsh working environment. It is therefore difficult to forecast a successful *WEC* technology based on concepts. With this caveat, and based on advances in prototypes, currently there seem to be two likely technologies that may be adopted for California wave energy projects in the near term, the Aqua Boy and the Sea Snake (Figure 1). The "Wells Turbine," another type of point absorber technology is simple in design, can be robust in real ocean environments, but has capacity factor limitations. Beyene (2009) has developed and tested a new flexible blade for the Wells Turbine that shows great promise,. The AquaBuoy (Fig. 1) is a point absorber with a hydraulic pump instead of a Wells Turbine, and seems to be a likely *WEC* technology of the near future. After many successful

ocean deployments, an AquaBuoy sunk in a test off the Oregon coast in 2007 (Callaway 2007). The deficiencies are now being corrected. A long snake like *WEC*, the Pelamis, Fig. 1, is in the early stages of full commercial testing in the northwest coast of Scotland. After a promising initial result, a Pelamis buoy off the Northern Portugal shore was disabled due to damage to the structure. The realistic impression one is left with is that there is no sea-tested technology that can be endorsed as a ready and reliable choice. An effort to study the impact of *WEC*, in the absence of a successful *WEC* design, is valid and very useful, but remains inevitably conjectural.

Figure 1: AquaBuoy Point Absorber (left) and Pelamis "Sea Snake" Line Absorber (right)

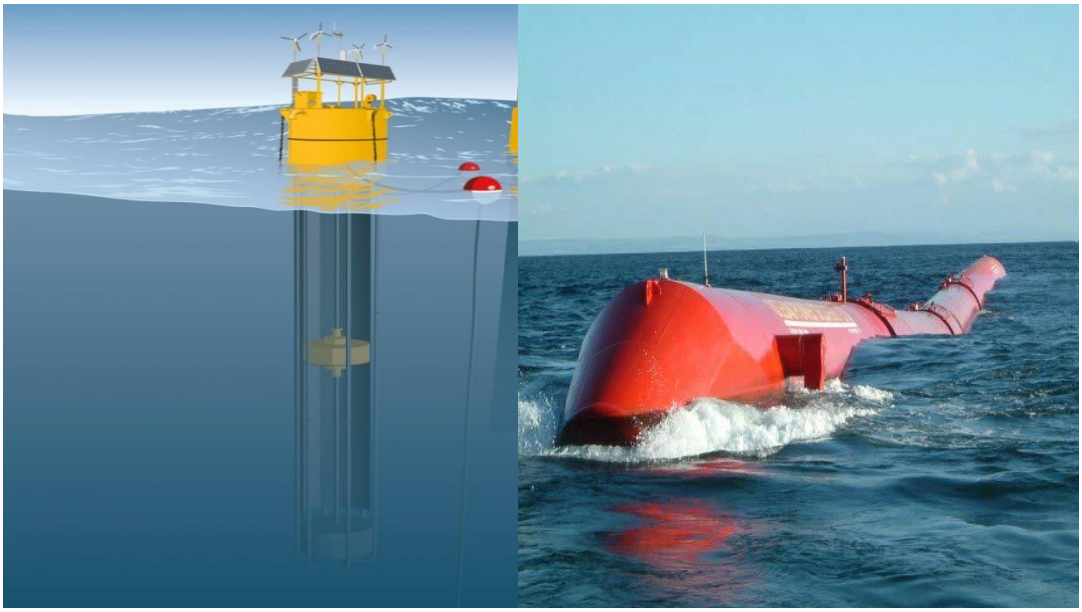

2.2 Impact Studies

Below, the researchers discuss the literature on anticipated adverse environmental effects of *WEC*s with the following categories:

a) Changes in wave conditions,

b) Mechanical intrusions,

c) Disturbances,

d) Interferences.

2.2.1 Changes in Wave Conditions

WEC operation is based on the principles of capturing the embedded energy which inevitably results in changes in wave parameters: reduced height, suppressed sediment transport and turbulence. These changes can be desired or undesired based on direct and temporary cost/benefit analyses. The changes will likely depend on existing wave conditions and parameters such as wave height, frequency, and prevalence of rogue waves.

The impact of rogue waves and violent pressure on *WEC* structures is important for the success of the technology. Destructive wave power can alter the impact of *WEC* on the environment, and as such the potential impact should be incorporated into the design process of *WEC* design and exploitation. Some aspects of these issues have already been addressed, (Bredmose et al 2004). In fact, the increase in frequency of rogue waves makes the subject matter even more relevant. The increasing number of reported rogue waves with unexpected large wave height ($Hmax/Hs$ >2.0), crest height ($hc/Hmax$ > 0.6), wave steepness and group pattern (e.g. Three Sisters) suggests a reconsideration of design codes and impact evaluation (Clauss et al. 2004). Progress in understanding wave conditions and structural forces combined with knowledge about their environmental impact makes the technology more possible than ever before.

The actual impact of *WEC*s on wave condition can be settled with extensive field data and measurement. The issue is relevant not only for recreational activities such as surfing, but also for near-shore turbulence affecting sea colonies. Few papers have tackled the issue of *WEC*s on wave parameters.

Black (2007) discusses energy absorption at the Wave Hub including the processes of diffraction, refraction and dissipation, and concludes that "Wave height attenuation should be less than 3-6% at beaches in the direct shadow of the wave hub in 'clean' (narrow-banded) swell". The conservative approach of modeling wave transmission is to assume that the *WEC* devices will absorb all wave energy, which doesn't happen in reality. The author suggests that for 100% wave height absorption through the wave hub, the impact at the shoreline could be as much as 30% height attenuation for a given swell condition. However, the author, taking into consideration other studies, concludes that the wave height attenuation is highly unlikely to exceed 20%, assuming 100% absorption. As such, the likely maximum impact on wave height at the shoreline is in the 3-6% range, a rate which will impact other derivative parameters and sediment transport only modestly.

Ahmadian et al (2012) investigated the significance of the layout of an array using modified version of tidal stream turbines on the power output and the hydro-environmental impacts array using the 'Depth Integrated Velocities And Solute Transport' (*DIVAST*) model. The study demonstrated that the impacts of the arrays on the water levels and the maximum water levels which are associated with the flood risk were very small. Although this study is for tidal energy conversion, some logical conclusions can be derived for *WEC*s.

2.2.1.1 Mechanical Intrusions

The presence of new mechanical structures such as moors and cables will alter the local sea environment. Marine organisms may colonize *WEC* structures and underground cables which may increase biodiversity. Langhamer (2010) reports that about 150 kg of organisms were estimated to have been attached to a 3 meter diameter buoy in just a few summers. The author suggests that such bio-fouling does not interfere with the buoy performance, and that it is acceptable to allow such growth on *WEC*s. The structural foundations can be attractive to marine organisms and may serve as artificial reefs.

Another relevant component of environmental impact study of *WEC* structures is their possible effect on the soft-bottom habitats. The above study examines macro-faunal assemblages in the seabed around *WEC* at a research site on the Swedish west coast during a period of 5 years. The research project concludes that *WEC*s may alter the surrounding seabed with an increase in organic matter, and that the deployment of *WEC*s at the specific site tended to have rather minor direct ecological impacts on the surrounding benthic community when compared to the natural species variances.

A comprehensive approach to environmental impact study should also include flying habitats that share the sea. Changes to energy budgets could impact reproduction and survival of birds. Langton et al (2011), outline the information needed for modeling the impact of *WEC*s on bird communities and conclude more information is needed on seabird foraging rates, flight behavior and ability to buffer against possible environmental fluctuations.

2.2.1.2 Disturbances

*WEC*s with grid connected power outputs will introduce anthropogenic disturbances such as electromagnetic fields (*EMF*s) and noise. Little is known about potential ecological impacts of *EMF*s and "artificial" noise. However, transmission cables with significant *EMF* are stretched across the sea bed. Cables have been stretched across sea beds connecting islands and even continents for decades. *WEC*s may increase the range of *EMF*s over a much greater area of the seabed as well as shore lines. Tricas et al. (2011) discuss the types of power cables and expected *EMF*s from representative cables, and summarize existing information on electro- and magneto-sensitivity of marine organisms including sharks, rays, and other species. The authors assert the need to understand power cable characteristics and predict their impacts on sea life including that from cumulative exposure.

In another case, sources of ambient noise have been identified and characterized in terms of their frequency content, relative level, and spatial and temporal variability. The mechanisms of noise generation in marine renewable devices have been identified and the sources of noise in a range of device types have been assessed (Richards et al. 2007). The study identifies noise spectrum levels for some marine renewable devices to assess the potential impact of device noise on receptors. The authors conducted a desktop study to identify mechanisms of marine noise generation and concluded that noise from these devices is not expected to result in significant impacts.

Other lateral but useful studies have been conducted on small water bodies, particularly on bluff erosion near lakes (Meadows 2005; Swenson et al 2006].

2.2.1.3 Interferences

Interferences with sea environment of toxicity resulting from paints, lubricants, and antifouling coatings of *WEC* structures have not been studied yet. However, there are general guidelines of toxicity, hazard, etc., as established by State and Federal agencies such as *Environmental Protection Agency.*

CHAPTER 3:
Current Assessment Tools and Their Performance Ranges

Studying the conversion of wave energy and its effects on the environment involves the use of several different types of computational models, each having a particular physical basis. Wave models describe the wind-induced creation and propagation of waves over domains of interest. Hydrodynamic models are used to study the interaction of *WEC*s with the wave resource at the fluid-structure interface. Ocean models describe circulation and currents on various scales, as well as variations in temperature, salinity and density. Sediment models show the evolution of suspended and settled sediment matter, including seabed morphology. Other related geophysical models include ocean ice models, ocean biological and chemical models, and atmospheric models.

3.1 Ocean Modeling

Ocean models are used to study the motion and state of seawater, its interaction with the atmosphere, and the transport of different types of materials in the oceans. The Earth's oceans comprise stratified fluids rotating with the planet beneath them. Its motion is caused by transfers of momentum and buoyancy, originated by forcing at the interface with the atmosphere. The Navier-Stokes equations relate this dynamically with good accuracy, representing many physical processes on numerous scales of time and space (Marshall et al 1997). The majority of computational ocean models use an approximation to the Navier-Stokes equations, called the hydrostatic primitive equations. This approximation is so widespread within oceanographic modeling that it can be considered standard and appropriate for large scale phenomena (Marshall et al. 1997).

Faithful modeling of ocean processes entails two principles, true representation of physical processes which have resolution at the time and space scales being used, as well as appropriate parametrization of sub-scale processes Figure 3 (Griffies at al. 2000). Ocean models typically orient their coordinate systems with the two horizontal directions perpendicular to a vertical coordinate based on the local plumb line. The reason for this is that horizontal transport is dominant over that in the vertical, due to the oceans' nature as a stratified, rotating fluid (Griffies at al. 2000). Three significant types of vertical coordinates have been traditionally used in ocean models, simple linear z-coordinates, ϱ-coordinates based on potential density, and σ-coordinates, which are following terrain (bathymetry). Each has advantages and disadvantages, and this selection is the most critical aspect of model construction (Griffies at al. 2000). In general, z-coordinates are well suited to the upper mixed layer, ϱ-coordinates to the interior, and σ-coordinates to the bottom boundary layer (*BBL*). More recently an S-coordinate has been developed to enable high resolution in upper ocean layers for terrain-following σ-coordinates (Song et al. 1994; Shchepetkin et al. 2005).

Table 1: Summary of the Three Spectral Wave Model Capabilities (Oh et al 2009)

	RefDif	***MIKE21BW***	***SWAN***
Refraction	Yes	Yes	Yes
Shoaling	Yes	Yes	Yes
Diffraction	Yes	Yes	Yes (?)
Wave-current interaction	Yes	Yes	Yes
Wave-wave interaction	No	Yes	Yes (?)
White-capping	No	No	Yes
Wave breaking	Yes	Yes	Yes
Reflection	No	Yes	Yes (?)
Transmission	No	Yes	Yes
Bottom friction Dissipation	Yes	Yes	Yes
Generation by wind input	No	No	Yes

Table 2: Summary of Ocean Model Types (Giffies et al 2000) 2000

Model Type					
z-Coordinate		ρ-coordinate (isopycnal)		σ- or S-coordinate	
Acronym	Developer	Acronym	Developer	Acronym	Developer
CANDIE	Dalhousie University	HIM	Geophysical Fluid Dynamics Laboratory	POM	Princeton University
COCO	Center for Climate System Research (Tokyo)	MICOM (HYCOM)	University of Miami; Los Alamos National Laboratory; Naval Research Laboratory, Stennis Space Center	SPEM (*ROMS*)	Rutgers; UCLA
GISS	Goddard Institute for Space Sciences	POSEIDON	Center for Ocean, Land, and Atmospheres; George Mason University		
Hadley	Hadley Centre	POSUM	Oregon State University		
HOPE	Deutsche Klimarechenzentrum				
MIT	Massachusetts Institute of Technology				
MOM	Geophysical Fluid Dynamics Laboratory				
MOMA	Southampton Oceanography Centre				
SEA	University of East Anglia				
OCCAM	Southampton Oceanography Centre				
OPA	Laboratoire d' Océanographie Dynamique et de Climatologie				
POP	Los Alamos National Laboratory				

Although spherical coordinates are an obvious choice for geophysical modeling, the polar region is problematic due to the singularities at the poles, as well as the convergence to small grid dimensions in this area (Griffies at al. 2000). Therefore standard practice is to convert horizontal coordinates onto a generalized orthogonal system. The usual horizontal discretization for ocean models uses a staggered Arakawa grid (Griffies at al. 2000; Arakawa et al. 1977). The B or C grids are used by the majority of models (Griffies at al. 2000).

Barotropic and baroclinic phenomena occur on different time scales in the ocean. This has led to a split system of time stepping, where the fast barotropic mode can be approximated as a two-dimensional, depth-averaged model, and the Courant Friedrichs Lewy (*CFL*) condition

determined by the baroclinic or slow mode (Griffies at al. 2000; Shchepetkin et al 2005). Many schemes are used to couple these two different model modes.

3.2 Wave Modeling

Wave models are used to model phenomena including transfer of energy from wind, inter-wave interaction, bottom friction, shoaling and surf breaking, sea level setup and setdown, transmission, reflection and refraction due to obstacles, diffraction, vegetation based damping, wave-driven currents, and transmission, reflection, refraction and diffraction due to obstacles (*SWAN* 2006). The foremost wave models in the coastal engineering industry are *SWAN*, the "BW" wave module of *MIKE21*, and the "S" or spectral version of *RefDif* (Oh et al 2009). *SWAN* is a phase averaging model based on an energy balance, *RefDif* and *MIKE21BW* are phase resolved models based on potential flow analysis. *RefDif* (refraction/diffraction) solves the mild slope equation. *Mike21BW* solves the Boussinesq-type equation. *SWAN* solves the action balance equation. *RefDif* is somewhat better for diffraction effects, but restricted in domain size, nonlinearity, direction, slope angle, and is monochromatic although different frequencies can be superimposed. *MIKE21BW* is better than *RefDif* for spectral interaction and dispersion, but is limited to long waves and by direction. *SWAN* is better for larger domains, nonlinearity and spectral applications and interactions as well as dispersion. *SWAN* is the only model of the three which can handle reflection, and most importantly wave generation and whitecapping from wind, but there are some issues with diffraction. *SWAN* has been chosen for this study because of its accessibility and adaptability as open source software, its native coupling with ocean models, and its dominance in wave forecasting along with related third-generation models *WAM* and *WAVEWATCH III*, (Jensen et al. 2002).

3.2.1 Modeling WECs

Hydrodynamic modeling of wave energy converters has made use of software developed for studying the interaction of waves with vessels and offshore structures. Many different schemes have been studied using commercial panel method code such as *WAMIT*, which incorporates linear wave theory with a Boundary Element Method solver using source and doublet singularities (Babarit et al. 2012; Gomes et al 2012). Another tool for modeling the hydrodynamics of marine structures is the *OrcaFlex* software, which is based on Finite Element Modeling using a lumped-mass analysis. Full Computational Fluid Dynamics (CFD) software can also be used to model hydrodynamic behavior. These models can be useful for studying the performance of *WEC*s under various conditions, but their use is outside the scope of this paper. Results of analyses using these models are available in the literature and have been used in the present study (Babarit et al. 2012).

The above table lists wave models, i.e., they cannot handle sediment transport alone, although at least *SWAN* and *RefDif* can be easily coupled with *ROMS* natively.

For sediment transport modelling, *COAWST, DIVAST, ORCAFLEX*, and *WAMIT* are some of the existing tools. The Coupled-Ocean-Atmosphere-Wave-Sediment Transport Model (*COAWST*)system is comprised of the Regional Ocean Modeling System (*ROMS*) ocean model,

the Weather Research and Forecasting (WRF) atmospheric model, the *SWAN* wave model, and the Community Sediment Transport Model (*CSTM*) sediment model.

ROMS serves as the ocean circulation model in *COAWST*, and is described as "a member of a general class of three-dimensional, free-surface, terrain-following numerical models that solve the Reynolds-averaged Navier-Stokes equations using the hydrostatic and Boussinesq assumptions" (Hedström 2012). The *ROMS* model uses atmospheric inputs including air temperature, pressure and humidity, surface radiation and other heat fluxes, wind speed or stress, evaporation and precipitation.

DIVAST is a hydrodynamic ocean/circulation model for coastal and estuarine applications which solves the depth integrated Navier Stokes equations with sediment model. There is also another hydrodynamic model for modelling structures known as *ORCAFLEX*, primarily for stresses and fluid-structure interaction of an actual wave converter, based on finite element with lumped mass. *WAMIT* is used to model vessels, with capacity to also model wave converters. It applies BEM/panel methods. There are more, closed-source tools to model various aspects of ocean and coastal parameters, which remain beyond the access and scope of this paper. Some comparative publications are available in the literature, for example Oh et al. (2009).

3.2.2 *SWAN*

To understand ocean energy potential, the researchers use the *SWAN* software. Sea states are modeled as a superposition of many wave trains, and are described in terms of three bulk statistics: characteristic wave height, characteristic wave period and characteristic wave direction. The significant wave height used in *SWAN* is H_{m0}, and is equal to four times the square root of the sea surface height variance:

$$H_{m0} = 4\sqrt{\mathrm{VAR}(\zeta)} \quad (1)$$

where VAR is the variance function and ζ is the sea surface height. From linear wave theory, the total wave power across a unit of length, for regular seas, is:

$$\frac{P}{l} = c_g(E_{tot}/A) \quad (2)$$

where c_g is the group velocity. E_{tot}/A is the total wave energy per unit surface area, and is related to the significant wave height H_{m0} as:

$$\frac{E_{tot}}{A} = \frac{\rho_0 g H_{m0}^2}{32} = \frac{1}{2}\rho_0 g\mathrm{VAR}(\zeta) \quad (3)$$

The variance density spectrum (or spectral energy density), $G(f)$, is obtained by performing a Fourier transform on the autocovariance of sea surface height, (*SWAN* 2006):

$$G(f) = 2\int_{-\infty}^{\infty} \mathrm{EV}(\zeta(t)\zeta(t-\tau))e^{-2\pi i f\tau}d\tau \quad (4)$$

for $f \geq 0$. EV is the expected value function. The variance spectrum density is so called because it has the property that [*SWAN* technical documentation]:

$$\mathrm{VAR}(\zeta) = \int_0^{\infty} G(f)df \quad (5)$$

If ambient currents exist, spectral energy density is not a conservative property, therefore the researchers introduce the spectral action density, $N(\sigma,\theta)$, which is conserved when currents exist and is defined as:

$$N = G/\sigma \tag{6}$$

The governing equation solved by *SWAN* is called the spectral action balance equation, and is expressed as, [*SWAN* technical documentation]:

$$\frac{\partial N}{\partial t} + \nabla_{\vec{x}} \cdot \left[(\vec{c}_g + \vec{U})N\right] + \frac{\partial c_\sigma N}{\partial \sigma} + \frac{\partial c_\theta N}{\partial \theta} = S_{tot}/\sigma \tag{7}$$

The terms on the left describe the evolution of wave energy kinematically, with the second term representing the spatial propagation of wave energy, and the third and fourth terms describing the transport of wave energy in the spectral space. The wave energy forcing effects on the right side comprise an energy source term due to wind, source/sink nonlinear 3- and 4-wave interaction terms, and energy sink terms for dissipation due to whitecapping, bottom friction, and depth induced breaking making up the source term on the right side are from wind, nonlinear 3- and 4-wave interactions, whitecapping, bottom friction and depth induced breaking. These terms include various empirical formulations, with whitecapping related to the ratio of wave height to wavelength, and breaking related to the ratio of wave height to bottom depth. The action balance equation is discretized using the Finite Difference method, and solved using Gauss-Seidel iteration.

The n-th moment of the variance density spectrum, [*SWAN* technical documentation]:

$$m_n = \int_0^\infty f^n G(f) df \tag{8}$$

is used to define various parameters – Equation (4) for example shows that the variance is equal to the 0th moment, and this moment is the basis for the significant wave height used by *SWAN*:

$$H_{m0} = 4\sqrt{m_0} \tag{9}$$

Different moments can also be combined to express various forms of the characteristic wave period.

$$T_{m-10} = m_{-1}/m_0 \tag{10}$$

For irregular waves in deep water, linear wave theory gives [*SWAN* technical documentation]:

$$\frac{P}{l} = \rho_0 g^2 H_{m0}^2 T_{m-10}/64\pi \tag{11}$$

SWAN can calculate and output various bulk parameter data such as H_{mo}, P/l, and various forms of characteristic period and direction, as well as spectral data $G(\sigma,\theta)$, at user selected points. To sum up the resource the researchers performed a line integral on the total energy transport across the 100m contour. Thirty-four points, equally spaced between 32.48°N and

32.74°N are sampled, and the annual average wave power across each of the i=33 line segments is calculated as, [*SWAN* technical documentation]:

$$P_{avg,i} = \frac{s_i}{2920}\sum_{n=1}^{2920}((\frac{P}{l})_{i,n} + (\frac{P}{l})_{i+1,n})/2 \quad (12)$$

where *i* is the index of line segments, from 1 to 33, *n* is the time step of each run, from 1 to 2,920 and *s* is the line segment length.

3.3 Sediment Transport (*COAWST* and *ROMS*)

In order to study the processes involved in the erosion, suspension, transport and deposition of sediment, the researchers use the Coupled-Ocean-Atmosphere-Wave-Sediment Transport Model, or *COAWST*, (Warner et al, 2008, 2010). This model comprises the Regional Ocean Modeling System (*ROMS*) ocean model, the Weather Research and Forecasting (*WRF*) atmospheric model, the *SWAN* wave model, and the Community Sediment Transport Model (*CSTM*) sediment model. The atmospheric model was not used in this study, instead the option of providing surface fluxes, forcing and boundary conditions via bulk parameters was used. *COAWST* enables two-way coupling between *ROMS* and *SWAN* with variables being transferred between the two models at user-defined time steps. The size of these time steps must be an integer multiple of each of the time steps used in the individual wave and ocean models.

To evaluate the impacts of *WEC*s on the wave field over the domain and by extension, the impacts on sediment conditions, the researchers first use the *COAWST* software to model the domain in the absence of *WEC*s. The researchers then alter the *SWAN* wave model portion of the software to simulate a reduction in wave energy due to *WEC*s. This altered wave model is coupled with the ocean and sediment model using *COAWST* to evaluate the effects of *WEC*s on sediment conditions.

The ocean circulation model used in *COAWST* is *ROMS*, (Hedström 2012). *ROMS* is described as "a member of a general class of three-dimensional, free-surface, terrain-following numerical models that solve the Reynolds-averaged Navier-Stokes equations using the hydrostatic and Boussinesq assumptions", (Hedström 2012). The *ROMS* model uses atmospheric inputs including air temperature, pressure and humidity, surface radiation and other heat fluxes, wind speed or stress, evaporation and precipitation. Boundary conditions include water level, momentum, salinity and temperature.

The governing equations solved by *ROMS* are the primitive equations – a formulation of the conservation of momentum, the advection-diffusion equation, the equation of state for seawater, and the continuity equation. The Reynolds-averaged formulation of the horizontal momentum equations in Cartesian coordinates are given as, (Haas and Warner 2009):

$$\frac{\partial U}{\partial t} + \vec{V}\cdot\nabla U - fV = -\frac{\partial \phi}{\partial x} - \frac{\partial}{\partial z}\left(\overline{U'W'} - \nu\frac{\partial U}{\partial z}\right) + F_U + D_U \quad (13)$$

$$\frac{\partial V}{\partial t} + \vec{V}\cdot\nabla V - fU = -\frac{\partial \phi}{\partial y} - \frac{\partial}{\partial z}\left(\overline{V'W'} - \nu\frac{\partial V}{\partial z}\right) + F_V + D_V \quad (14)$$

The prime notation indicates a variation around the mean; the overbar indicates an average over time. The hydrostatic assumption gives as a force balance in the vertical dimension:

$$\frac{\partial \phi}{\partial z} = \frac{-\rho g}{\rho_0} \tag{15}$$

Note that variations in density are significant and accounted for in this equation where the density is multiplied by the acceleration of gravity, *g*, in the buoyancy term. These variations are neglected elsewhere in the momentum equations due to the Boussinesq approximation.

Conservation of mass for an incompressible fluid is given by:

$$\frac{\partial U}{\partial x} + \frac{\partial V}{\partial y} + \frac{\partial W}{\partial z} = 0 \tag{16}$$

The equation of state for seawater is expressed as:

$$\rho = \rho(T, S, P) \tag{17}$$

The nonlinear equation of state used in this study is based on the UNESCO EOS-80 formulation and was developed to compute the density *in situ* from potential temperature, salinity and pressure, [Jackett and McDougall].

Transport of tracer type variables are governed by the advection-diffusion equation:

$$\frac{\partial C}{\partial t} + \vec{V} \cdot \nabla C = -\frac{\partial}{\partial z}\left(\overline{C'W'} - \nu_\theta \frac{\partial C}{\partial z}\right) + F_C + D_C \tag{18}$$

ROMS is discretized horizontally onto an orthogonal curvilinear grid. The Arakawa-C grid used is shown in Figure 4 with grid coordinates ξ and η. Density, temperature, salinity and sea surface height are prescribed at ϱ-points in the centers of cells, velocities are prescribed at cell edges. ψ-points define grid cell nodes. Boundary conditions are given by values on and outside the outer edges.

Figure 2: *ROMS* Arakawa-C Staggered Grid, (Hedström 2012)

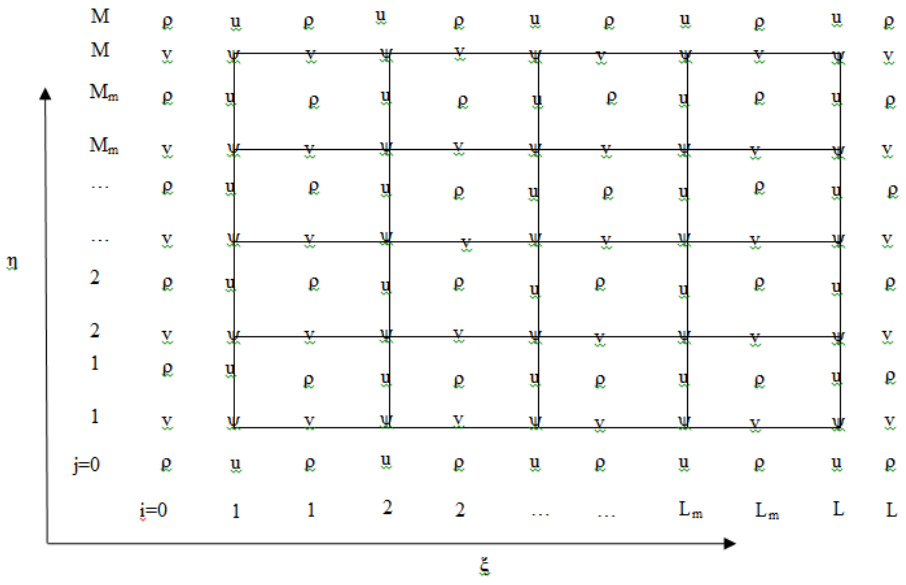

ROMS has multiple methods available for topography-following vertical discretization. This allows for increased resolution in surface and mixing levels as well as in the bottom boundary layer. Vertical velocities are evaluated at cell tops and bottoms, horizontal velocities and state variables are prescribed at cell centers. Cell thicknesses vary spatially and in time, since both sea surface height and bathymetry can change versus a reference datum level, (Hedström 2012).

ROMS has several available schemes for dealing with vertical and horizontal advection and mixing of both momentum and tracer type variables (active and passive), atmospheric and bottom boundary layers, lateral boundary conditions, and pressure gradient. In the coupled *COAWST* system *ROMS* receives values from *SWAN* for wave height, wave direction, peak and average wavelength, wave bottom and average period, energy dissipation due to breaking, white-capping and bottom friction, wave bottom orbital velocity, and breaking wave fraction. In the coupled *COAWST* system, *SWAN* receives values from *ROMS* for depth-averaged current velocity, sea surface height, and bottom depth, (Hedström 2012).

Figure 3: Energy flux calculated at depths from 200m to shore at Site A. (Jarocki et al 2010).

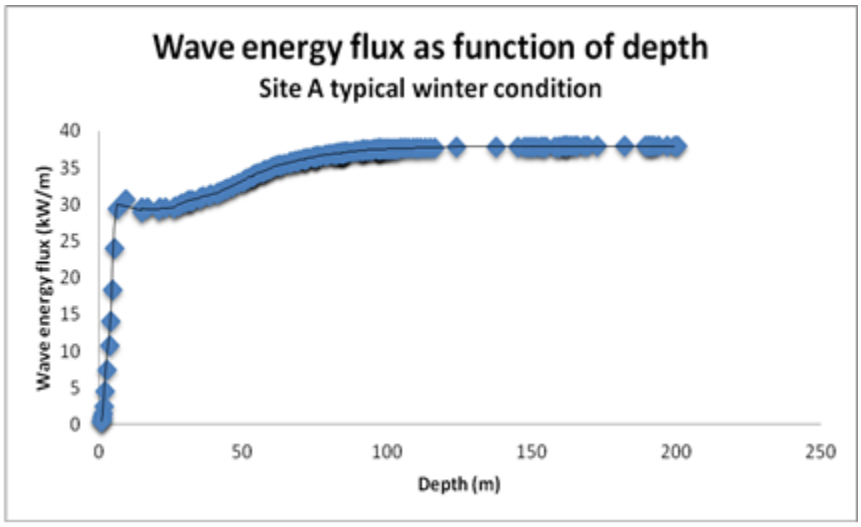

3.3.1 *SWAN* Model without *WEC*s Inserted in the Wave Field

Jarocki et al (2010) give an excellent description of *SWAN* model results versus CDIP and NDBC wave buoy data for two sites: Site A, 4 miles offshore at Morro Bay and Site B, 4.5 miles west of Vandenberg Air Force Base (*VAFB*). This analysis will not be repeated here, but the conclusion was that the wave buoy data and *SWAN* estimates agreed well. Table 3 and Figures 3, 4, 5, and 6 below are used with permission from (Jarocki 2010). The *CDIP* and *NDBC* buoy data (Table 3) are dense in time coverage and sparse in spatial coverage of all the water depths from 200m to the surf zone. In Figures 3 and 4 the steep drop of wave energy flux at depths less than 10m is what is expected from bottom friction loss. The drop in wave energy flux from 100m to 10m water depth has a lesser slope than the loss for water depths from 10m to the surf zone, but this is too deep for bottom friction loss, Hwang et al, to be the cause according to the classical shallow water wave propagation literature. Having an early inclination that the loss in wave

energy flux from 100m to 10m water depth was difficult to explain from the literature, Beyene and Wilson (2003) performed the analysis shown in Figure 5 from wave buoy data only, and a much more significant wave energy loss slope was observed than for Sites A and B. No reason is known for this currently, but it will be investigated thoroughly in this effort. The apparent difference in wave energy flux loss from 100m to 10m water depth between Northern and Southern California locations must be understood before one can model the impact of *WEC*s on the wave energy flux decrease.

Figure 4: Energy Flux Calculated at Depths from 200m to Shore at Site B (Jarocki 2010).

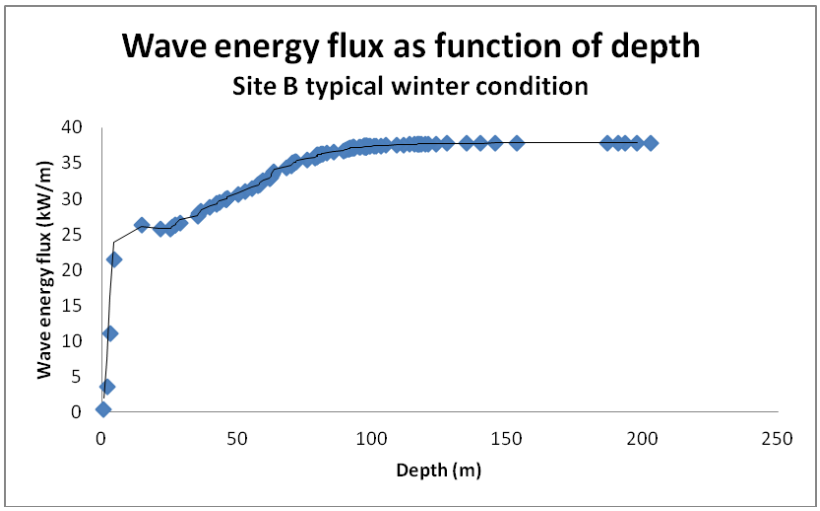

Figure 5: Wave Energy Flux as a Function of Depth Measured at Observation Buoys in Northern California (Jarocki 2010)

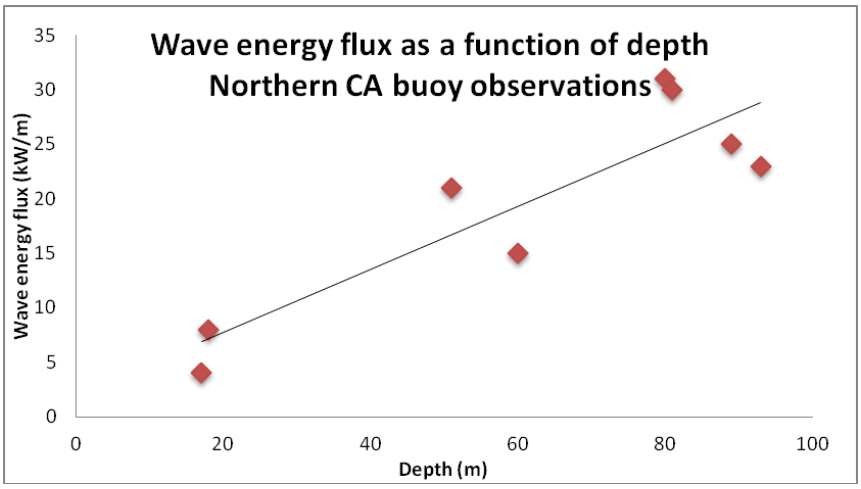

Figure 6: Google Earth Image of *CDIP* and *NBDC* Stations Used in Study (Jarocki 2010)

Table 3: NBDC and CDIP Buoy Records Analyzed (Jarocki et al)

Station	Location	Latit. (Deg. North)	Long. (Deg. South)	Depth (m)	Data Coverage
CDIP 0076	Diablo Canyon	35.21	120.86	22.9	1983-2002
NBDC 46062	Point San Luis	35.10	121.00	379.0	1197-2001
NBDC 46011	Santa Maria	34.88	128.87	185.9	1980-2001
NBDC 46023	Point Arguello	34.71	120.97	384.1	1982-2001
CDIP 0120	Pt. Arguello Harbor Outer	34.57	120.63	5.8	1978-1979
CDIP 0019	Pt. Arguello Harbor Inner	34.57	120.63	2.5	1978-1980

The Literature on the Impact of *WEC*s insertion on the wave energy flux shoreward is very sparse (Zetterman et al. 2009). Furthermore, *SWAN* currently only allows one to insert "island spikes" connected to the bottom. In the future, the researchers plan to derive more realistic wave energy flux absorption algorithm that can be ingested into the *SWAN* model.

3.3.2 The Presence of Waves with Significant Wave Heights Greater than 15m 4 to 5 Miles Offshore

Ocean wave propagation from storms in the North Pacific are modeled using *Wavewatch III* in deep water, and as they approach shore, the *Wavewatch II* ocean parameters are used to initiate the *SWAN* model for propagation to the *WEC* site 4 or 5 miles offshore to the surf zone. These wave model studies for extreme storms and the analysis of the historical wave buoy records near the California coast show that a significant wave height greater than 15m is an extremely rare event. However, this large wave event would be predictable by *Wavewatch III* and *SWAN* at the *WEC* location if it ever occurred (Beyene and Wilson 2003).

There are no realistic storms that create waves with significant wave heights of 15m or greater at *WEC* locations 4 or 5 miles offshore in California. It must be emphasized that waves with significant wave heights exceeding 15m at *WEC* locations 4 or 5 miles offshore is a totally different phenomena than single rogue waves exceeding 15m *Wavewatch III*, *SWAN*, nor any other wave model can currently predict large, single rogue waves. Significant wave height by definition is an average of the largest 1/3 of any set of waves. Rogue waves may have large periods, such as Tsunami waves generated from underwater earthquakes, usually increase in wave height. In this case the rogue wave has a relatively low wave height 4 or 5 miles seaward, but become very large as they enter very shallow water near the surf zone. The area 4 or 5 miles offshore is a good area to install a *WEC* field because there is very little ocean bottom friction to diminish the wave's energy, and large waves of any type are extremely rare off the California coast that far off shore. The last recorded destructive rogue wave heavily damaged the Long Beach pier in the early 1930s, and the lack of wave modeling capability at that time prevented the assessment of what caused this wave. There was no reported damage off shore from this wave, only damage in shallow water.

Few comprehensive studies have been conducted to assess the impact of *WEC*s on the environment. Krivtsov et al (2012) use the *OrcaFlex* model to assess the scouring effect on bottom sediments and consequent disruption of benthic habitats. The output from *OrcaFlex* is then imported to Matlab to calculate the affected area using the time series of coordinates of touch down points of the mooring lines. The results show that the area affected by the leading mooring line increases with the increase in wave height.

Millar et al (2007) use the *SWAN* wave model to assess change of shoreline wave climate caused by the installation of a wave farm rated at 30 MW. The results suggest that the magnitude of effects decreases linearly as wave energy transmitted increases, and that the predicted change in shoreline wave climate is small. The authors suggest that the effects vary with location and wave direction. The model also concludes that 90% wave energy transmission produces an average change in significant wave height at the shoreline of 1 cm or less over 11 months, with a maximum change of as high as 4 cm coming sporadically. It then follows that the effects introduced by such wave hub will be insignificant.

Palha et al (2010) use *RefDif* to model the energy extraction from wave farms. Three different sinusoidal incident wave conditions and five different wave farm configurations were considered, varying the position of the wave farm, its number and the width of the navigation

channels at each wave farm. The results for each configuration in terms of the change of the wave characteristics for three representative wave conditions were presented.

Notice that Millar et al. (2007) chose to use the *SWAN* model for the propagation of waves and the absorption-transmission of energy by the wave farm. This version is a third generation wave model that propagates a wave spectrum. The authors opted for hypothetical wave energy devices, hence choosing values of energy absorption in a wide range varying between very low and near total energy absorption by the wave farm. This enabled the determination of a range, and more importantly, a maximum for the effects of the installation of such wave energy farm on the wave climate near-shore. Also, due to the lack of a choice of a specific wave energy device, the authors did not have available a magnitude transmission function hence all frequencies present in the spectrum were affected in the same way. In the approach presented here, the choice for the *RefDif* model, a single frequency propagation model, lies in two reasons: the use of a single sinusoidal wave which enables a first safe use of the specifications of the wave energy device without possible effects arising from different absorption values for different frequencies; possibility in the future of the same methodology to be used for the different components of the spectrum of a wave state, each component with the corresponding energy absorption specified by the manufacturer. In this case, given that there was a specific wave energy device, one could use the specific working conditions given by the manufacturer, that is, for each wave state one knows the energy absorption by the device. This also allowed for another point of study: the effect of the shape of the wave energy farm not only on the wave climate near-shore, but also on the total energy absorption by the wave energy farm, specifically in situations of shadowing between groups of devices. As will be seen, nevertheless the differences in the methodologies used – specially the numerical models used for *SWAN* (Millar et al. 2007), Boussinesq (Hedström 2012) and *RefDif* (the present work) - the trend results, i.e., the order of magnitude of the wave height variation and affected direction are very similar.

Oh et al. (2009) present the performance of three spectral wave models using *RefDif*, *MIKE21BW* module, and *SWAN*, which were then compared to laboratory or field experimental data. The authors claim that all the numerical models simulated fairly well shoaling and breaking of waves propagating on a plane sloping beach. However, the model accuracy was reduced in simulating waves propagating over a barred beach. Sensitivity of the models to bathymetry, refraction, and diffraction were presented.

3.4 Testing and Monitoring

The simulation model combining wave and erosion impacts are still in the early stages of development. Furthermore, the available tools are not coupled to data acquisition systems to validate these models. There are technologies under development to track the environmental impact of wave energy generation technologies (ZD Net 2014). The idea is to develop sensors and communications infrastructure with real-time data collection capabilities to be hosted and processed in the 'cloud' so as to explore underwater noise created by *WEC*s, for example, which in turn will be evaluated for its impact on the marine ecosystem.

A site was built in 2004 for the purpose of studying environmental impact of *WEC* near Lysekil on the Swedish West coast, 2 km offshore covering an area of 40 000 m^2, to run until the end of 2013, (Leijon et al. 2008). Several *WEC*s were connected to produce a variable voltage in amplitude and frequency which was then connected to a marine substation, where the voltage from each *WEC* was rectified, alternated and transformed for the grid using a 1 kV cable. Sediment samples were taken annually including before *WEC* devices were deployed to determine species composition and site biodiversity. The site capacity was boosted in 2007 by installing additional buoys, some dedicated to biological research alone. The preliminary results suggest that the effect of biofouling on energy absorption can be neglected.

In another study of the sort, a high definition video was used to monitor the ecological impacts from *WEC* deployment was installed to monitor wave energy impact in September 2010, (Renewable Energy Focus 2010). The outcome of this project is still unknown.

CHAPTER 4:
Tools to Assess the Environmental Impact of Power Generation from *WEC*s

The species pool in a particular sea locality is defined by its biogeographic identity and uniqueness. The evolution of the species pool is a dynamic process even when anthropogenic interventions are absent.

On exposed shores, benthic organisms experience greater wave-induced forces and consequently face a higher risk of breakage or dislodgement from the rock and consequently their persistence. Wave action increases wetting of upper shore species and distribution of nutrient food supply, affecting foraging times in manners unknown. Sheltered shores may experience reduced water motion but may also experience greater sediment deposition and siltation at the same time. The response of species to these stress levels would be different and difficult to evaluate.

Competition for space or resources often reduces the diversity of species, but diversity can often be higher at intermediate levels of disturbances (Caswell 1978). Some species and scenarios such as sheltering from algae or mussel beds, can improve conditions for other species which may increase the local biodiversity as a result. Some species build structures that alter the physical shelters leading to changes in the species assemblage. Wave attenuation or flow reduction will often promote sediment trapping, offering new habitats in place of species that are sensitive to high sediment load. The prevalence of species strongly depends on wave gradient, i.e., limpets prevent establishment of algae on wave beaten shores whilst algal persistence is probably controlled by wave action (Hawkins et al 2007; Jonsson et al. 2006).

4.1 Tools for Impact Assessment

As part of the impact assessment a preliminary field assessment of physical and biological features should be carried out to characterize the *WEC* site and its immediate surroundings (defined by GPS coordinates) by experienced coastal ecologists. A map of the bathymetry should be prepared. Biotopes and sediment characteristics (grain size, oxic layer) should be characterized.

Evidence of scouring around any hard substrates should be noted and key species such as mussels and *sabellaria* worm should be recorded as they play an important role in filtration by reducing porosity. They can also interfere with performance of *WEC* systems if in large mass. Winkles and topshells are important for controlling algal growth (Jenkins et al 1999; Boaventura et al. 2002), whereas green algae may be a nuisance. *Fucoids*, on the other hand, can signal wave exposure (Raffaelli et al 1996). Ratio of dead to live barnacles may be a measure of scouring on the structures. Starfish and the gastropod *Nucella*, which feed on mussels, i.e., can control their growth (Minchin and Duggan 1988). Seagrasses may stabilize the coastline, and *capitella* are indicators of organic enrichment in soft bottoms (Airas and Rapp 203). It is also important to identify other alien species that may potentially impact the *WEC* environment.

Accumulation of algal and seagrass detritus on the beach should be quantified over a period of time. *WEC* is likely to increase this accumulation rate. From a recreational viewpoint, the accumulation has a negative impact. However, it may also stabilize the coastline (Alongi et al 1985). Dead shell assemblages should be examined to obtain information on the diversity of mollusk in the region. Artificial and natural boundaries between terrestrial and marine habitats should be surveyed for all seasons, noting vegetated banks, sand dunes, coastal lagoons, etc., and documented with photographs. Baseline ecological surveys should also be conducted for local and far field effects (Hawkins et al 1983). Organic matter should be estimated using, for example, the oxidation method, and granulometry should also be quantified using nested sets of sieves or automated system (Holme and McIntyre 1971).

4.2 Cost Benefit

One technique for appraising environmental impact of interventions such as *WEC*s is the use of Cost-Benefit Analysis (CBA). Contrary to CBA, a Cost-Effectiveness Analysis (CEA) is employed to select a scheme from among various design options. CEA uses the same steps as in CBA, but uses only the costs, not the benefits, thus incorporating only construction and financial costs – without the intangibles. Eight steps of CEA analyses are presented as, [Hawkins et al, 2007]:

Step 1: Definition of the project.

Step 2: Identification of project impacts.

Step 3: Relevant economic impacts.

Step 5: Monetary valuation of relevant effects.

Step 6: Discounting.

Step 7: Applying the Net Present Value (NPV) test.

Step 8: Sensitivity Analysis.

Detailed classification of costs and benefits as well as inventory of coastal assets is presented by (Hawkins et al, 2007) in which the authors use the concept of economic value defined on the basis of Willingness To Pay (WTP), "the maximum amount of money a person is willing to exchange to acquire a good or service that he (she) considers desirable". This allows monetary value to be placed on non-marketed goods such as a coastal defense. Defining economic value allows quantifying CBA with a broadly defined class of benefits, not only with direct monetary transaction. Projects may have equity and environmental values not quantifiable in the context of monetary transactions, which imposes different appraisal methods for different types of values. An overview of the valuation techniques are presented in the literature (Haab and McConnel 2002).

Mitigation benefits or costs such as reducing sedimentation and values for direct consumptive use such as land and fisheries as well as values type for non-consumptive use such as bird

viewing, waterfowl hunting, and recreational beach visitation is discussed in Bower and Turner (1998), Fankhauser (1995), and in Penning Rowsell et al. (1992).

Table 4 summarizes the proposed environmental impact assessment tool with phases in the columns and classes of effects presented in the rows. Table 5 is a detailed presentation of phase and class of effects.

Table 4: Target Tools to Assess Environmental Impact of *WEC* Systems

	Construction (1)	**Operation and maintenance (2)**	**Decommissioning (3)**
Wave condition, sediment, etc. (A)	Tool 1A	Tool 2A	Tool 3A
Intrusions, mechanical (B)	Tool 1B	Tool 2B	Tool 3B
Disturbances, *EMF*, etc. (C)	Tool 1C	Tool 2C	Tool 3C
Interferences. Haz, toxicity, (D)	Tool 1D	Tool 2D	Tool 3D

Table 5: Detailed Classes of Tools to Assess Environmental Impact of *WEC* Systems

Tool 1 (Construction)	
Wave Conditions (1A)	• Will traffic to WEC site affect wave conditions? • Will temporary buildups for the permanent system construction impact wave conditions?
Subsea and Onshore cables, Mooring systems, *WEC* devices, Vessel traffic (1B)	• Will there be any damage to archaeology sites? • Interfere with on or offshore scenic routes and places? • Have there been review of effects of other similar projects relative to cables and mooring of offshore platforms (oil, wind turbine, etc.)? • Have there been review of effects of known vessel traffics from oil, wind turbine, etc.? • Will traffic and temporary buildups affect access to beaches and other important port outlets?
	• Will laying cables affect sea and shore habitats (fisheries, benthos etc.)? • Will laying cables affect sea and shore habitats?
	• Will mooring affect sea and shore habitats?
	• Will construction or towing to the site of *WEC* devices affect sea and shore habitats?
	• Will vessel traffic increase within or near breeding, resting and molting periods and places of sea birds species?
Noise, *EMF*, etc. (1C)	• Will the noise level of traffic and construction impact beach and sea lives including humans?
Hazardous, toxic, etc. substances, (D)	• Will there be hazards or toxic releases that affect sea life during the construction period?
Tool 2 (Operation and Maintenance)	
Wave Conditions (2A)	• Will during exploitation affect wave conditions? • Will changes in wave conditions affect sediment transport? • Have modelling been done to show impact of changes on wave and sediment? (**Model developed by PIs, Section 4**)

Presence of moored structures, operation of *WEC* devices, overhead-lines and substations, maintenance (2B)	• Will there be physical damages to sea life from passage through *WEC* devices? • Will mooring blocks on sea bed affect the nature of sea life? • Will mooring chains moving on the seabed damage sea life? • Will there be loss to aesthetic value of the landscape?
	• Will traffic generated by regular maintenance of *WEC*s, mooring, cables, etc., affect breeding, resting and molting of sea life?
Noise, *EMF*, etc. (2C)	• Will presence of subsea cables in seabed create *EMF*? • Will increased level of noise and vibrations affect mammals dependent on sound for navigation?
Hazardous, toxic, etc. substances, (2D)	• Will there be marine debris, leakages of fluids such as hydraulic, paints, antifoul, and spill of oil affecting sea life? • Will leaks be washed on shore? • Will emissions of toxic substance such as anti-fouling affect breeding, resting and molting of sea life? • Will there be personnel permanently housed at the plant? • How is human waste disposed of?
Tool 3 (decommissioning)	
Wave Conditions (3A)	• Will enhanced traffic affect wave conditions? • Will temporary buildups for removing the system impact wave conditions?
Removal of *WEC* system, mooring, and cables, (3B)	• Will there be effects of towing and traffic of large vessels on sea life? • What is the fate of the removed materials? • Will removal affect newly formed colonies and habitats that have become dependent on moors and cables?
Noise, *EMF*, etc. (3C)	• Will the noise level of traffic during decommissioning have impact on beach and sea life including humans?
Hazardous, toxic, etc. substances, (3D)	• Will decommissioning add or leave any new or built up toxic or hazardous residue?

4.3 Wave Side Modelling

Software tools for modeling hydrodynamic are divided into three groups: (a) flow models, (b) wave models and (c) computational fluid dynamics, (Hawkins et al, 2007). An example of flow modeling tool is the *Delft3D-FLOW*, used for lakes, estuaries, bays, coastal areas and seas. *Delft3D* can switch from 2D simulation, - vertically averaged to 3D mode to investigate the model behavior before going into full 3D simulations, (Hawkins et al, 2007). The built in modules addressing a specific area of interest such as flow, water quality, wave propagation, and sediment transport, are dynamically interfaced.

The hydrodynamic module, *Delft3D-FLOW*, is a multi-dimensional hydrodynamic simulation program that calculates non-steady flow and transport phenomena resulting from tidal and meteorological forcing on a curvilinear, boundary-fitted grid. In 3D simulations, the hydrodynamic module applies the so-called sigma co-ordinate transformation in the vertical, which results in a smooth representation of the bottom topography. It also results in a high computing efficiency because of the constant number of vertical layers over the whole computational domain.

MIKE21 is another comprehensive modeling software tool for 2D hydraulic simulation in lakes, estuaries, bays, coastal areas and seas where stratification can be neglected, (Hawkins et al, 2007).

SHORECIRC (C.A.C.R., University of Delaware) is a quasi-3D numerical tool developed to simulate currents and long waves forced by wind as well as short waves. It solves the depth integrated continuity and momentum equations. Its 3D effect is simulated using solution for the 3D current profiles with solution for the depth-integrated 2D horizontal equations, (Putrevu et al. 1999). *SHORECIRC* is coupled with REF-DIF.

Other flow models include *COPLA* and *LIMCIR*, offering different capacities of dimensional simulation, availability, and shore line capabilities.

4.4 Wave Modelling Tools

Wave models include *BMV, DELFT-TRITON, MIKE21BW, MIKE21PMS, OLUCA-SP, RedDif, LIMWAVE* each offering varying capabilities of suitability for near-shore, computing time, and time variance.

BMV (C.A.C.R., University of Delaware, U.S.A.; University of Roma TRE, University of Genova, University of Catania, Italy) is a 1D model based on the Boussinesq equation. (Svendsen, et al 1996) thus derived without making the assumption of irrotational flow; coupling with the vorticity transport equation which helps account for vorticity-induced wave-breaking.

The model can provide accurate description of the flow in the surf zone. Further developments have been targeted to include turbulence, allowing the eddy viscosity to vary over the water depth. Evolution of this model has gone through some universities, and the latest versions that solve the vorticity transport equation with eddy viscosity at each computational point (Briganti et al. 2004).

Shallow waters have relatively large waves with more non-linear effects than those in deep water. These nonlinearities also result in that wave components of different frequencies propagate at different speeds. Standard shallow-water modeling tools designed for very long waves do not take such frequency dispersion into account. The *TRITON* model includes both non-linear wave behavior and frequency dispersion. *TRITON* accounts for shoaling, refraction due to depth variations, frequency dispersion and diffraction, as well as non-linear wave-wave interactions, wave breaking, and wave reflection. The model is therefore suitable for coastal regions and harbors with coastal structures, (Hawkins et al, 2007). *TRITON* has been coupled to the spectral model *SWAN*.

MIKE21BW is a tool for studies and analyses of wave in ports, harbors and coastal regions. It can be used to assess design conditions of coastal structures in these areas. More applicable to wave energy would be *MIKE21PMS*, which is based on equations governing the refraction, shoaling, diffraction and reflection of linear water waves propagating on a gently sloping bathymetry. The parabolic approximation neglects diffraction along the wave direction, i.e., neglects backscatter which means modelling of wave conditions in the vicinity of reflecting structures would be inaccurate. There exists the ability to simulate directional and frequency

spreading of the propagating waves using linear superposition with *MIKE21PMS* for any water depth on a gently sloping bathymetry, capable of reproducing shoaling, refraction, dissipation due to bed friction and wave breaking, forward scattering and partial diffraction, (Hawkins et al 2007).

The Coastal Modelling System (*SMC*) developed by the University of Cantabria. Two relevant hydrodynamic modules of this package are *OLUCA-SP* and *COPLA. OLUCA-SP* is a wave propagation model based on linear wave theory and parabolic approximation of the mild-slope equation, similar to *RefDif* and *MIKE21PMS*. It can include the effect of currents.

COPLA offers simulation abilities of water circulation and level variations in the near-shore as a response to wave forcing, solving vertically and time-averaged continuity and momentum equations in two horizontal dimensions. The currents are driven by radiation stress gradients. The model accounts also for turbulent diffusion and bottom friction.

RefDif (University of Delaware) solves the parabolic approximation of the mild-slope equation and can simulate the effect of wave shoaling, refraction, wave-breaking and bottom friction and approximate diffraction, - without the ability of modeling wave reflection. *RefDif* considers monochromatic waves. However, random sea states can be modelled using linear superposition of each component, (Hawkins et al 2007).

4.5 Fluid Dynamic Modelling Tools

Examples are COBRAS, DELFT-SKYLLA, and NS3. *COBRAS* (Cornell University/University of Cantabria) is a 2DV numerical modeling tool with capabilities of simulating wave-induced motions around coastal structures and processes including shoaling, reflection, transmission, overtopping, porous flow, wave breaking, and run-up. It is also capable of simulating nonlinear effects and turbulence generation as well as transport in the fluid and permeable regions (Hawkins et al. 2007).

The model can handle complex geometries and multi-layered structures - submerged or floating. The model has been extensively validated.

DELFT-SKYLLA is a Volume-of-Fluid Navier-Stokes model for wave interaction with coastal structures.

Over the past few decades, a number of advanced spectral wind-wave models, known as 3G models such as *WAMDI, WAVEWATCH III, TOMAWAC*, and *SWAN* (Tolman 1991; Benoit *et al*. 1996; Booij et al. 1999) have been developed. These models solve the spectral action balance equation without restrictions on the spectrum for the evolution of wave growth.

SWAN is an extension of the deep water third-generation wave model which incorporates deep water processes of wave generation, dissipation (including due to bottom friction), depth-induced breaking, and the quadruplet wave-wave interactions from the WAM model (Komen *et al*., 1994). It has been extensively validated, and it is available at no cost, which makes this powerful tool a very desirable choice. It has undergone some important evolutionary

changes to make it more user-friendly, and the development of *WHEAT* is one such improvement.

Jove Sciences, Inc.'s (Po-PI) new **Wave Height and Energy Automation Tool (*WHEAT*)** Version 2.0 software makes it easy to insert *WEC* fields of all types into the wave field to assess their performance and environmental impact. *WHEAT* is a breakthrough for environmental agencies assessing the impact of proposed *WEC* developments offshore and for *WEC* developers estimating the performance of potential *WEC* fields they are proposing to install using all types of seasonal wave environments. The most time consuming and difficult part of the entire *WEC* impact effort is to develop the software to make the *SWAN* model user friendly. Currently, *SWAN* is one of the most user unfriendly wave models ever developed, and only academic scientists and engineers, who can spend man months of spin up time, use *SWAN* extensively. *WHEAT* represents a very significant breakthrough toward making *SWAN* easier to use for *WEC* developers, ocean wave modelers, and environmental agencies alike. The database inputs to *SWAN* include the ocean wave environment (significant wave height, wave direction, and wave period), near shore bathymetry, and the bottom geology from the *WEC* site to the surf zone. *WEC* performance assessment organizations and environmental impact agencies may not afford this learning spin up time, and manual input of these data bases and *WEC* fields make the manual running of *SWAN* an extremely time consuming and economically unfeasible effort. *WHEAT* will have a very significant impact on the *WEC* industry in the future. *WHEAT* is a Java-based Graphical User Interface (GUI) that streamlines the process of downloading bathymetry data from various websites, converting this downloaded data, running the *SWAN* wave model, and then displaying the results.

See Appendix A for more details.

Summary of the tool developed to assess the environmental impact of power generation from *WEC*s: Summarizing the *SWAN* oceanographic model used in this analysis the researchers will show how much impact there is on waves arriving in the surf zone after passing over the Wave Energy Converter (*WEC*) installations 4 to 5 NM seaward. Thus, if there is very little impact on energy flux density or significant wave height by the *WEC* installation, then there will be little impact on oceanographic near shore parameters, such as near shore currents and beach erosion. However, if *SWAN* shows that an Existing *WEC* installation has a large impact on significant wave height, then the *DELFT 3D* model can be used to model the near shore oceanographic impact for specific *WEC* installations. A real, but manageable, environmental barrier to *WEC* installation approvals is the potential for *WEC*s to break loose from their moorings during high sea states and potentially injure or kill people, or damage infrastructure ashore. To mitigate this environmental barrier for *WEC* installation approval, the wave parameters at the *WEC* site must be forecast accurately at least 72 hours in advance, and the PIs have vast experience in running Wavewatch III, the Coupled Oceanographic and Atmospheric Mesoscale Prediction System (*COAMPS*), and other modern wave and storm forecast models. A rule of thumb among *WEC* manufacturers is to have *WEC* moorings withstand waves of 15 meter significant wave height or less, and so the focus is to forecast extreme wave conditions. Tools to accomplish this will be summarized.

***SWAN* Runs to Assess Environmental Impact of Deep Water *WEC* Installations:** The "Bottom Line" conclusion of the analyses presented in this section is that *WEC* fields have little or no impact on the wave field propagating shoreward. It takes islands to impact energy flux density (*EFD*) and significant wave height (H_s) to produce noticeable differences compared to *SWAN* runs with no "obstacle" (i.e., *WEC*s) in the wave field. Remember the attached is for a very large obstacle (a 100m island with low "flow through"), not a small 8m *WEC* that will be used to simulate a *WEC* "point absorber". For *WEC*s in *SWAN*, JOVE has developed software to insert *WEC* "point absorbers" of realistic size, geometric position based on minimum *WEC* spacing for safety, height above and below the mean water depth, and a "flow through" factor between 1.0 (zero blockage) and 0.0 (complete blockage).

The *EFD* scale in Figure 7 is 25-30 kW/m for red, 20-25 kW/m for orange, and 15-20 kW/m for yellow. Light blue is the surf zone and dark blue is land. Even for this large *WEC* "obstacle, the *EFD* is homogeneous a few nm shoreward of the *WEC*s.

Figure 7: Energy Flux Density for a Large 100m WEC

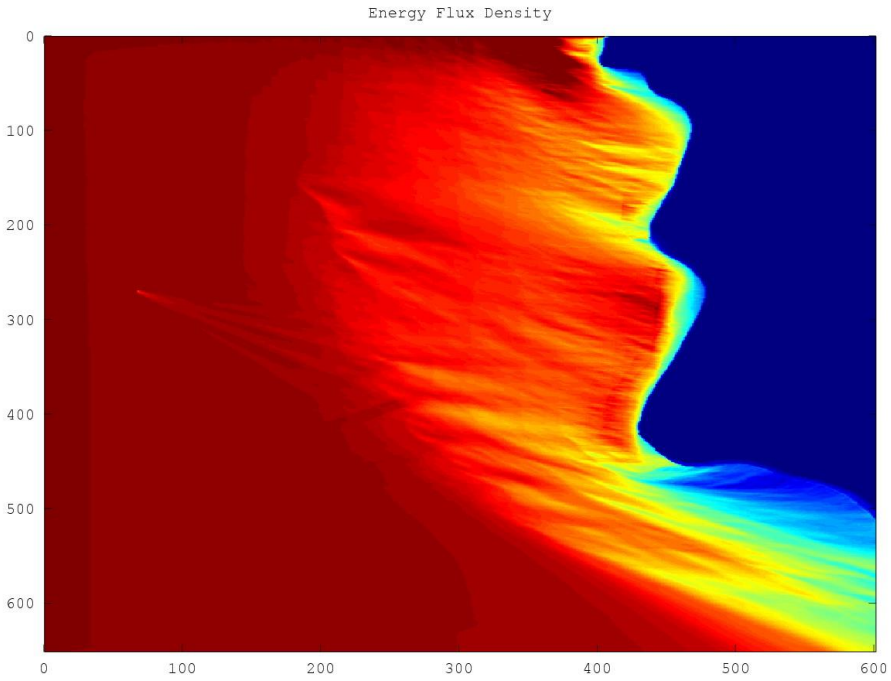

WEC placed at 45 degrees to the incident west wave field approximately 4.5 nm west of Point Arguello near Vandenberg Air Force Base.

Drawing an analogy from a California Energy Commission Wave Resource Study (Beyene and Wilson, 2003) to understand the *SWAN* output, assume an AquaBuoy (Figure 1) point absorber is 8m by 8m and extends 30m below the mean water depth. For the California coast north of Point Conception (Beyene and Wilson, 2006(a)) the typical winter EFD was ~ 30 kW/m of ocean wave crest, and AquaBuoy's capacity factor optimistically was 20% so that it extracted ~ 6.0 x 8m or 48 kW of power from the wave. If the AquaBuoys were spaced 100m apart (minimum

safety distance), and if there were a line of 10 AquaBuoys, the power extracted would be ~ 480 kW. The total power in the wave incident upon the line of 10 *WEC*s is 1100m x 30 kW/m = 3.3 MW. Thus, the percentage of wave power extracted by the *WEC*s is ~14.5%. This creates a very small diffraction/refraction zone shoreward of the *WEC* line, but is quickly filled in by the waves on both sides of the *WEC* line. Little or no impact on the near shore environment results from this basic analysis. Now the *SWAN* results are shown to be consistent with this analysis above, when one employs *SWAN*'s flow through factor to model *WEC*'s capacity factor as a function of wave height.

4.5.1 Impact of *WEC* Point Absorbers on the Ocean Environment

An array of 10 *WEC* point absorbers like the AquaBuoy was placed parallel to the shore (north-south) approximately 4.5 nautical miles off shore west of Vandenberg Air Force Base (*VAFB*) as shown in Figure 8. This site was chosen by Dr. Wilson of Jove Sciences, Inc. because it is near Oil Platform Irene and in an ideal location for a *WEC* installation based on its excellent wave resource. A realistic *WEC* capacity factor of 20 percent was assumed, and modeled in *SWAN* by using an 80 percent "energy flow through" factor. The *WEC* size of 9m was used to simulate the point absorber size, and Figures 13 and 14 show the *SWAN* runs outputting H_s and *EFD*s from the *WEC* location to the surf zone near Point Arguello. A significant wave height of H_s = 3m incident on the *WEC* array from the west was assumed, and one can clearly see the refraction/defraction wave height pattern shoreward of the *WEC* array in Figure 9 numerous *WEC* point absorbers can be installed in deep water locations and the total EFD shoreward is reduced far less than 10%. A very significant amount of work was required to develop this *SWAN* tool by Jove Sciences, Inc., and it is hoped that *WEC* developers and environmental agencies alike can how valuable the *WHEAT* tool can be in practical applications.

Figure 8: *WEC* Location Point Arguello near Vandenberg Air Force Base

The WEC location 4.5 nm West of Point Arguello near Vandenberg Air Force Base (Google earth)

The reason that the *EFD* diffraction/refraction pattern in Fig. 14 is more pronounced than the H_s pattern in Fig. 9 is that *EFD* depends on H_s^2, but the total amount of wave energy extracted by

this 10 *WEC* array compared to the total amount incident at the *WEC* location is minimal. Stated in simple terms there is an enormous amount of wave energy available off California's coast, with very little chance of impacting the ocean environment nearshore for any safe spacing of *WEC*s. However, this must be determined on a specific case by case basis, and the *WHEAT* tool developed here is ideal for this application.

The zoomed diffraction/refraction patterns of H_s and *EFD* from Figures 9 and 10 are shown in Figures 11 and 12, respectively. A very useful potential result for spacing of multiple *WEC* rows seaward of the 10 *WEC* array analyzed here now becomes apparent. If the predominate wave direction for this location is from the west [Beyene and Wilson, 2006(a)], than the second *WEC* row should be placed 'in between" the north/south locations of the western most *WEC* row to be located in an *EFD* peak. This is common sense, but it is encouraging that it is predicted by *SWAN*, a comprehensive ocean wave model.

Since *EFD* is proportional to H_s^2 the color plots of *SWAN EFD* outputs in Figures 12 and 13 look more dramatic than the corresponding H_s plots in Figures 9 and 10 above. While H_s in Figures 9 and 10 show a decrease from the initial 3.0m to ~ 2.7m just landward of the *WEC* column, the effect dissipates by the time the waves reach the surf zone. If the normal weather pattern without *WEC*s results in this small decrease in H_s there is no impact on the wave environment from deep water to the surf zone, so there is likewise no long term impact from one column of ten *WEC*s analyzed here. As the wave direction changes from due west as assumed in the *SWAN* runs made here to other directions the interference patterns shown in Figures 9 through 12 will also "wash out".

To analyze the impact of having two and ten north-south columns of *WEC*s instead of one column as analyzed above, the *WEC* columns were staggered in the north-south direction so that *WEC*s in adjacent columns were not blocked by the *WEC* to the seaward side. The results are shown in Figures 13 and 14, and the conclusion is that a two column *WEC* field also has little impact shoreward, while the ten column *WEC* field is starting to have an impact outside the surf zone. The *WEC* developer and environmentalist are likely on the same side of this issue, because the *WEC* developer does not want to place the *WEC*s in areas where the *EFD* has been diminished shoreward. The possible combination of *WEC* geometries to optimize total *EFD* output and minimize *WEC* environmental impact shoreward of the *WEC* position are almost infinite, but the *WHEAT* tool developed here will be critical for both the *WEC* developer and environmental agency to agree on a final geometry.

Figure 9: Significant Wave Height (H_s) resulting from a *SWAN* run for 10 *WEC*s of 9m diameter and spacing of 100m between adjacent *WEC*s, showing little impact

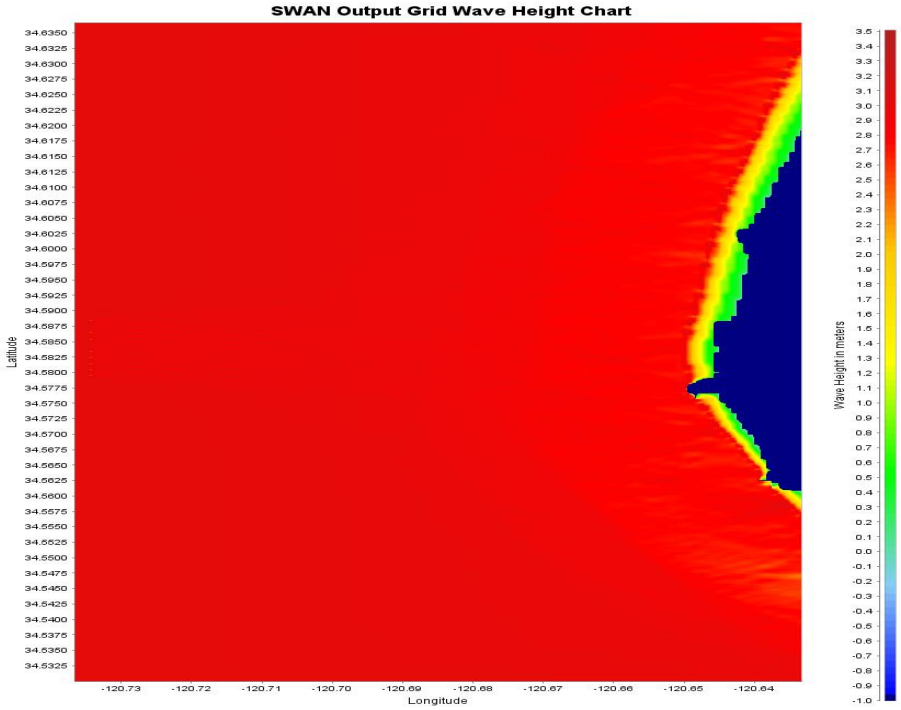

Figure 10: Zoomed plot of H_s from Fig. 12 showing peaks and nulls in the H_s field

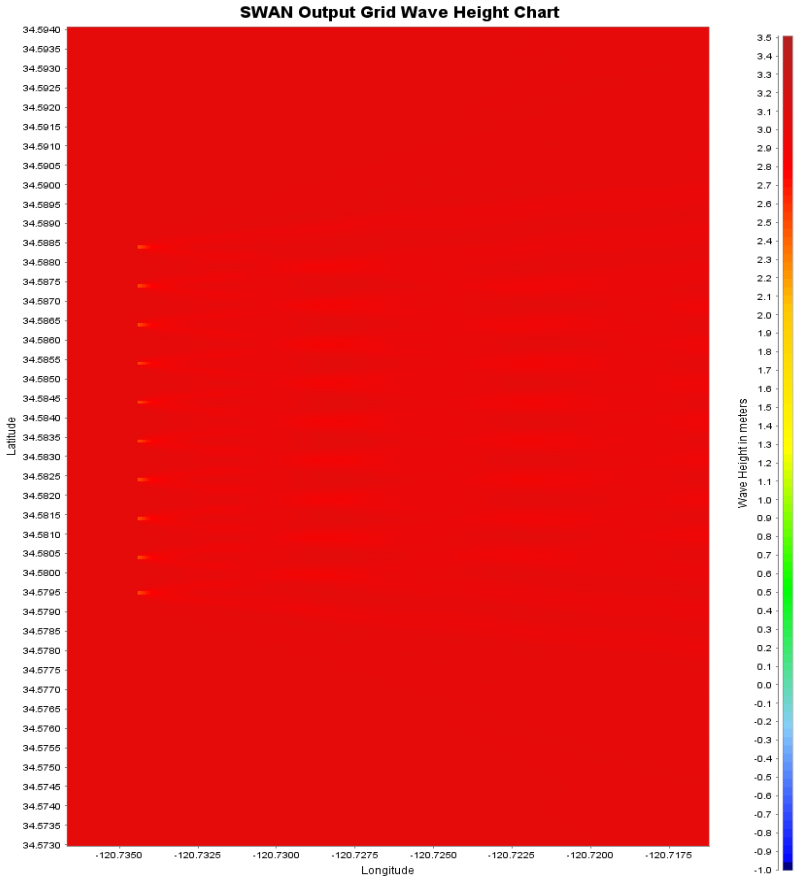

The authors speculate that for this location near VAFB a point absorber *WEC* field of 5 columns of 30 *WEC*s each would be a reasonable initial starting point that would optimize *WEC* output power and minimize impact on the wave environment shoreward of the *WEC* field. If each *WEC* had a rated output at a 3.0m H_s of 200 kW and a capacity factor of 20%, the output power at the *WEC* location would be 6 MW produced in a 3.0 x 0.5 = 1.5 km^2 area of ocean. There is an almost endless supply of offshore wave energy north of Point Conception that has minimal impact on the ocean environment.

The area off Moro bay is very similar to the *SWAN* runs made for VAFB, and there is no need to show redundant data. Also, a line absorber such as Pelamis can be modeled as a series of point absorbers using the *WHEAT* tool for the *SWAN* runs, and the Pelamis north-south spacing in the North Portugal project is so large (for safety reasons) that no detrimental ocean wave impact will occur.

Finally, the part-load problem has been addressed by Beyene and Wilson (2006(b)), and one only needs to know the specific *WEC* capacity factor variation as a function of wave height and direction from the *WEC*'s "resonance wave height". Then a *WEC* developer could use the

WHEAT tool to estimate the *WEC* field output by season throughout the year given the measured wave tri-statistics (wave height, direction, and period).

Figure 11: Energy Flux Density (kW/m) resulting from a *SWAN* run for 10 *WEC*s of 9m diameter and spacing of 100m between adjacent *WEC*s

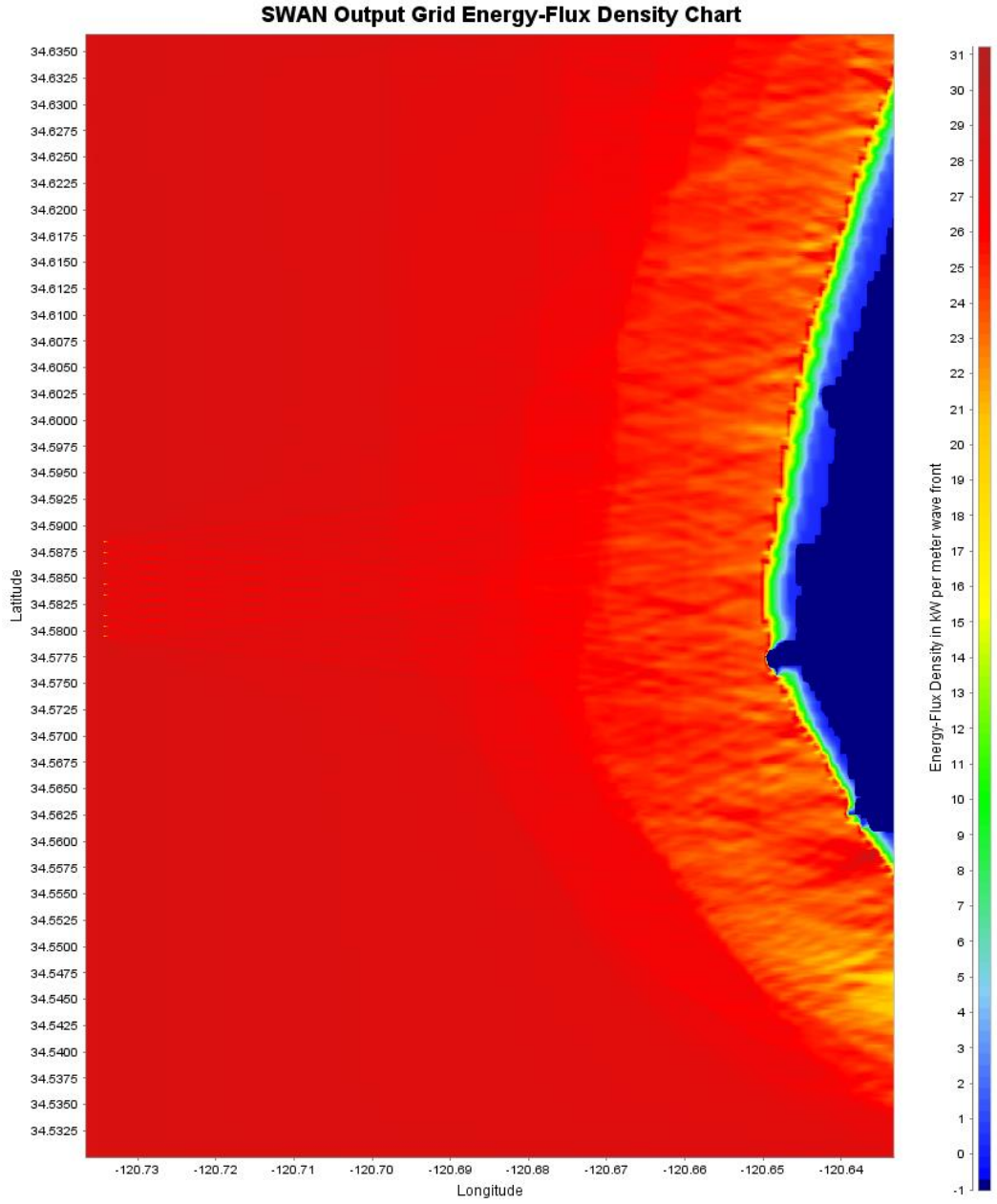

Figure 12: Zoomed plot of *EFD* from Figure 13 showing peaks and nulls in the *EFD* field

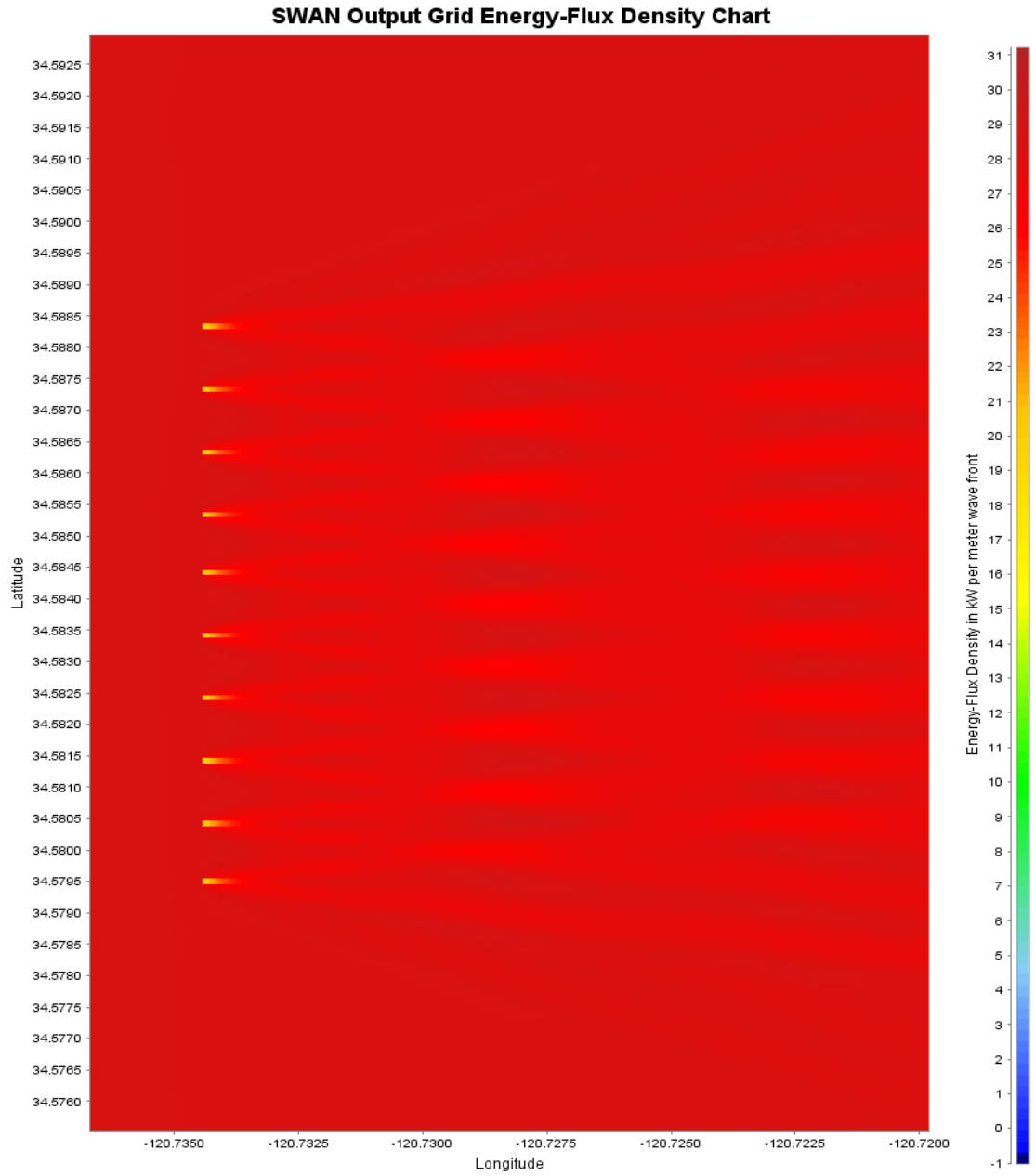

4.5.2 Tools for Large Wave Event Probability and Accurate 72 Hour Forecasts

Wavewatch III and *SWAN* are run every 6 hours on large computers at the Navy's Fleet Numerical and Meteorological Oceanographic Center (FNMOC) in Monterey CA. The problem with *SWAN* that was solved by this effort was the "User Unfriendliness" of it for the *WEC* user who needs to run *SWAN* for numerous scenarios on a PC with various *WEC* fields inserted into the *SWAN* wave propagation path. The FNMOC model runs are not useful for the *WEC* analyst, but are very good for 6 to 72 hour wave forecasts. To the authors' knowledge, FNMOC has never forecasted a 15m significant wave height 4 or 5 miles off shoe near the California coast.

Figure 13: Energy Flux Density (kW/m) resulting from a *SWAN* run for two North-South Columns of 10 *WEC*s each with 9m diameter and spacing of 100m between adjacent *WEC*s

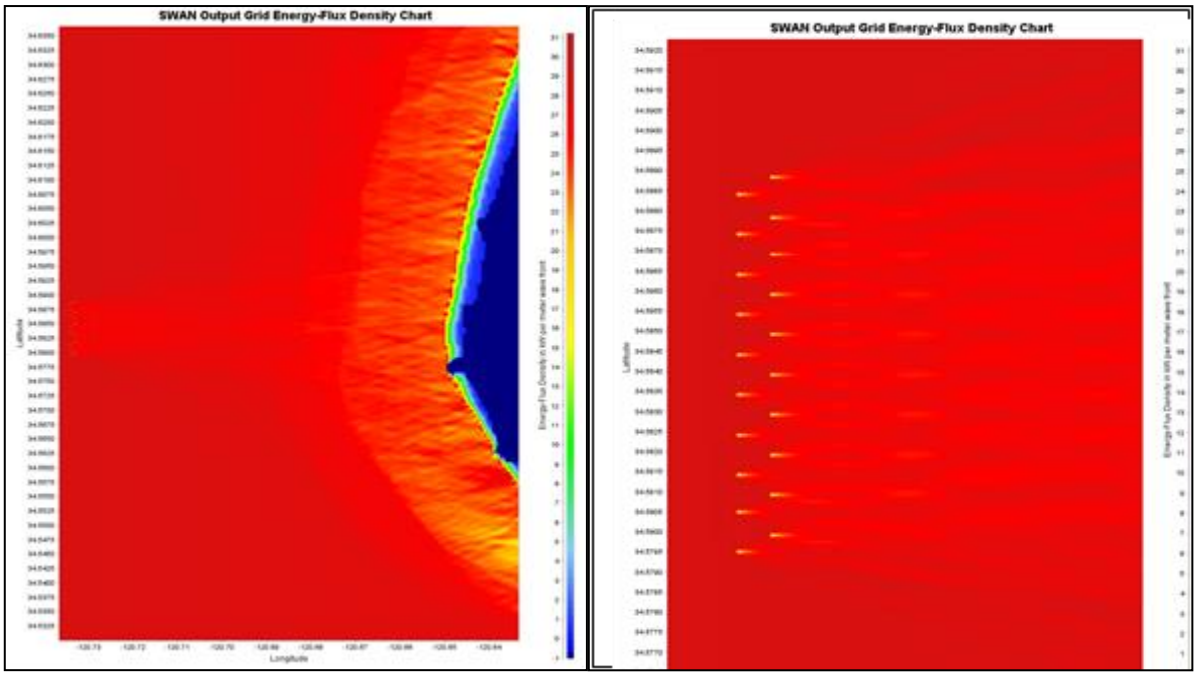

Figure 14: Energy Flux Density (kW/m) resulting from a *SWAN* run for ten North-South Columns of 10 *WEC*s each with 9m diameter and spacing of 100m between adjacent *WEC*s

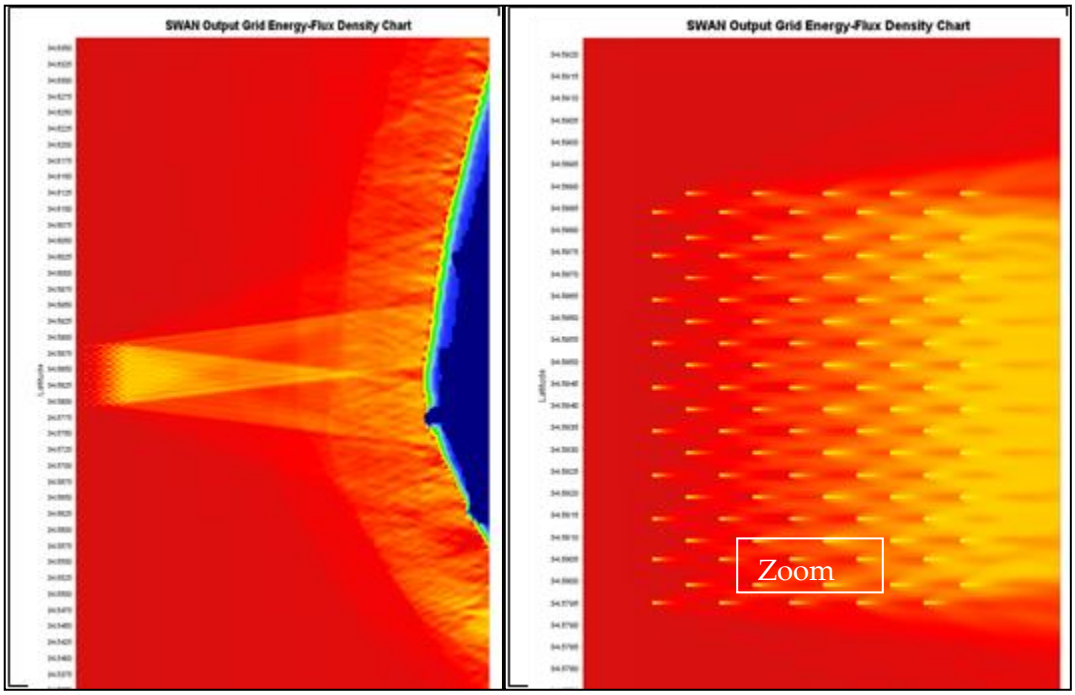

Jove Sciences, Inc. has been working with an Australian Company to address the large wave issue by using a very innovative camera system that accurately estimates actual wave height near a buoy mounting at sea or a shore mounting near the surf zone. Every *WEC* installation of the future should have a set of buoys deployed seaward of the *WEC* location, as well as in the *WEC* location, so that early warning of large approaching waves can be transmitted in time for the *WEC*s to be secured for high seas.

4.6 Sediment Side Modelling

Sediment can be accounted for in *ROMS* using options based on the *CSTM* software. The model is initialized with a user-defined number of bed layers having user-defined thicknesses. The user also defines a changeable number of sediment classes, each class having defined characteristics such as grain size, porosity, etc. When the critical shear stress is exceeded at the bottom boundary, erosion occurs. When the shear stress drops below a user-defined threshold, deposition occurs. New layers are formed when deposited material exceeds a user-defined thickness. The number of layers is held constant by merging or dividing the bottom layer as necessary (Warner, 2008). A depiction of the model processes is shown in **Error! Reference source not found.**. The model is capable of handling both cohesive and non-cohesive sediment types (mud and sand). Important user inputs include the thickness required to create a new layer, initial bed conditions, as well as median grain diameter, suspended sediment concentration, grain density, settling velocity, erosion rate, critical shear stress, and porosity for each sediment class.

Figure 15: CSTM Sediment Model, [Warner et al, 2008]

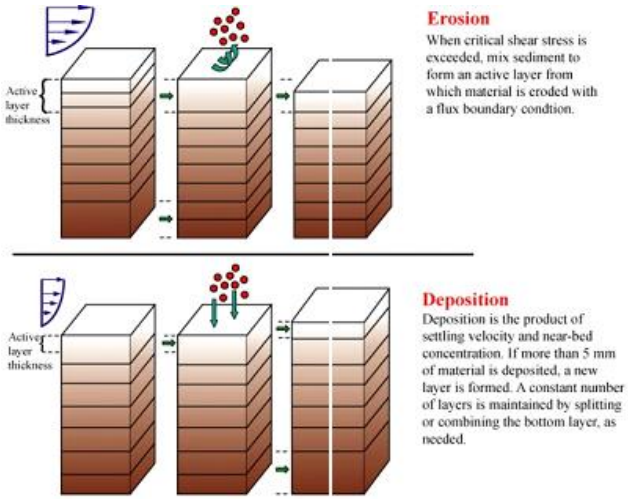

4.6.1 Oceanographic Concepts

Coastal sediment processes are a subset of general sediment processes in which stresses at the interface of a fluid and the bed beneath it combine with fluid flows to result in the erosion, suspension, transport and deposition of sediment. A combination of forces from currents and waves acts to erode sediment and carry the suspended particles, resulting in morphological

changes. These processes can be affected by artificial structures such as *WEC*s [Nam et al]. Sediment patterns can have environmental impacts in coastal areas including water quality and beach erosion.

4.7 Model Coupling

Coupling in *COAWST* is achieved using the Model Coupling Toolkit *(MCT). MCT* is a parallel software protocol using message passing interfaces to facilitate two-way coupling between *ROMS* and *SWAN*. *MCT* handles the allocation of processors, transfer of data between models, and interpolation of transferred data fields. A schematic of the model coupling with transferred data types is shown in Fig. 16.

Figure 16: Schematic of Model Coupling

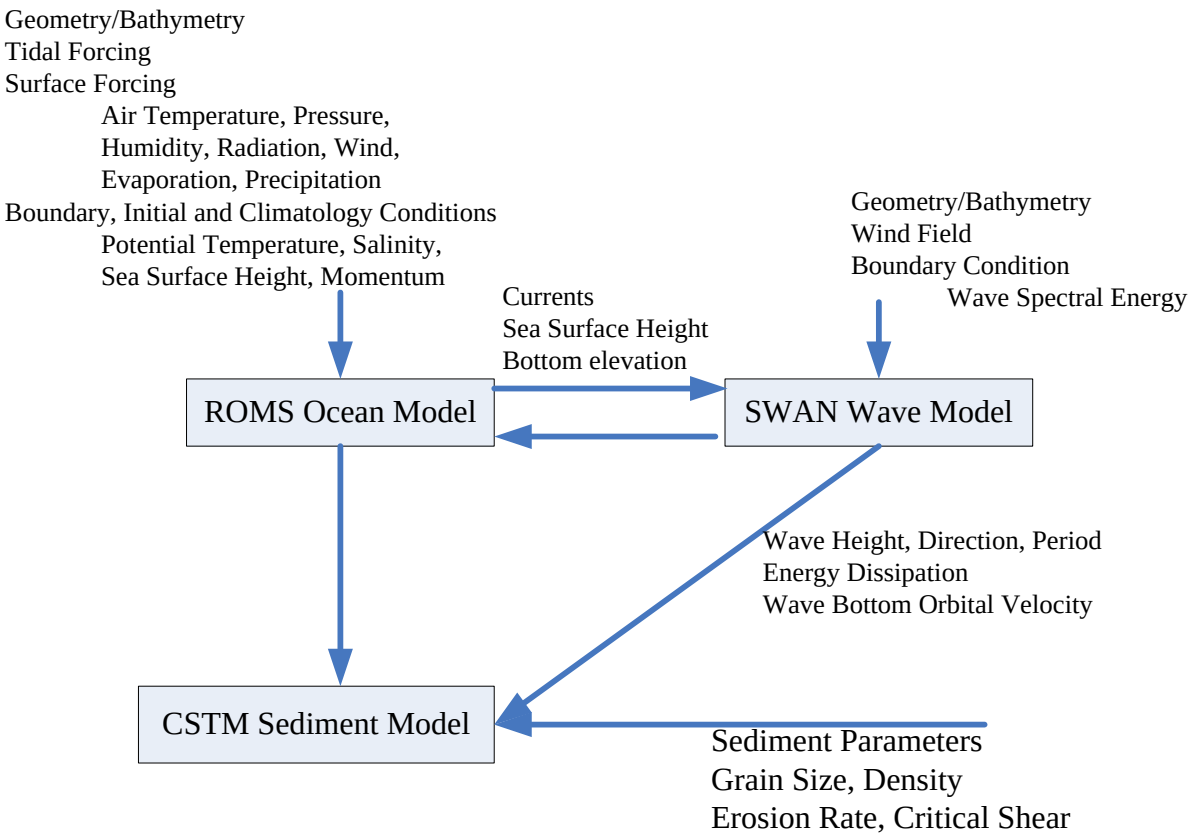

4.8 Case Study

4.8.1 Wave Side

The researchers choose a contour of 100m depth just west of the city of San Diego, California, USA. The depth contour is confined to lie between latitudes of 32.48°N and 32.74°N, shown in Fig. 17. *SWAN* was used to model the wave resource over one full year at this contour. The resulting energy profile along the contour was then, and ultimately used to implicate possible sediment transport capacities.

Figure 17: Bathymetric (depth) Data for the Proposed Domain of Interest. Solid Line Indicates 100m Depth Contour

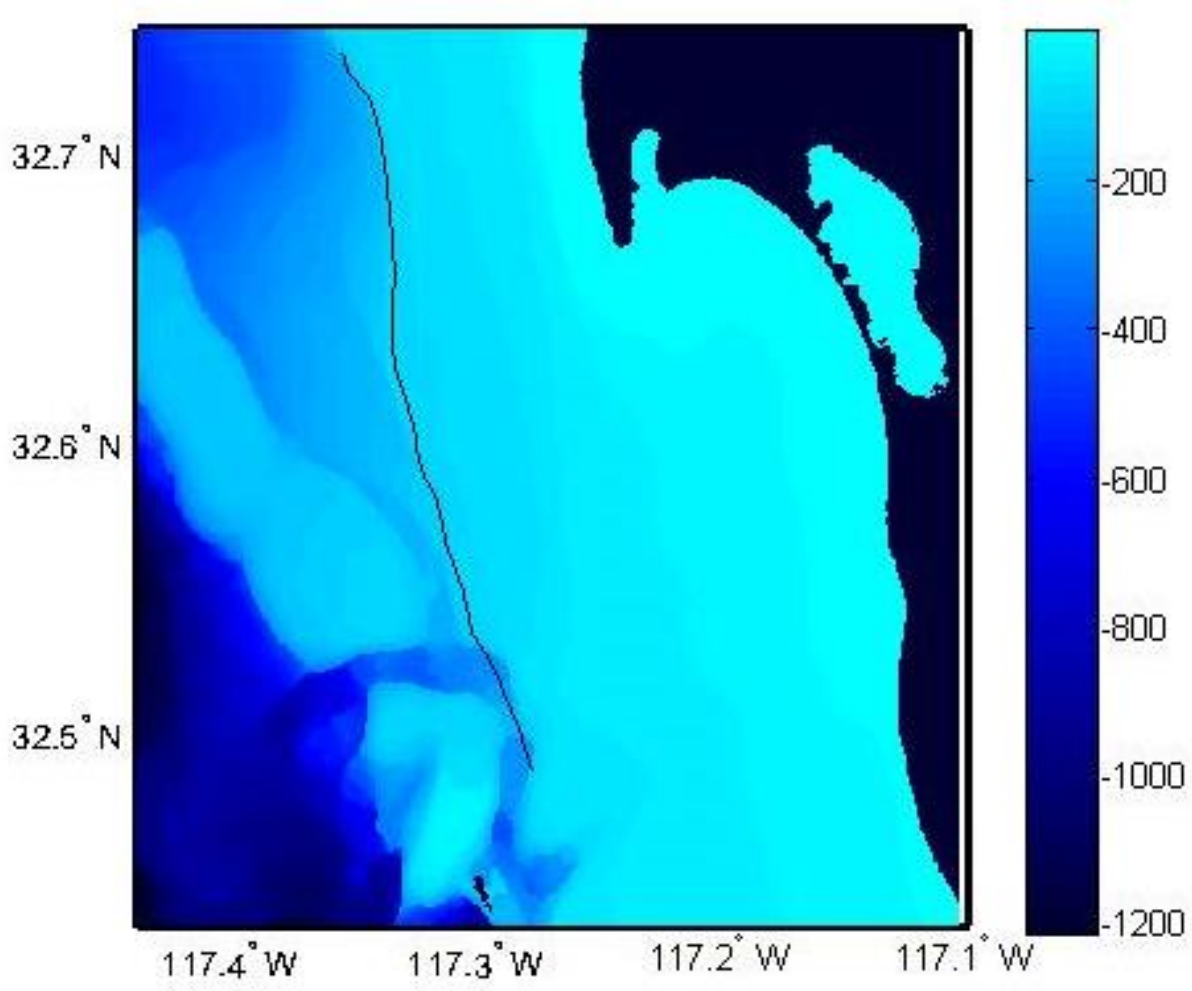

In order to accurately predict wave energy potential, the researchers solve over the entire domain of interest and average over the entire calendar year of 2010. The wind field input used was six hour interval, 0.25° resolution, 6-satellite blended data from the National Climactic Data Center (*NCDC*). This data required a small amount of interpolation. Wave boundary conditions are obtained from three hour interval Wavewatch III hindcast data from the Marine Modeling and Analysis Branch (*MMAB*) of the Environmental Modeling Center (*EMC*) of the National Center for Environmental Prediction (*NCEP*). This is full discrete spectral data for all directions and frequencies from 0.0412 Hz to 0.406 Hz, for three points: 32.43°N -117.33°W, 32.63°N -117.44°W and 32.75°N -117.37°W. The bathymetric data is 1-arcminute resolution *ETOPO1* model data obtained from the National Geophysical Data Center (*NGDC*). Water level data is obtained from the National Ocean Service (*NOS*) Center for Operational Oceanographic Products and Services (*CO-OPS*) for station number 9410230. The resulting system was simulated on a laptop equipped with an Intel Core 2 Duo T6500 processor with 4GB of RAM,

utilizing a grid resolution of 20x22. With a time step value of 3 hours, the entire simulation required around 30 hours of CPU time. A typical *SWAN* command file is shown in Appendix 2.

SWAN can calculate and output various bulk parameter data such as H_{m0}, P/l, and various forms of characteristic period and direction, as well as spectral data $G(\sigma,\theta)$, at user selected points. To sum up the resource the researchers perform a line integral on the total energy transport across the 100m contour. Thirty-four points, equally spaced between 32.48°N and 32.74°N are sampled, and the annual average wave power across each of the i=33 line segments is calculated as:

$$P_{avg,i} = \frac{s_i}{2920}\sum_{n=1}^{2920}\left(\left(\frac{P}{l}\right)_{i,n} + \left(\frac{P}{l}\right)_{i+1,n}\right)/2 \qquad (19)$$

where i is the index of line segments, from 1 to 33, n is the time step of each run, from 1 to 2,920 and s is the line segment length.

The *WEC* efficiencies and the wave farm have been condensed to single values rather than a set of various values for different conditions. This is because of the lack of validated data for varying operating conditions. These values and the electrical and water capacity values calculated using them should be seen as a yardstick giving ranges for the potential of different technologies.

4.8.2 SWAN Output

Was generated for a grid coincident with the computational and bathymetric grids, as well as along a 100m depth contour line. Figure 18 shows a typical significant wave height (scaled by color), which was relatively constant over the domain at around 3.3m. The arrows point in the mean wave direction and are scaled by the average wave period.

Figure 18: Significant Wave Height and Direction

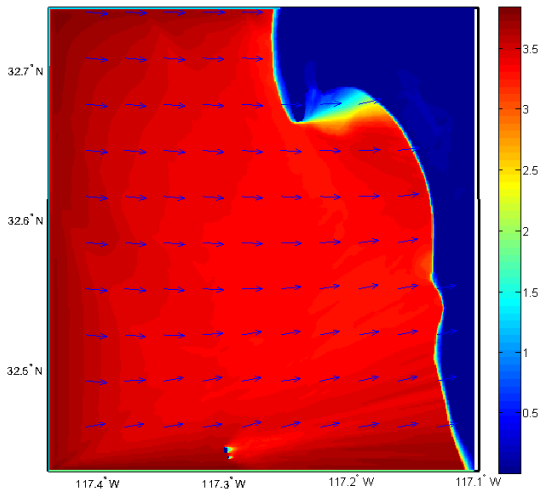

To show the annual variation in H_{m0}, the researchers chose one point of interest along the 100m depth contour, at 32.69°N 117.34°W, and present the *SWAN* output for significant wave height

at that point throughout the year (Figure 19). Figure 20 shows the total wave energy per meter of wave crest at this location throughout the year.

Figure 19: Significant Wave Height Over the Calendar Year 2010 at 32.69°W 117.34°W

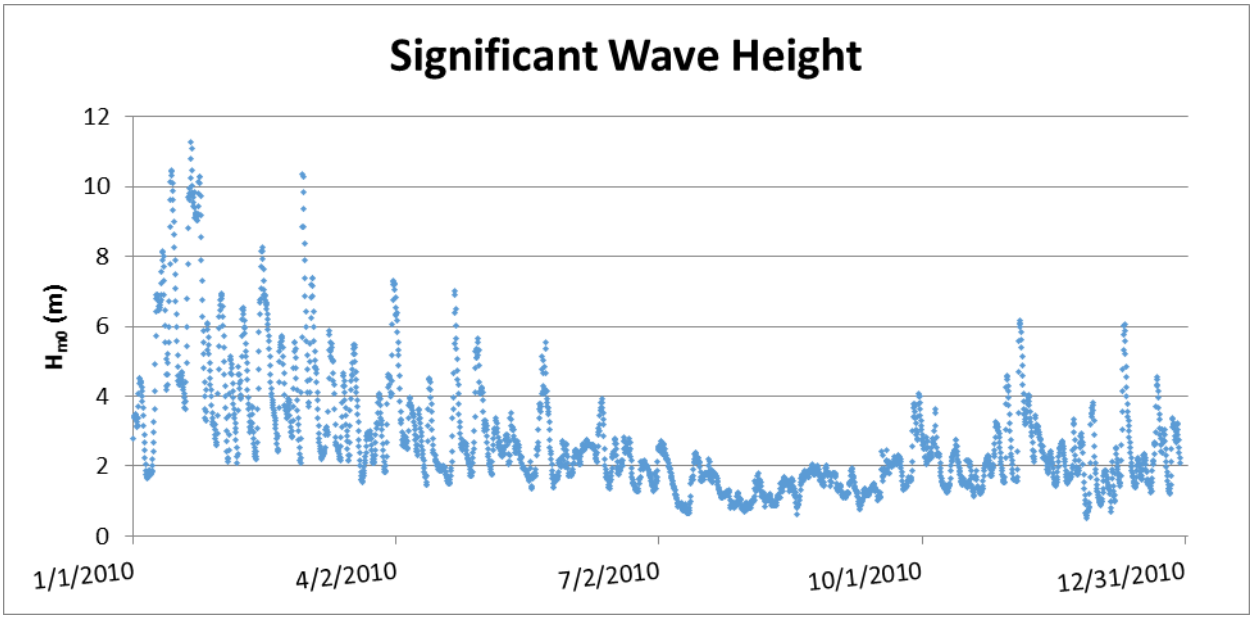

Figure 20: Wave energy over the calendar year 2010 at 32.69°W 117.34°W

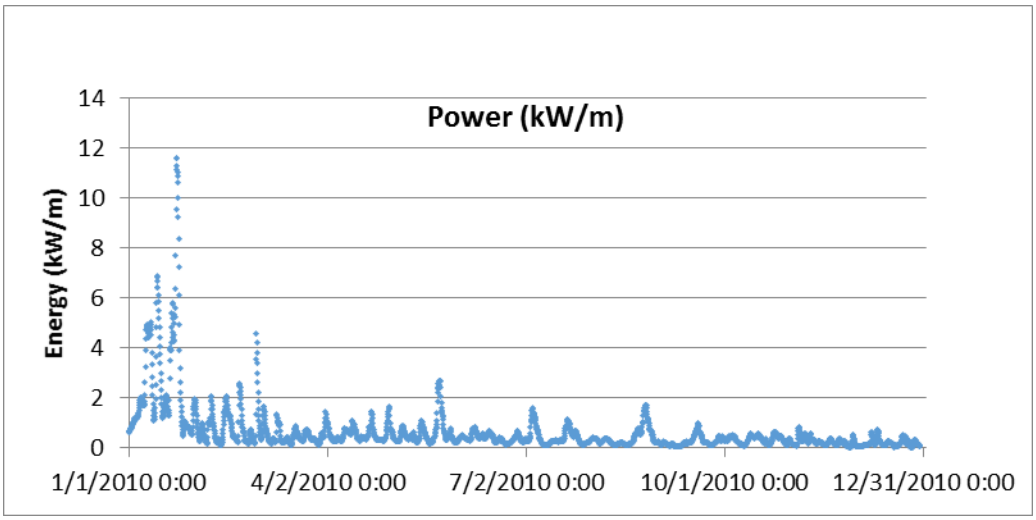

Figure 21 shows a typical snapshot of the energy density spectrum at this location, showing both a narrow banded low frequency swell and higher frequency wind waves. Figure 22 shows a typical snapshot of the directional energy spectrum for this location. Figure 23 shows the power along the 100m contour; the average is around 2.9 kW/m. In fact, this is much lower expected for much of the US pacific coast, as is seen in Wilson and Beyene (2007).

Figure 21: Spectral Energy Density

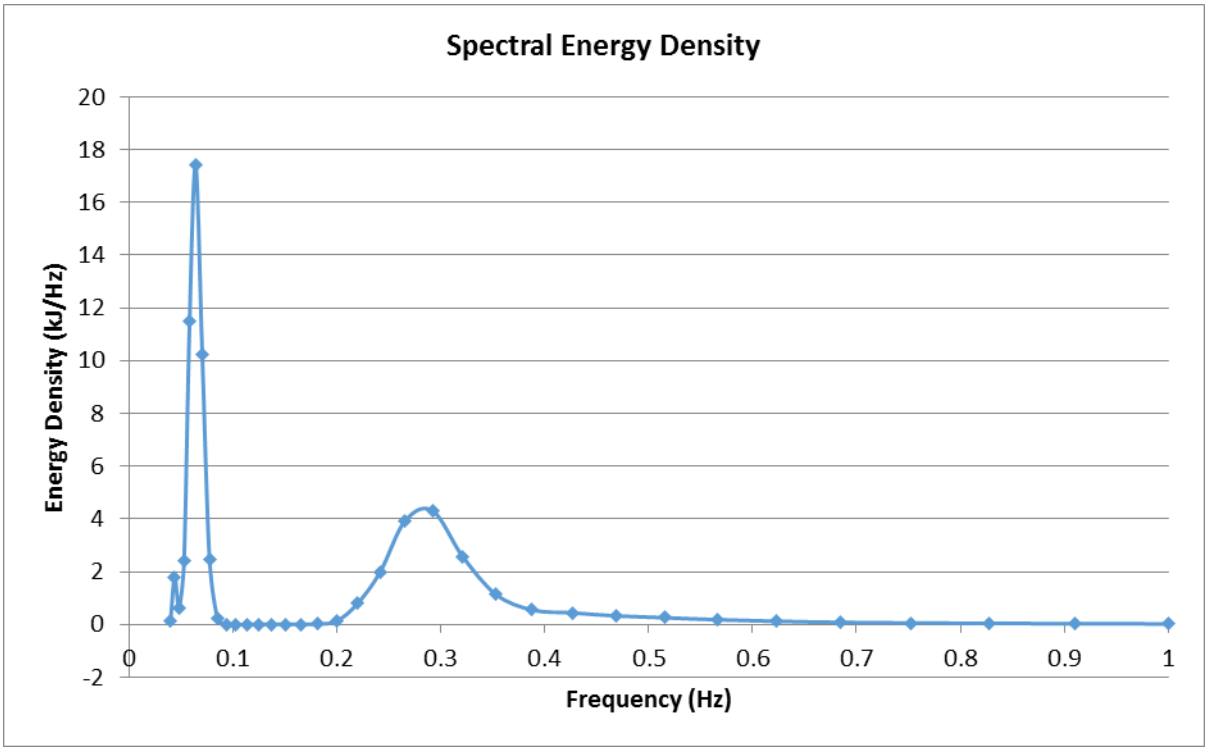

Figure 22: Directional Energy Spectrum

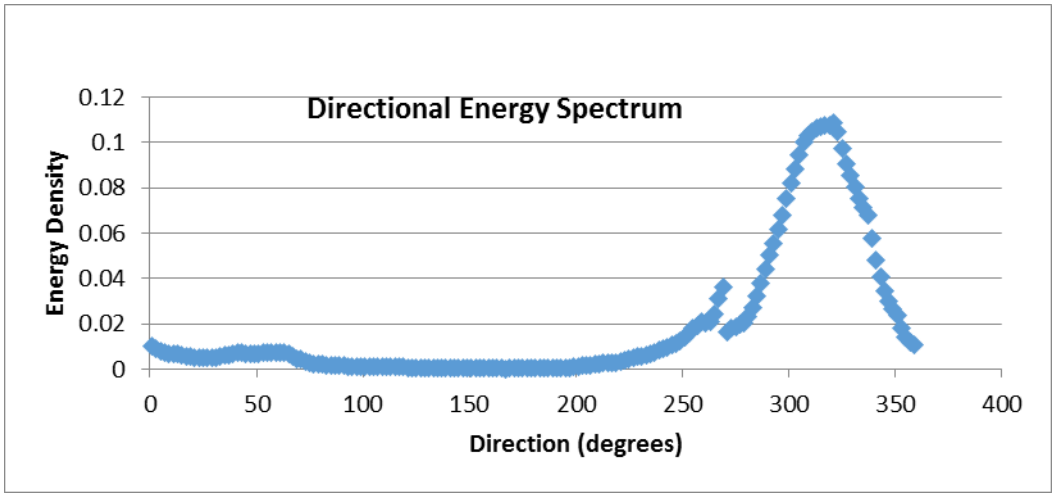

Figure 23: Available Wave Power per Meter Along 100m Depth Contour

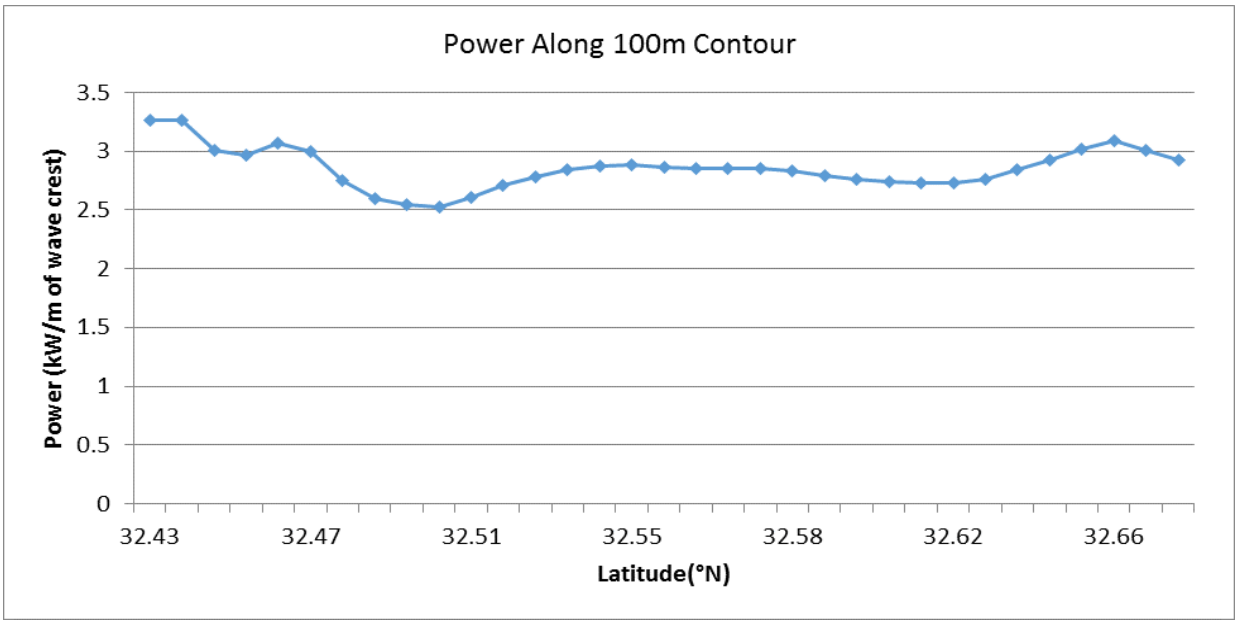

4.8.3 Impact of *WEC* Devices on Sediment Transport

A naturally occurring reef can provide a fair comparison of full energy absorber (Figure 24). In order to study the effects of *WEC*s on sediment processes, the researchers modeled the coast of Southern California using the *COAWST* coupled wave-ocean-sediment model. To study the effects of *WEC* operation on the marine environment the researchers first use *COAWST* to model a selected domain over the entire month of October, 2009. The researchers then selected a smaller subdomain whose western boundary covers the location of the wave converter placement area. The *COAWST* model is used to model the subdomain over the same time period, using the *SWAN* spectral energy output from the larger run as the wave energy boundary condition. To simulate the effects of *WEC*s, the spectral energy is reduced by a factor of 0.5 across two grid cells. Figure 25 shows the bathymetry for the model as well as the nested domain. This raw bathymetry is used for the *SWAN* model directly but is smoothed before being used for the *ROMS* grid in order to eliminate pressure gradient errors. The depth is in meters, positive down. *COAWST* output variables for both runs are then compared to evaluate the environmental impact of *WEC*s.

Figure 24: Naturally Occurring Near Full Energy Absorbing Riff

Figure 25: Raw Bathymetry and Outline of Nested Domain

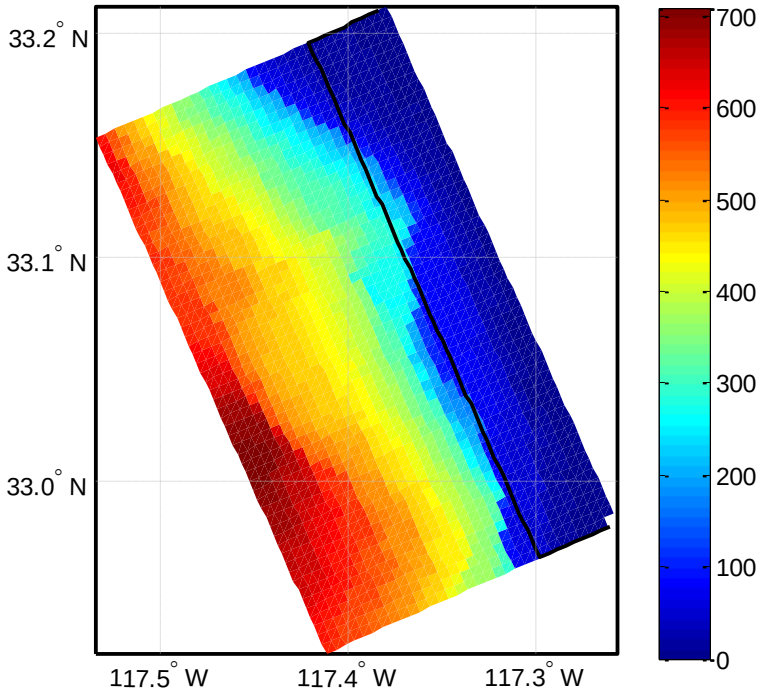

The bathymetric data used is 3-arcsecond resolution Coastal Relief Model data obtained from the National Geophysical Data Center (*NGDC*) (National Oceanic and Atmospheric Administration 2014). Forcing data including air temperature, pressure, humidity, wind, radiation flux, and rainfall rate are from the Climate Forecast System Reanalysis (*CFSR*) performed by the National Centers for Environmental Prediction (Saha 2010). Tidal forcing constituents are from the *TPXO7.2* tidal model (Egbert et al. 1994). Wave boundary conditions are obtained from three hour interval Wavewatch III hindcast data from the Marine Modeling and Analysis Branch (*MMAB)* of the Environmental Modeling Center (*EMC*) of the National Center for Environmental Prediction). The initial, boundary and climatological ocean conditions are from the *HYCOM + NCODA* Global 1/12° Analysis. The *COAWST* command files for the

larger run are shown in Appendix B and include the coupling file, the ocean file, the *SWAN* file and the sediment file.

Figure 26 shows the depth integrated current and wave heights at the 400th time step. The arrows lengths are proportional to the current velocities, and the color scale gives the wave heights in meters. The white contour lines show bottom depths in 100m increments.

Figure 26: Depth-Integrated Current

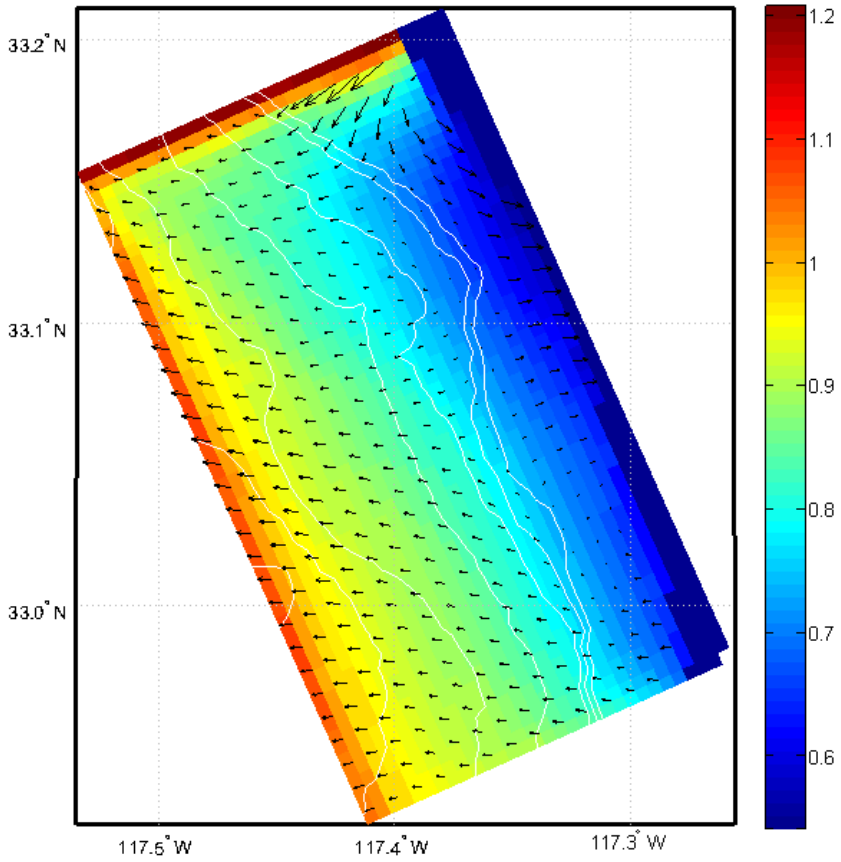

4.9 Coupled Model Results

After running the *COAWST* model over both the larger and nested domains for the selected time period, the changes in calculated wave heights, sediment bed thicknesses, water column sediment concentrations, energy density and bottom wave orbital velocity were calculated by subtracting the calculated parameters obtained from the nested run with wave energy removed, from those obtained in the original run. Figure 27 shows the difference in significant wave height, in meters, for the nested subdomain at the 410th time step. The effect of removing the energy along the western boundary can be seen clearly in the two grid cells which represent the location of the *WEC*s. Note also that the difference decreases rapidly with distance from the *WEC* location.

Figure 27: Difference in Wave Height Over Nested Domain

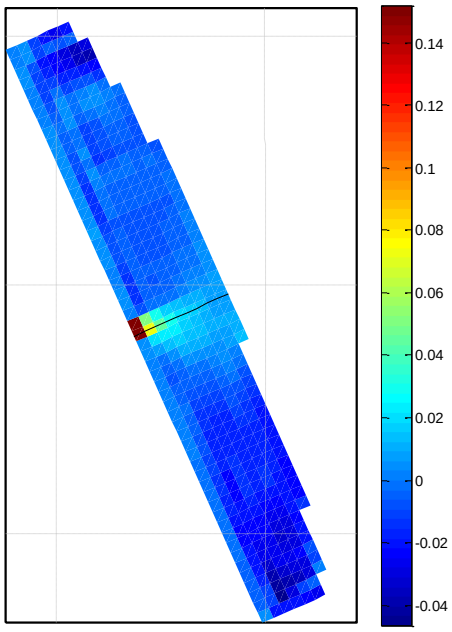

Figure 28 shows the difference in wave height at the 410th time step, in meters, along grid points with j indices equal to 29 along the η-direction. This cross section line is shown in Fig. 27. This plot shows that the effect of the *WEC*s on the amount of wave energy present decreases quickly as the wave energy propagates toward the coastline.

Figure 28: Wave Height Before and After Wave Farm

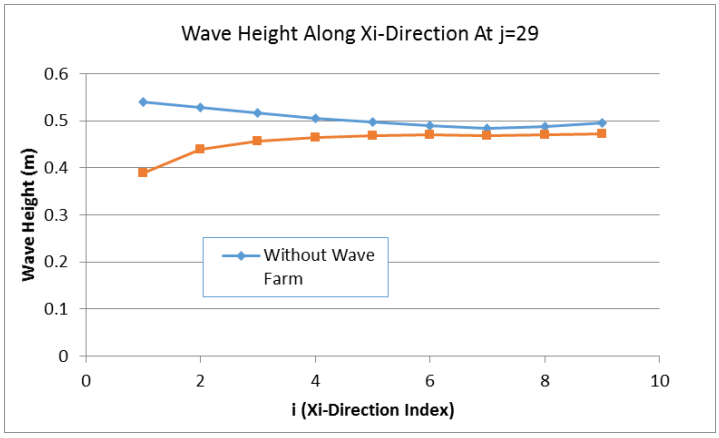

Figure 29 shows the difference in spectral energy density at 117.33°W, 33.09°N at the 410th time step, with and without the wave farm. This shows the modeled reduction in energy due to the *WEC*s shortly towards shore from the wave farm.

Figure 29: Spectral Energy Density Before and After Wave Farm

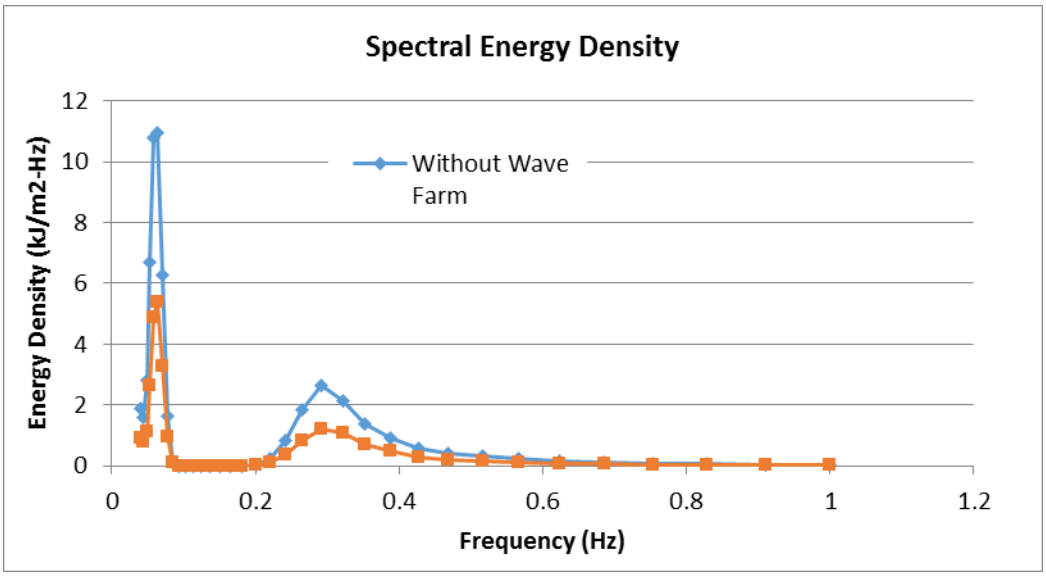

Figures 30, 31, and 32 show the energy densities, in kJ/m²-Hz-°, at the 410th time step for points at 117.36°W, 33.077400°N, 117.34°W 33.08°N, and 117.32°W 33.09°N respectively. The radial coordinates are given in Hz. These points all lie along the line shown in Figure 27. These illustrate the dominant wave period and directions associated with the highest energy densities. Note also that, for this high energy scenario, the reduction in wave energy remains significant as the energy propagates shoreward.

Figure 30: Energy density a) before wave farm b) after wave farm c) difference at 117.36°W, 33.08°N

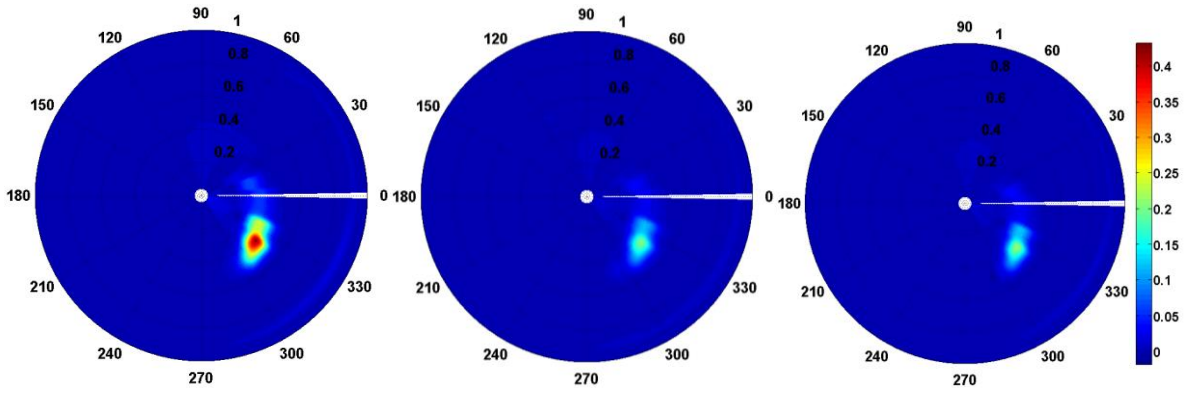

Figure 31: Energy density a) before wave farm b) after wave farm c) difference at 117.34°W 33.08°N

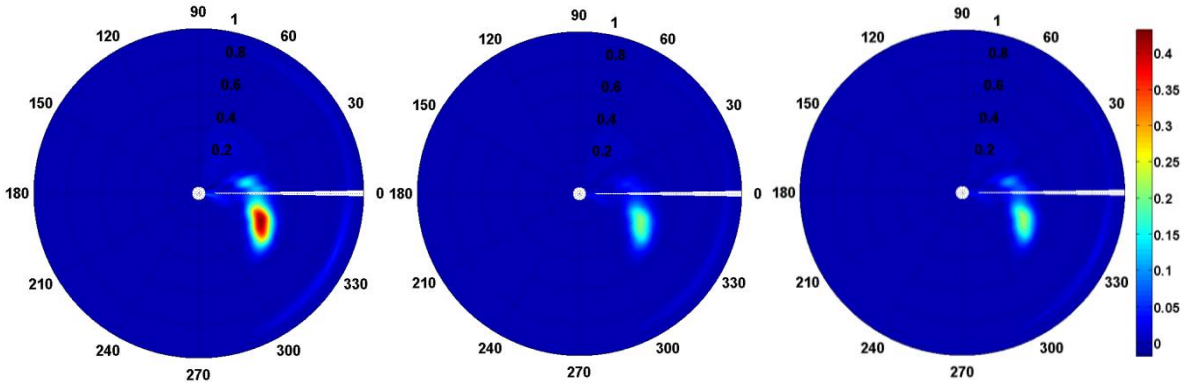

Figure 32: Energy density a) before wave farm b) after wave farm c) difference at 117.32°W 33.09°N

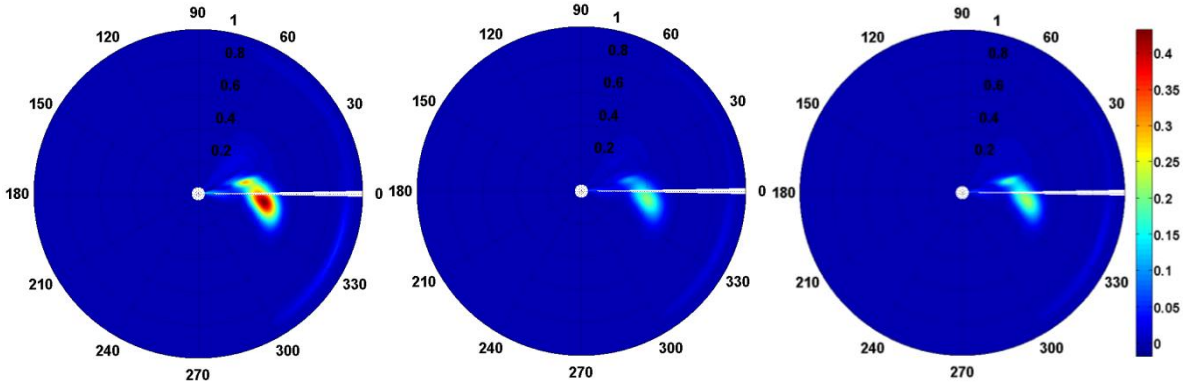

Figure 33 shows the bottom wave orbital velocity with the wave farm as a fraction of that before the wave farm. This metric is important as it represents one of the critical mechanisms by which sediment is eroded, transported and deposited. The plot clearly shows the effects of the wave farm which decrease in the direction of wave propagation. However, these effects are minor in nature, especially with increasing distance from the *WEC*s.

Figure 33: Fraction of Bottom Wave Orbital Velocity After Wave Farm

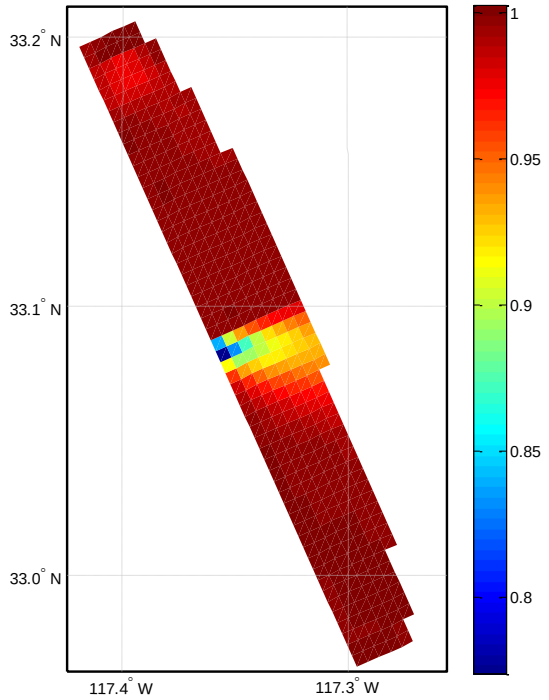

Figure 34 shows the difference in sediment bed thickness, measured in meters, for the 410th time step at the end of the month. This plot shows a slight increase in sediment deposition south of the *WEC* location, as well as a slight decrease in the vicinity of the *WEC*s. Overall, the effect of the *WEC*s on the sediment bed environment is seen to be quite small.

Figure 35 shows the difference in net sediment deposition at the 410th time step, in meters, at grid points with j indices equal to 29 along the η-direction. This cross section line is shown in Fig. 34. This graph shows that, although there is a significant difference in sediment accretion near the *WEC*s, this difference practically disappears as the wave energy moves toward the shore. It is notable that there is sediment deposition that occurs with the wave farm in areas where it did not occur without *WEC*s.

Figure 36 shows the difference in large grain size sediment concentration, in kg/m^3 for the 200th time step. The vertical cross section shown is for the row with index j=29 in the η-direction. This cross section line is shown in Figure 34. The y-axis of the plot is the depth given in meters, and the x-axis is the longitude in degrees east. This plot shows that the change in sediment concentration due to *WEC*s is confined to the lowest levels of the water column. In general one can see that the effect of the wave farm on the suspended sediment environment is very small.

Figure 34: Difference in Bed Thickness Over Nested Domain

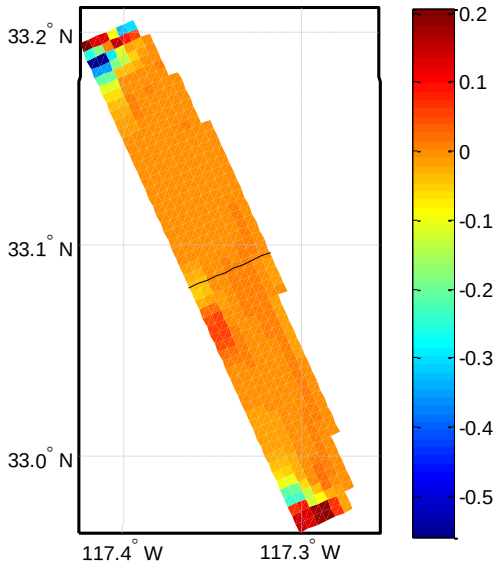

Figure 35: Sediment Deposition Before and After Wave Farm

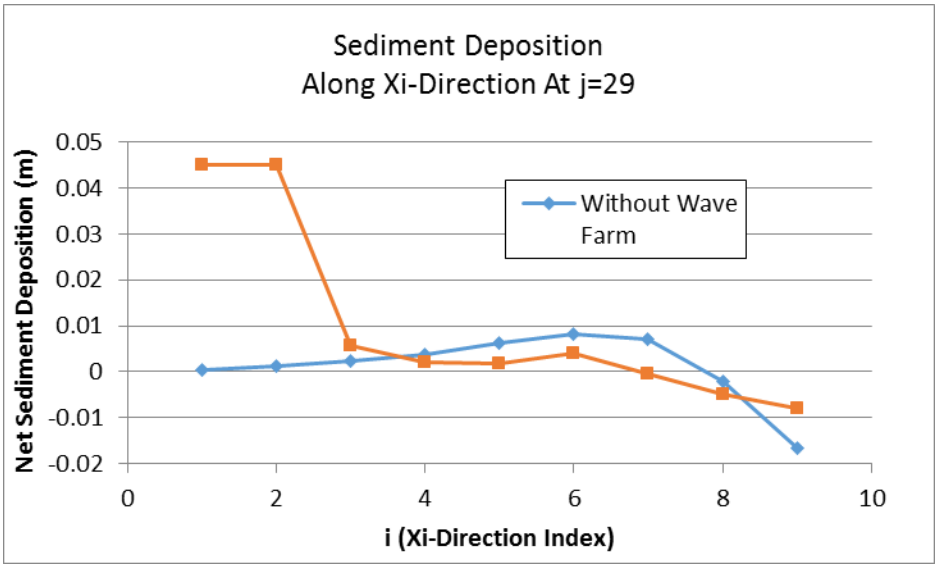

Figure 36: Difference in Large Grain Sediment Concentration over Cross Section of nested Domain

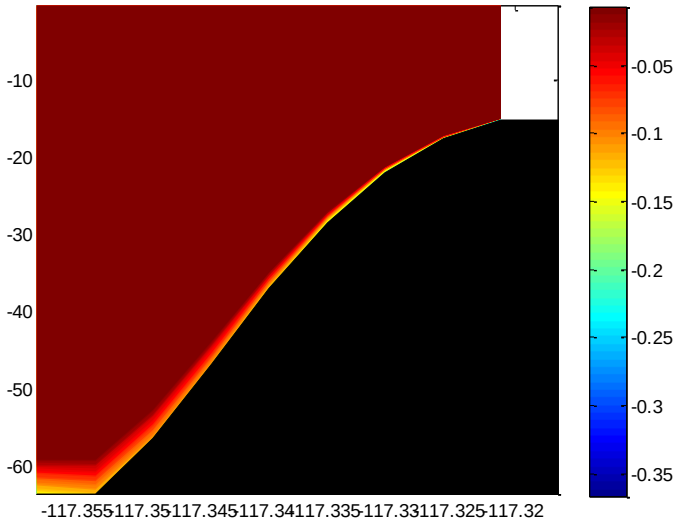

Figure 37 shows the difference in large grain sediment concentration in kg/m^3 for the 410th time step at grid points with j indices equal to 29 along the η-direction. This cross section line is shown in Figure 36. The concentrations shown are calculated at the lowest vertical grid point at each horizontal location. This graph illustrates the insignificant environmental impact of the removal of wave energy due to *WEC*s.

Figure 37: Sediment Concentration Before and After Wave Farm

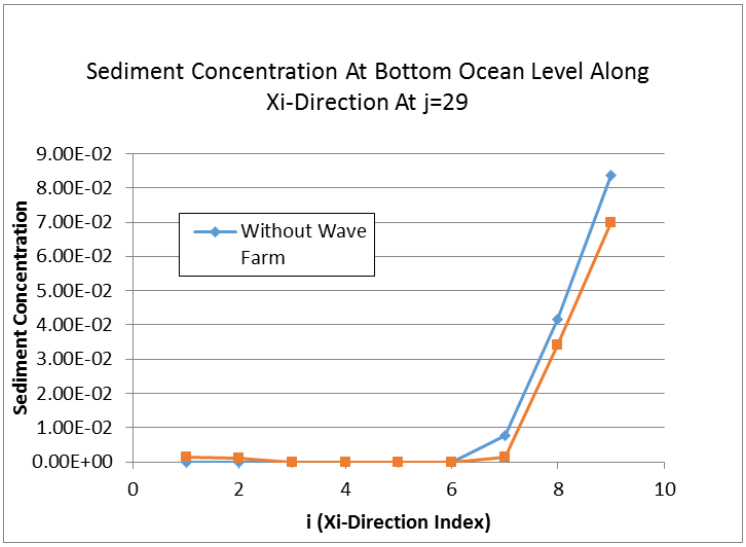

CHAPTER 5:
Summary and Conclusion

This report provides:

- a synthesis of applicable literature;
- a review and summary of current assessment tools and their performance ranges; and
- a summary of the Wave Energy Environmental Assessment Tool

To develop environmental effect assessment tool for WECs, relevant target areas that may change concentration, migration, and reproduction of sea and benthic habitat as well as the shore environment are categorized in four groups as they relate to:

- Changes in wave conditions: (height, direction, frequency) which will then impose alterations in sediment transport and deposition,
- Mechanical intrusions - of *WEC* devices and structures altering animal movements and migrations, including risks of entanglement or strike by moving parts.
- Disturbances: this may include noise during construction and operation as well as electromagnetic fields (*EMF*),
- Interferences with sea environment: toxicity of paints, lubricants, and antifouling coatings of *WEC* structures.

Under Chapter 4, the researchers present a summary of the tool developed to assess the environmental impact of power generation from *WEC*s. Table 4 summarizes the proposed environmental impact assessment tool with phases in the columns and classes of effects presented in the rows. Table 5 is a detailed presentation of phase and class of effects. Section 4.1 describes the newly developed wave parameter input tool, *WHEAT* Version 2.0, which makes it easy to insert *WEC* parameters into the wave field to assess their performance and environmental impact. The most time consuming and difficult part of the *WEC* impact assessment effort is the complexity of the *SWAN* architecture, generally regarded as one of the most user unfriendly wave models. *WHEAT* represents a very significant breakthrough toward making *SWAN* easier to use for *WEC* developers, ocean wave modelers, and environmental agencies alike.

In Section 4.2 the researchers present the sediment side modeling tool, *ROMS*. The model is initialized with a user-defined number of bed layers, each layer having defined characteristics such as thickness, grain size, porosity, etc. When the critical shear stress is exceeded at the bottom boundary, erosion occurs. When the shear stress drops below a user-defined threshold, deposition occurs. New layers are formed when deposited material exceeds a user-defined thickness. The number of layers is held constant by merging or dividing the bottom layer as necessary.

The wave and sediment modeling tools are coupled as discussed in Section 4.3. Results of the coupling technique are presented as a case study in Section 4.4.

The environmental assessment tool presented in Table 5 is designed to cover the life of the WEC system, from design stages to decommissioning, covering three sections:

1) Construction phase, (Tool 1);
2) Operation and Maintenance (Tool 2); and
3) Decommissioning phase (Tool 3).

Once the presence of undesirable environmental effect is predicted, subjective evaluation of the intensity of such effects and the validity of any mitigating factors or alternative and compromise options are not directly tied to environmental assessment tool development, hence legislative advices and decisions must be considered available parts of the assessment tool.

Finally, at least based on the case study presented in this report, it can be said that - generally the effect of a wave farm on suspended sediment environment is very small. Of the three phases, operation and maintenance should be given serious consideration because of its duration - compared to the construction and decommissioning phases.

CHAPTER 6:
Future Plan

The proposed environmental assessment tool needs to be expanded and validated. This continuation is necessary as wave energy technology is at its infancy, expecting rapid growth and evolution. This requires continuous iteration for model adaptation to accommodate latest developments. Parameter sensitivities, identification, and fine-tuning of *WEC* models for different manufacturers are needed to link manufacturer suggested parameters and generic environmental assessment tools. It would also be necessary to revise/improve assessment tools to include legislative inputs and updates, and design best case design guidelines. The most serious problem such an environmental assessment tool faces currently is lack of a field data, an operating *WEC* system in any part of the country. An operating site would not only serve as a validation for the tool, but it will also offer better understanding of wave parameters as well as provides practical engineering feedback for design improvements.

The availability and use of future *WEC* data collected from operational sites will be accessed to validate *WEC* models by different agencies, predict their stability, design improved and effective controls, etc. Eventually, communication with ASME, IEEE, and the *WEC* community is important to create and then continue refining standards and guidelines for *WEC* development.

GLOSSARY

Term	Definition
BFL	Bottom Friction Loss
CDIP	Coastal Data Information Program
CFD	Computational Fluid Dynamics
CFSR	Climate Forecast System Reanalysis
COAMPS	Coupled Oceanographic and Atmospheric Mesoscale Prediction System
COAWST	Coupled-Ocean-Atmosphere-Wave-Sediment Transport Model
CSTM	Coastal Sediment Transport Model
DIVAST	Depth Integrated Velocities And Solute Transport
EMC	Environmental Modeling Center
EMF	Electromagnetic Fields
EPA	Environmental Protection Agency
FNMOC	Fleet Numerical and Meteorological Oceanographic Center
GUI	Graphical User Interface
MCT	Model Coupling Toolkit
MMAB	Marine Modeling and Analysis Branch
NCEP	National Centers for Environmental Prediction
NDBC	*National Data Buoy Center*
NGDC	National Geophysical Data Center
OWC	OWC
PTO	Power Take Off
RFD	Energy Flux Density
RefDif	Refraction/Diffraction Model
ROMS	Regional Ocean Modeling System
SWAN	Simulating *WAves* Nearshore
TAPCHAN	Tapered Channel

VAFB	Vandenberg Air Force Base
WEC	wave energy conversion
WAMIT	Wave Analysis MIT
WHEAT	Wave Height and Energy Automation Tool
WRF	Weather Research and Forecasting

REFERENCES

Ahmadian R. and Falconer A.R. (2012). Assessment of array shape of tidal stream turbines on hydro-environmental impacts and power output, *Renewable Energy* 44. Pages 318-327.

Airas S. and Rapp H.T. (2003). Correlations between environmental gradients and the abundance of selected marine invertebrates. Institutt for Fiskeri-or Marinbiology Rapport. 7 28 pages.

Alongi, D.M. and Tenore, K. R. (1985). Effects of detritus supply on trophic relationships within experimental benthic food webs. I. Meiofauna-polychaete (Capitella capitata [type11 Fabricius) interactions. J. Exp. Marine Biology and Ecology 88: 153-166.

Arakawa A. and Lamb V. (1977). Computational design of the basic dynamical process of the UCLA general circulation model, *Methods in Computational Physics,* vol. 17, pp. 173-265.

Babarit A., Hals J., Muliawan M., Kurniawan A., Moan T. and Krokstad J. (2012). Numerical benchmarking study of a selection of wave energy converters, *Renewable Energy,* vol. 41, pp. 44-63, 2012.

Bedard R, Jabobsen T.P, Previsic M, Musial W., and Varley R. (2010). An overview of ocean renewable energy technologies, *Oceanography* 23(2):22–31, http://dx.doi.org/10.5670/oceanog.2010.40.

Benoit M., Marcos F., and Becq F. (1996). Development of a third-generation shallow-water wave model with unstructured spatial meshing. *Proc. 25*th Int. Conf. Coastal Engineering, ASCE, Orlando, 465-478.

Beyene A. and Peffley J. (2009). Constructal Theory, Adaptive Motion and Their Theoretical Application to Low Speed Turbine Design, American Society of Civil Engineers, *Journal of Energy Engineering, Vol. 135, No 4, Pages 112-118, Dec.*

Beyene A. and Wilson J. (2003). California Wave Energy Resource Study, Final submitted to California Energy Commission, Sacramento, California.

Beyene, A. and Wilson J. (2005). Wave Energy Capacity and Part-load Operation, Sea Technology, pp 45-48.

Beyene A. and Wilson J. (2006a). Parameter Variation and Part-load Efficiencies of Wave Energy Conversion, American Society of Civil Engineers (ASCE*), Journal of Energy Engineering*, April Vol. 132: 1, p. 15.

Beyene, A. and Wilson J. (2006b). Comparison of Wave Energy Flux for Northern, Central, and Southern Coast of California Based on Long Term Statistical Wave Data, Energy: the International Journal, Elsevier, Vol. 31, p. 1520-1533.

Beyene A. and Wilson J. (2007). Digital Mapping of California Wave Energy Resource, *International Journal of Energy Research*, Vol. 31, page 1156-1168.

Beyene A. and Wilson J. (2008). Wave Energy Conversion: Prospects and Challenges, *Sea Technology*, Vol. 49, No. 5, page 43-46.

Black, K.P., ASR Ltd, (2007). Marine Consulting and Research, Review of Wave Hub Technical Studies: Impacts on inshore surfing beaches. Report for the South West of England Regional Development Agency.

Boehlert W.G., McMurray R.G., and Tortorici E.C., editors. (2007). Report on Ecological Effects of Wave Energy Development in the Pacific Northwest. A Scientific Workshop, October 11–12, 2007. National Oceanic and Atmospheric Administration. http://farallones.noaa.gov/manage/pdf/sac/13_02_workshop/wave_energy.pdf. Accessed Feb. 2014.

Booij N., Ris C.R., and Holthuijsen H.L. (1999). A third-generation wave model for coastal regions, Part I, Model description and validation, *J.Geoph.Research*, 104, C4, 7649-7666.

Bredmose H., Peregrine H., Bullock G., Obhrai C., Muller G., and Wolters G., Extreme wave impact pressures and the effect of aeration. (2004). International Workshop on Water Waves and Floating Bodies, abstract. http://www.iwwwfb.org/Abstracts/iwwwfb19/iwwwfb19_04.pdf. Accessed Dec. 2013.

Briganti, R., Musumeci, R. E., Bellotti, G., Brocchini, M., and Foti, E. (2004). Boussinesq modeling of breaking waves: Description of turbulence. *J. Geophys. Res*., 109, C07015

Budal K., Falnes J., Iversen C.L., Lillebekken M.P., Oltedal G., Hals T. and Høy S.A (1982). The Norwegian wave-power buoy project, Proc. Of the 2nd Symposium on Wave Energy utilization, Trondheim, Norway, (ISBN 82-519-0478-1).

Boaventura D., Re P., Fonseca C.L, and Hawkins S.J. (2002). Intertidal rocky shore communities of the continental Portuguese coast: analysis of distribution patterns, *Marine Ecology* 23, 69-90.

Bower, B. and Turner, R.K., (1998). Characterizing and analyzing benefits from integrated coastal zone management. *Ocean and Coastal Management* 38, 41-66.

Callaway, Ewen. (2007). Energy: To catch a wave. *Nature* ***450****, 156-159.* November 7. http://www.nature.com/news/2007/071107/full/450156a.html. Accessed Feb. 2014.

Caswell, H. (1978). Predator-mediated coexistence: a nonequilibrium model. *Am. Nat*., 112, 127–154.

Clauss G., Stutz K., and Schmittner C. (2004). Rogue wave impact on offshore structures, Offshore Technology Conference, Houston, Texas, U.S.A., 3-6 May.

Clément A., McCullen P., Falcão A., Fiorentino A., Gardner F., Hammarlund K., Lemonis G., Lewis T., Nielsen K., Petroncini S., Pontes T.M., Schild P., Sjöström O.B., Sørensen C.H. and Thorpe T. (2002). Wave energy in Europe: current status and perspectives, *Renewable and Sustainable Energy Reviews,* vol. 6, pp. 405-431.

Dalton G., Alcorn R. and Lewis T. (2010). Case study feasibility analysis of the Pelamis wave energy convertor in Ireland, Portugal and North America," *Renewable Energy,* vol. 35, pp. 443-455.

Davies P. (2005). Wave-powered desalination: resource assessment and review of technology, *Desalination,* vol. 186, pp. 97-109.

Dolman S. and Simmonds M. (2010). Towards best environmental practice for cetacean conservation in developing Scotland's marine renewable energy, *Marine Policy* 34 1021–1027.

Egbert, D.G., Bennett F.A .and Foreman G.G.M. (1994). TOPEX/POSEIDON tides estimated using a global inverse model, "*Journal of Geophysical Research: Oceans,* vol. 99. pp. 24821-24852.

Falcão F.D. (2010). Wave energy utilization: A review of the technologies," *Renewable and Sustainable Energy Reviews,* pp. 899-918.

Falnes J. (1993). Research and development in ocean-wave energy in Norway". In: *Proceedings of International Symposium on Ocean Energy Development*, 26-27 August, Muroran, Hokkaido, Japan, (ed. H. Kondo) pp 27-39.

Fankhauser, S. (1995). Valuing Climate Change: the Economics of the Greenhouse. , London: Routledge. 194 pages.

Frid C., Andonegi E., Depestele J., Judd A., Rihan D., Rogers S., and Kenchington E. (2012). The environmental interactions of tidal and wave energy generation devices, *Environmental Impact Assessment Review* 32 133–139.

Gomes R., Henriques J., Gato L. and Falcão A. (2012). Hydrodynamic optimization of an axisymmetric floating oscillating water column for wave energy conversion, *Renewable Energy,* vol. 44, pp. 328-339.

Graham N.E. and Diaz H. (2001). Evidence for intensification of North Pacific winter cyclones since 1948. *Bull Am Meteorol Soc* 82:1869–1893.

Grant J.A., Bryden I., McGregor G.P., Stallard T., Swales K.J., Turner K., and Wallace R. (2008). Concurrent and legacy economic and environmental impacts from establishing a marine energy sector in Scotland, *Energy Policy* 36 2734– 2753.

Griffies S.M., Böning C., Bryan O.F., Chassignet P.E., Gerdes R., Hasumi H., Hirst A., Treguier M.A. and Webb D., (2000). Developments in ocean climate modelling, *Ocean Modelling,* vol. 2, pp. 123-192.

Haab C. T. and McConnell E. K. (2002). Valuing Environmental and Natural Resources: The Econometrics of Non-Market Valuation. Edward Elgar Publishing. Cheltenham, U.K. 326 pages.

Haas K. A. and Warner J. C. (2009). Comparing a quasi-3D to a full 3D nearshore circulation model: 1035 SHORECIRC and *ROMS*. *Ocean Modeling*. 26, 91-103.

Hawkins J.S., Burcharth F.H., Zanuttigh B., and Lamberti A. (2007). Environmental Design Guidelines for Low Crested Coastal Structures. Elsevier Science. Amsterdam. 448 pages.

Hawkins S.J. (1983). Interaction of Patella and macroalgae with settling Semibalanus balanoides (L.*) J. of Experimental Marine Biology and Ecology* 71, 55-72.

Hedström K. S. (2012). Draft Technical Manual for a Coupled Sea-Ice/Ocean Circulation Model (Version 4), U.S. Department of the Interior, Bureau of Ocean Energy Management. http://www.people.arsc.edu/~kate/ROMS/manual_2012.pdf, accessed Feb 2014.

Henderson R. (2006). Design, Simulation, and testing of a novel hydraulic power take-off system for the Pelamis wave energy converter, Renewable Energy, vol. 31, no. 2, pp. 271-283.

Holme N.A. and McIntyre A. D. Eds. (1971). Methods for the study of Marine Benthos, Blackwell Scientific Publishers, Oxford. IBP Handbook No, 16. Blackwell Sci. Publ., Oxford and Edinburgh. F. A. Davis, Philadelphia. 346 p.

Hwang P. A., Xu D., and Wu J. (1989). Breaking of wind-generated waves: Measurements and characteristics. *J. Fluid Mech*, 202, 177–200.

Jackett R.D. and McDougall T. (1995). Minimal Adjustment of Hydrostatic Profiles to Achieve Static Stability, *Journal of Atmospheric and Oceanic Technology*, vol. 12, pp. 381-389.

Jarocki D. (2010), Wave Energy Converter Performance Modeling and Cost of Electricity Assessment. Master's Thesis. California Polytechnic State University, San Louis Obispo. http://digitalcommons.calpoly.edu/cgi/viewcontent.cgi?article=1288&context=theses. Accessed Feb. 2014.

Jenkins R.J, Norton T. A., Hawkins S.J. (1999). Settlement and post-settlement interactions between Semibalanus balnnoides (L.) (Crustacea: Cirripedia) and three species of fucoid canopy algae. *J. exp. mar. Biol. Ecol*. 236: 49-67.

Jensen R., Wittmann P., and Dykes J., (2002). Global and regional wave modeling activities, *Oceanography,* vol. 15, pp. 57-66

Jonsson, P.R., Granhag, L., Moschella, P.S., Aberg, P., Hawkins, S.J., and Thompson, R.C. (2006). Interactions between wave action and grazing control the distribution of intertidal macroalgae. Ecology 87, 1169 - 1178.

Kofoed P.J., Frigaar P., Friis-Madsen E. and Sørensen C.H. (2006). Prototype testing of the wave energy converter wave dragon, *Renewable Energy,* vol. 31, no. 2, pp. 181-189.

Komen G.J., Cavaleri L., Donelan M., Hasselmann K., Hasselmann S. and P.A.E.M. Janssen M. P. (1994). *Dynamics and Modelling of Ocean Waves*, Cambridge University.

Krivtsov V. and Linfoot B. (2012), Disruption to benthic habitats by moorings of wave energy installations: A modelling case study and implications for overall ecosystem functioning, *Ecological Modelling*, 245: 121-124.

Langhamer O. (2010). Effects of wave energy converters on the surrounding soft-bottom macrofauna (west coast of Sweden), *Marine Environmental Research* 69 374–381.

Langton R., Davies M.I., and Scott E.B. (2011). Seabird conservation and tidal stream and wave power generation: Information needs for predicting and managing potential impacts, *Marine Policy* 35 623–630.

Leijon M., Bostrom C., Danielsson O., Gustafsson S., Haikonen K., Langhamer O., Stromstedt E., Stalberg M., Sundberg J., Svensson O., Tyrberg S., and Waters R. (2008). Wave Energy from the North Sea: Experiences from the Lysekil Research Site, *Surv Geophys* 29:221–240, DOI 10.1007/s10712-008-9047.

Marshall J., Hill C., Perelman L. and Adcroft A., (1997). "Hydrostatic, quasi-hydrostatic, and nonhydrostatic ocean modeling, *Journal of Geophysical Research,* vol. 102, pp. 5733-5752.

Meadows A.G. (2005). Cumulative Habitat Impacts of Nearshore Engineering, J. Great Lakes Res. 31 (Supplement 1):90–112, Internat. Assoc. Great Lakes Res.

Millar L.D., Smith M.C.H., and Reeve E.D. (2007). Modelling analysis of the sensitivity of shoreline change to a wave farm, *Ocean Engineering* 34: 884–901.

Minchin D. and Duggan C.B. (1988). The distribution of the exotic ascidian, Styela clava Herdman, in Cork Harbour. *Irish Naturalists Journal* 22: 388-393.

Nam T.P., Larson M., Hanson H. and Hoan X.L. (2009). A numerical model of nearshore waves, currents, and sediment transport, *Coastal Engineering,* vol. 56, pp. 1084-1096.

National Oceanic and Atmospheric Administration (NOAA). (2014) U.S. Coastal Relief Model, NOAA National Geophysical Data Center. Web page: http://www.ngdc.noaa.gov/mgg/coastal/crm.html. Accessed Feb. 2014.

Oh H.S., Suh D.K., Son Y.S., and Lee Y.D. (2009). Performance Comparison of Spectral Wave Models Based on Different Governing Equations Including Wave Breaking, *Korean Society of Civil Engineers Journal of Civil Engineering* 13(2):75-84.

Pacific Gas &Electric. 2014. WaveConnect Projects. Web page: http://www.pge.com/about/environment/pge/cleanenergy/waveconnect/. Accessed Feb. 2014.

Palha A., Mendes L., Fortes J.C., Brito-Melo A., and Sarmento A. (2010). The impact of wave energy farms in the shoreline wave climate: Portuguese pilot zone case study using Pelamis energy wave devices. *Renewable Energy* 35 62–77.

Penning-Rowsell E.C., Green C.H., Thompson P., Coker A., Tunstall S., Richards C. and Parker D.J. (1992). The Economics of Coastal Management: A Manual of Benefit Assessment Techniques Gower, Belhaven Press, London.

Price R. (2009). Trends in emerging tidal and wave energy collection technology, *Marine Technology Society Journal,* pp. 101-116.

Putrevu U. and Svendsen, I. A. (1999). Three-dimensional dispersion of momentum in wave-induced nearshore currents, *Eur. J. Mech. B/Fluids*, 83-101.

Raffaelli D.G. and Hawkins S.J. (1996). Intertidal ecology, Chapman & Hall, London.

Renewable energy focus. (2010). HD video monitoring of wave energy impact. Web page: http://www.renewableenergyfocus.com/view/12446/hd-video-monitoring-of-wave-energy-impact/ Posted September, 14. Accessed Feb., 2014.

Richards D.S., Harland J.E., and Jones A.S. (2007). Underwater Noise Study Supporting Scottish Executive Strategic Environmental Assessment for Marine Renewable, Report produced by QinetiQ Ltd, Cody Technology Park, Farnborough, Hampshire, GU14 0LX.

Saha E.S. (2010). The NCEP Climate Forecast System Reanalysis, *Bulletin of the American Meteorological Society,* vol. 91, pp. 1015-1057.

Shchepetkin A. F. and McWilliams CJ, "The regional oceanic modeling system (*ROMS*): a split-explicit, free-surface, topography-following-coordinate oceanic model," *Ocean Modelling,* vol. 9, pp. 347-404, 2005.

Song Y. and Haidvogel D, "A semi-implicit ocean circulation model using a generalized topography-following coordinate system," *Journal of Computational Physics,* vol. 115, pp. 228-244, 1994.

Svendsen I. A., Veeramony J., Kirby J. T. (1996). Verification of Boussinesq model for breaking waves, presented at *AGU Fall Meeting*, San Francisco.

SWAN (2006). SWAN Technical Documentation. University of Delft, The Netherlands. SWAN Cycle III version 40.51., http://cisweb1.ucsd.edu/~falk/modeling/swantech.pdf, accessed Feb. 2013.

Swenson J.M., Wu H.C., Edil B.T., and Mickelson M.D. (2006). Bluff Recession Rates and Wave Impact along the Wisconsin Coast of Lake Superior, *J. Great Lakes Res.* 32:512–530, International Assoc. Great Lakes Res.

Thompson R.C, Wilson B.J, Tobin M.L, Hill A.S. and Hawkins S.J. (1996). Biologically generated habitat provision and diversity of rocky shore organisms at a hierarchy of spatial scales, *Journal of Exp. Marine Biology and Ecology*, 202, 73-84.

Tolman, H.L. (1991). A third-generation model for wind waves on slowly varying, unsteady and inhomogeneous depths and currents, *J. Phys. Oceanogr*., 21, 6, 782-797.

Tricas T. and Gill A. (2011). Effects of EMF's from Undersea Power Cables on Elasmobranchs and Other Marine Species, Final Report, by Normandeau Associates, Inc. for U.S. Department of the Interior, Bureau of Ocean Energy Management, Regulation and Enforcement.

U.S. Department of Energy, Energy Efficiency and Renewable Energy, Wind and Hydropower Technologies Program (2009). Report to Congress on the Potential Environmental Effects of Marine and Hydrokinetic Energy Technologies. December. http://www1.eere.energy.gov/wind/pdfs/doe_eisa_633b.pdf

Valério D., Beirão P. and Sá da Costa J. (2007). Optimisation of wave energy extraction with the Archimedes Wave Swing," *Ocean Engineering,* vol. 34, no. 17, pp. 2330-2344.

Vantorre M., Banasiak R. and Verhoeven R. (2002). Extraction of sea wave energy: a mathematical evaluation of a point absorber in heave, *International series on advances in fluid mechanics,* vol. 32, pp. 193-204.

Warner C.J., Armstrong B., He R. and Zambon B.J. (2010). Development of a Coupled Ocean–Atmosphere–Wave–Sediment Transport (COAWST) Modeling System, *Ocean Modelling*, vol. 35, pp. 230-244.

Warner C.J., Sherwood R.C., Signell P.R. Harris KC and Arango GH, (2008). Development of a three-dimensional, regional, coupled wave, current, and sediment-transport model," *Computers & Geosciences*, vol. 34, pp. 1284-1306.

Wilson J. and Beyene A. (2007). California Wave Energy Resource Evaluation, *Journal of Coastal Research*, Vol. 23, No. 3, page 679-690.

ZD Net. (2014). IBM analytics will test environmental impact of wave energy tech. Web page: http://www.zdnet.com/blog/green/ibm-analytics-will-test-environmental-impact-of-wave-energy-tech/19312. Accessed Feb., 2014.

Zetterman A. and Wilson J. (2009). Wave Energy Converter Absorption, Undergraduate Oceanography Project, University of Colorado.

NOMENCLATURE

c_σ,c_θ	wave propagation in spectral space
$\vec{c}_g$	group velocity, m/s
C	tracer type variable, e.g. temperature, salinity, sediment concentration
d	water depth, m
D_U, D_V, D_C,	horizontal diffusion terms
E_{tot}/A	total energy per unit surface area, J/m^2
EMF	electromagnetic field
f	frequency, Hz
f(x,y)	Coriolis parameter
F	wave farm density, %
F_U, F_V, F_C,	*ROMS* forcing terms
g	gravitational acceleration, 9.81 m/s^2
$G(f, \theta)$	variance density spectrum (energy density spectrum), m^2/Hz-radian
h	sea floor depth (relative to datum height), m
H_c	crest height
H_{m0}	significant wave height in *SWAN*
H_{max}	maximum wave height
H_s	significant wave height
i	*ROMS* grid ξ-direction index
j	*ROMS* grid η-direction index
k	wavenumber, radians/m
$N(f,\theta)$	action density spectrum
P/l	*power per unit length, kW/m*
P	*total pressure*
Q	*freshwater production flow rate (m^3/s)*
S	wave energy source/sink term
S	salinity, P.S.U.

t	time
T	wave period, s
T	potential temperature, K
U,V,W	current velocity components, m/s
$\vec{V}$	current velocity vector, m/s (U,V,W)
x,y,z	cartesian coordinates, m

Greek symbols

ζ	sea surface height, m
η	*ROMS* Arakawa-C grid local coordinate
η_{WEC}	wave converter efficiency
θ	direction
ν	viscosity
ξ	*ROMS* Arakawa-C grid local coordinate
ρ_0	seawater density, 1025 kg/m^3
$\rho_0 + \rho(x,y,z,t)$	total density calculated *in situ* by *ROMS*
σ	relative frequency(radians/s)
φ	dynamic pressure, $\varphi=P/\rho_0$
ω	absolute frequency(radians/s)

APPENDIX A:
Wave Energy Automation Tool (*WHEAT*) Instructions

Prerequisites: *WHEAT* needs the following at a minimum to run:

A Java-supported Operating System (OS). *WHEAT* has been tested on Windows and Linux OSes but has been written to be as cross-platform as possible so it should run on other OSes as well.

Oracle's Java Runtime Environment (JRE) version 1.7 update 21 or newer. Download the latest version of their JRE from here:

https://java.com

It should not matter whether you install the 32 or 64 bit version of Java--either should run *WHEAT*. *WHEAT* has only been tested using Oracle's Java Virtual Machine (JVM) and has NOT been tested using any other Java variant. You may be able to run *WHEAT* with one of these other variants:

https://en.wikipedia.org/wiki/List_of_Java_virtual_machines

...but your mileage may vary and some of the components may not function properly.

The *WHEAT* GUI can run with just Java installed. But, to do any useful work you will also need the following:

Simulating WAves Nearshore (*SWAN*). Download the latest version from here:

http://swanmodel.sourceforge.net/download/download.htm

WHEAT itself does not require much in terms of CPU, RAM, video, and hard disk requirements, but *SWAN* does. Typically, most machines built in the last few years are good enough but your expectations of computational speed may vary. If in doubt, please see these sites for details about whether the hardware you are using is sufficient:

Java:

https://www.java.com/en/download/help/sysreq.xml

SWAN:

http://swanmodel.sourceforge.net/download/download.htm

Installation:

Jove Sciences' *WHEAT* is packaged as a Java ARchive (JAR) file and is intended to be run on machines that have Java version 1.7 or newer already installed on it. Therefore, in order to run *WHEAT*, install the latest version of Java. Install *SWAN* as well. The installation of *SWAN* is beyond the scope of this document so please go to the *SWAN* website for detailed installation instructions:

http://swanmodel.sourceforge.net/online_doc/swanimp/swanimp.html

...if compiling from source code. If you are installing precompiled binary

files, see here for more:

http://swanmodel.sourceforge.net/download/download.htm

The one important part, as far as *WHEAT* is concerned, is that after *SWAN* is installed, the *SWAN* directory is included in the user's PATH environment variable. If not, *SWAN* will not run correctly and *WHEAT* will not properly detect *SWAN*.

Once you have installed both Java and *SWAN*, *WHEAT* is ready to be used. *WHEAT* has no specific installation instructions.

Running WEAT:

Once Java is installed it will associate itself with all files that have a .jar extension in their name. Therefore, in order to run *WHEAT*, browse to where the weat.jar file is located on your machine and then double-click on it in a GUI explorer window in order to run the tool. Note that other applications, such as compression tools, may also associate themselves with the .jar extension, so if you double-click on the weat.jar file and the *WHEAT* GUI does not appear, some other application may be attempting to open the file. In this case,

right-click on the file and browse to the Java Runtime Environment you have installed in order to make Java run the file.

An alternative method to running the tool, if you are so inclined, is to open a console/terminal/DOS window and change directory (CD) to the location where the weat.jar file is located and then type the following into the window to run the tool:

```
java -jar weat.jar
```

The command above presumes that the java executable file is in one of the directories in your environment's PATH variable. If java is not found, you may need to specify the complete path to Java. It's default location is here:

Windows (64-bit):

C:\Progra~1\Java\jre7\bin\java.exe

Windows (32-bit):

C:\Progra~1\Java\jre7\bin\java.exe

...or:

C:\Progra~2\Java\jre7\bin\java.exe

Linux:

/usr/bin/java

...but it may be elsewhere on your system Specifying the absolute path to Java would make the above commands look like these:

C:\Progra~1\Java\jre7\bin\java.exe -jar weat.jar

C:\Progra~2\Java\jre7\bin\java.exe -jar weat.jar

/usr/bin/java -jar weat.jar

Using *WHEAT*:

When *WHEAT* is run a main GUI window is first displayed.

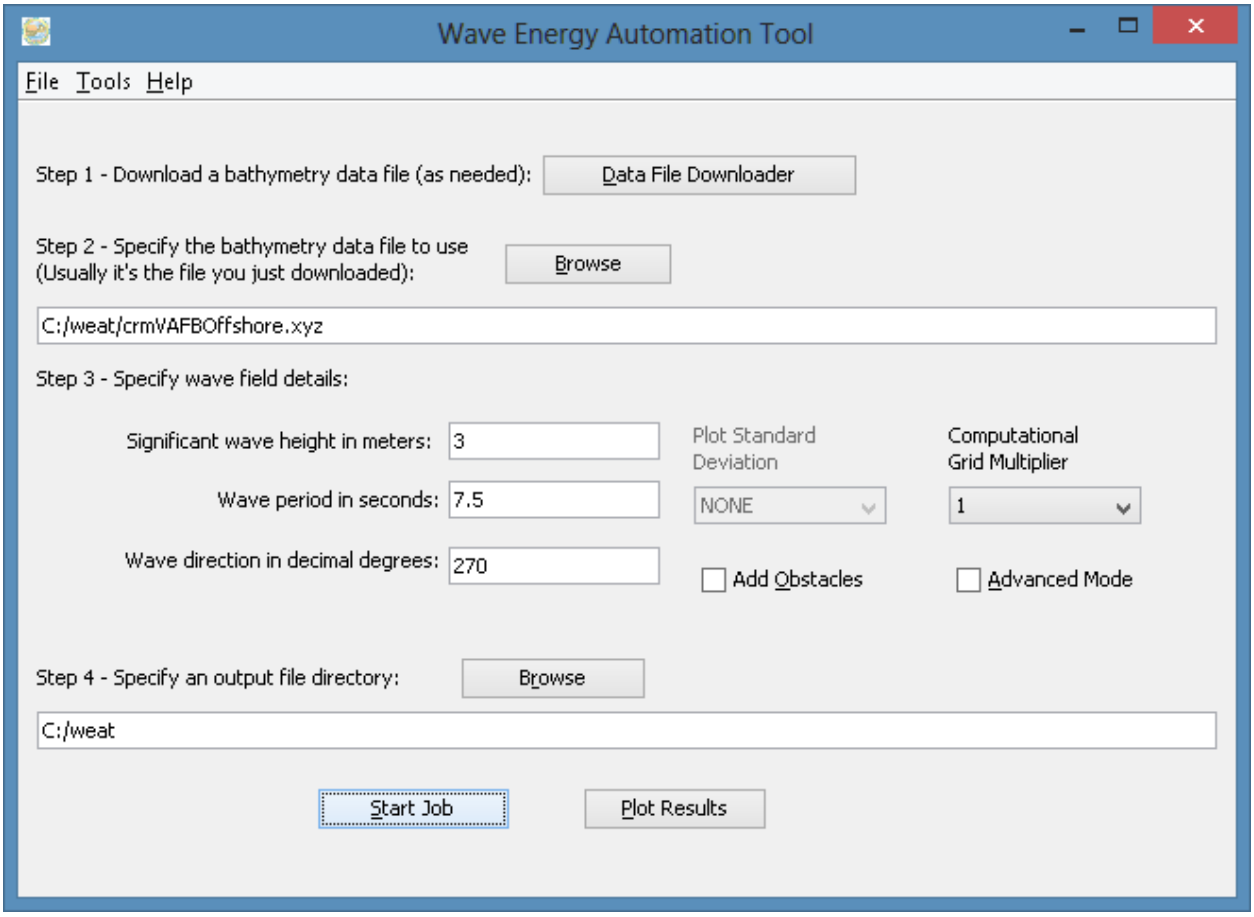

Figure A 1: The main *WHEAT* GUI

Once the *WHEAT* GUI is displayed, you will first want to ensure that *WHEAT* was able to correctly detect your desired version of *SWAN*. Open the Tools → Options dialog and ensure that the swanrun (Linux) or swanrun.bat (Windows) file is properly specified.

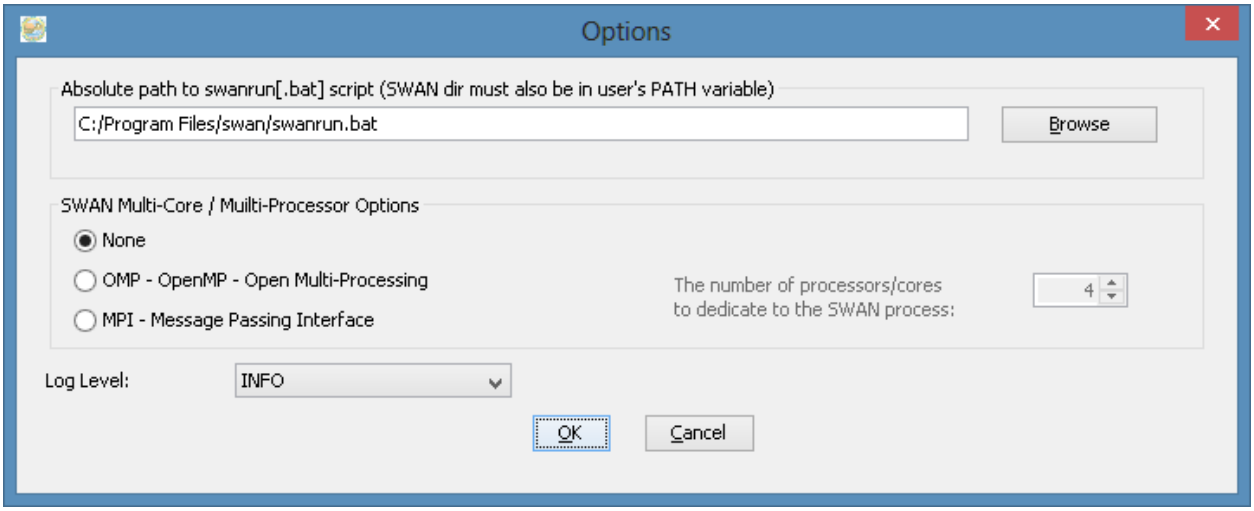

Figure A2: The *WHEAT* options dialog

If *WHEAT* is unable to automatically locate your swanrun (Linux) or swanrun.bat (Windows) script, it means that there is no swanrun/swanrun.bat file found anywhere in your environment's PATH variable. You will need to fix this prior to proceeding by modifying your PATH to include the directory where you installed *SWAN*. If you modify your PATH variable while WEAT is running, you will need to close and reopen *WHEAT* in order for this change to affect *WHEAT*.

If you need to download data files, in the main *WHEAT* window, press the Data File Downloader button to open a web browser that will act as a data file downloader.

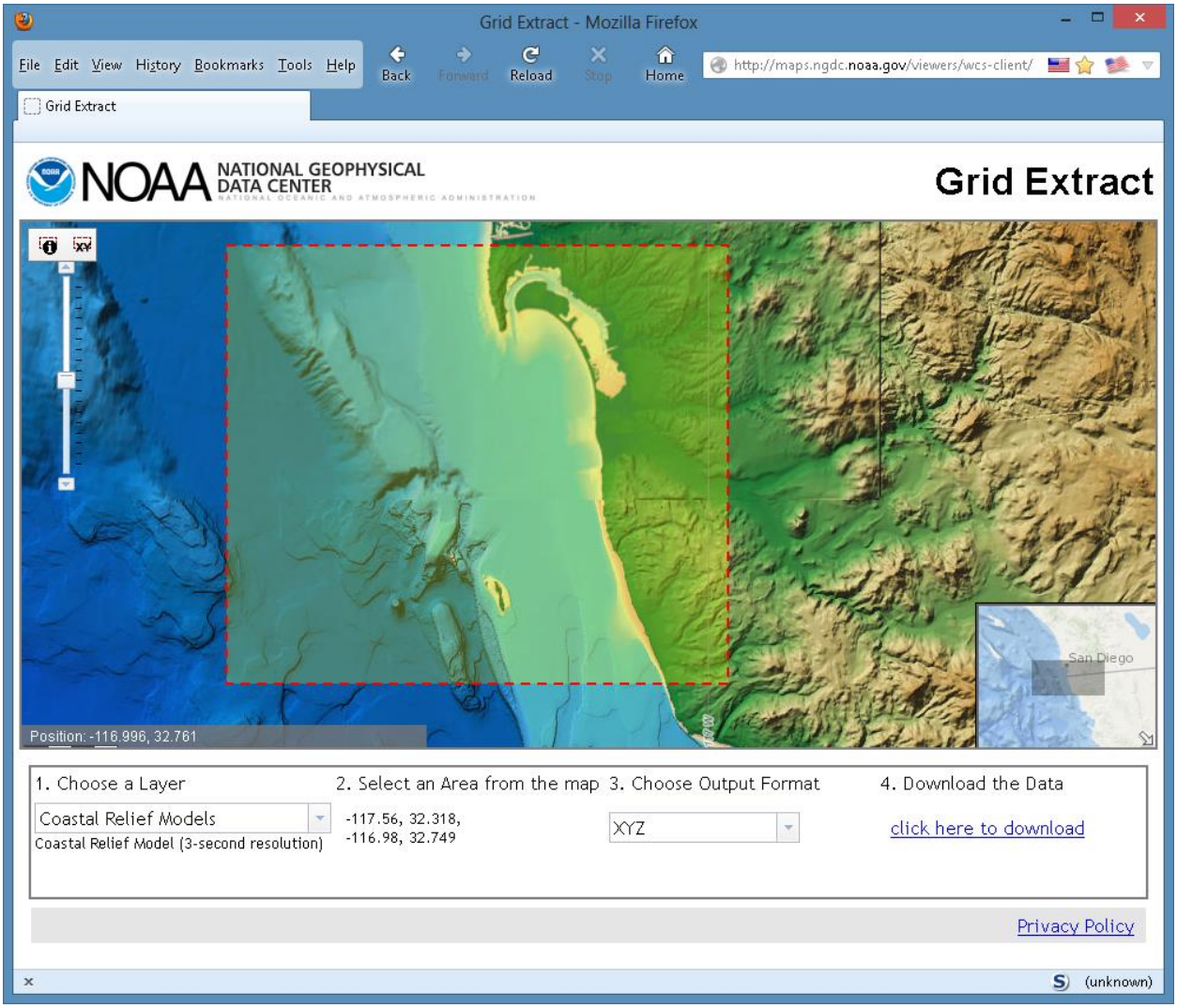

Figure A3: The NOAA website where XYZ bathymetry data can be downloaded

If your system does not support opening a browser, then a Data File Downloader window will be displayed instead. The Data File Downloader dialog is only accessible when *WHEAT* cannot start a web browser.

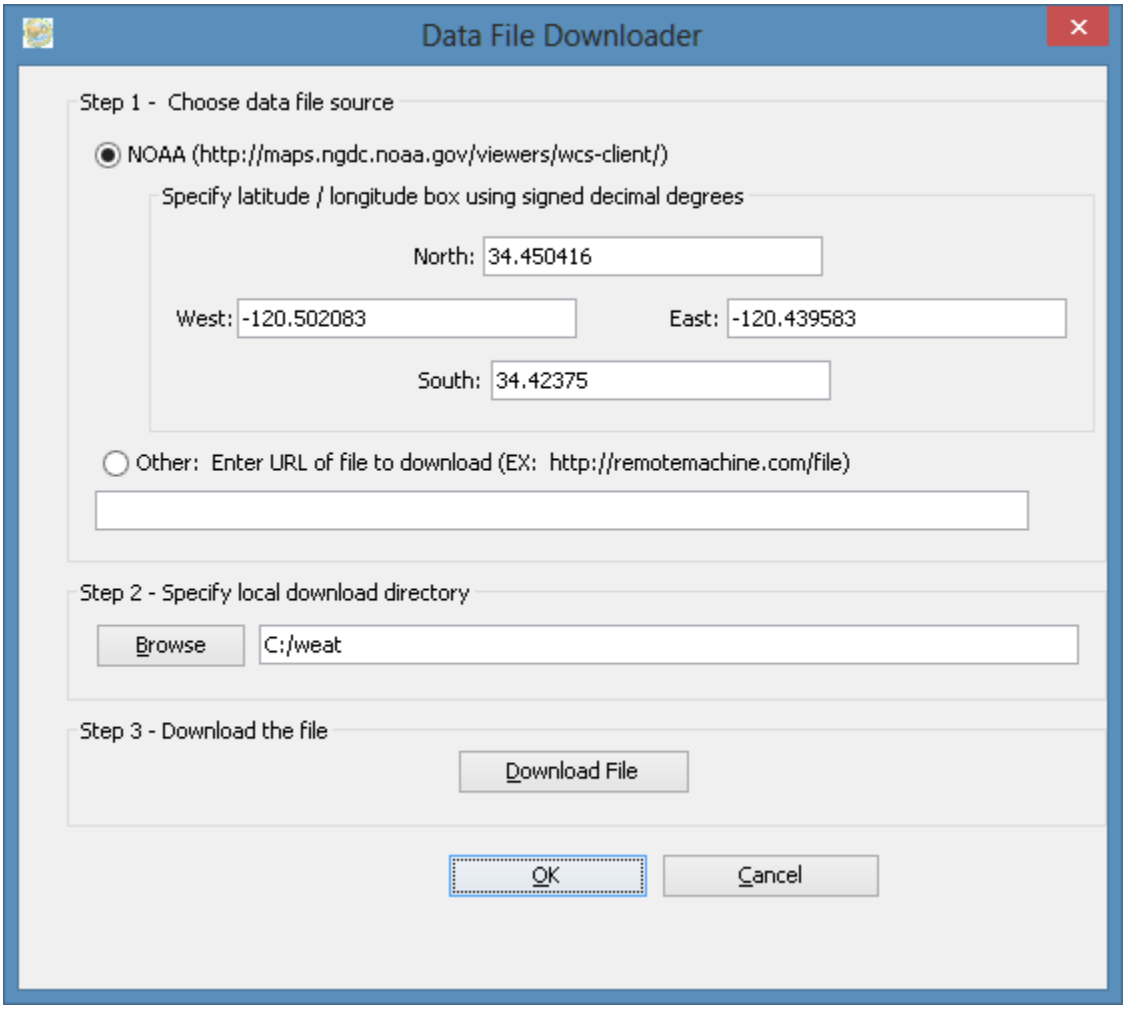

Figure A4: The Data File Downloader dialog

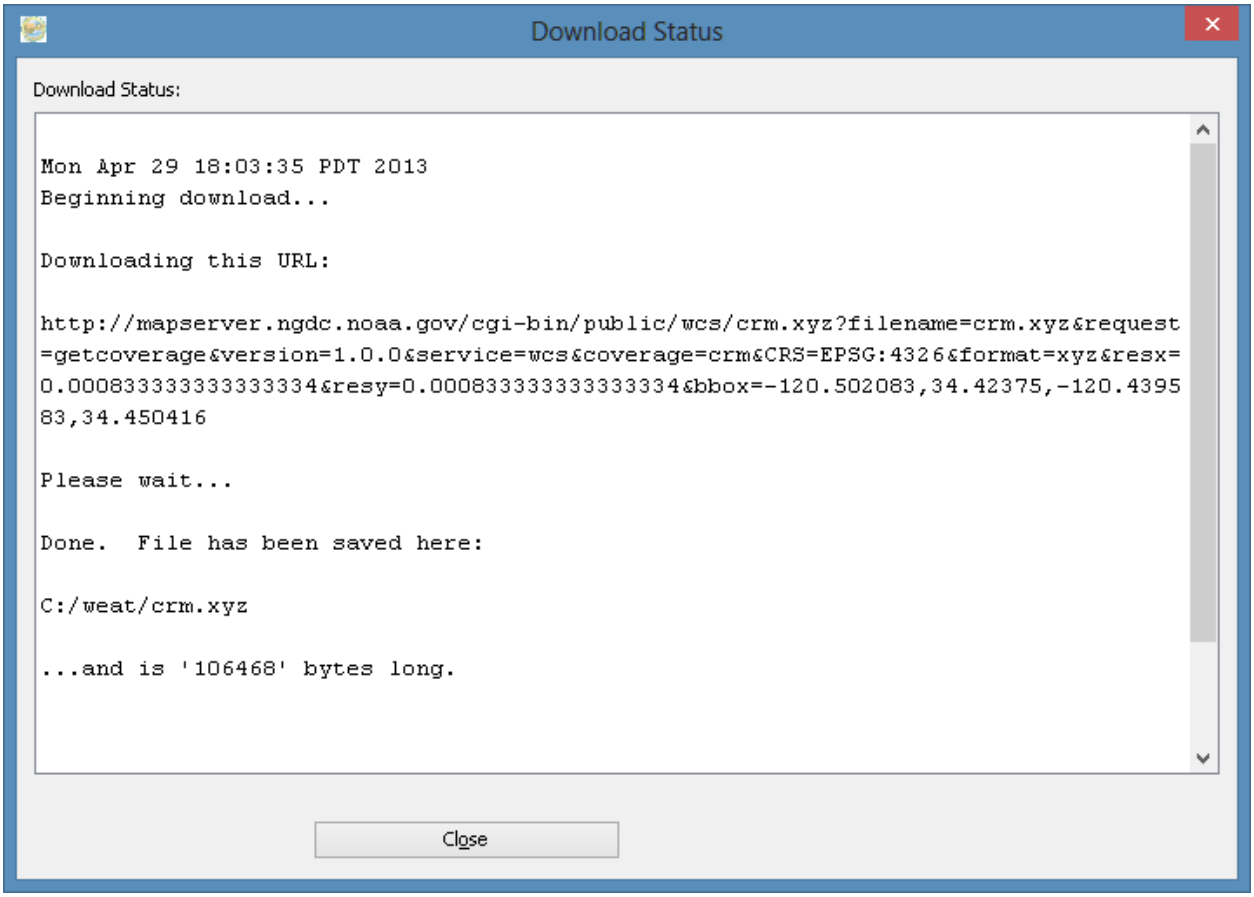

Figure A5: The data file download status dialog (Only show when NOT using a web browser to download an XYZ data file)

After you are done downloading one or more files, either close the browser or press OK to close the Data File Downloader window and return to the main *WHEAT* window. The current version of the *WHEAT* Data File Downloader window does not provide visual feedback in the form of a map when selecting a region, so it might be difficult to determine the area you are interested in by latitude and longitude alone. In that case the other alternative to using the *WHEAT* downloader is to download bathymetry data files in ASCII XYZ format using some other means and then using the *WHEAT* GUI to point to this file. For example, you can browse here:

http://maps.ngdc.noaa.gov/viewers/wcs-client/

...and download one or more files manually. To do so, select the "Coastal Relief Models" Layer, select a small rectangular region to process, select "XYZ" Output Format, and then click "Download the Data" to save the XYZ file on your local machine.

If you intend to run *SWAN* with many different inputs but the same data file, then this download step only needs to be done once since the data file will then be stored on your local machine from then on.

Once you have a local XYZ data file, you can enter all the needed inputs to *SWAN* in the main *WHEAT* window and then press the Start Job button to begin the process of converting the XYZ file, running the *SWAN* model, and then displaying the results.

Every time you press the "Start Job" button, a directory is created where all the files related to this run are stored. The directory will have the following name scheme:

yyyy-mm-dd_hh-mm-ss

...and be located in the directory that you specified here:

"Step 4 - Specify an output file directory"

So, if you specify this location:

/home/user/weat

...as the output directory, you will see this directory created:

/home/user/weat/yyyy-mm-dd_hh-mm-ss

...containing all the files related to this job.

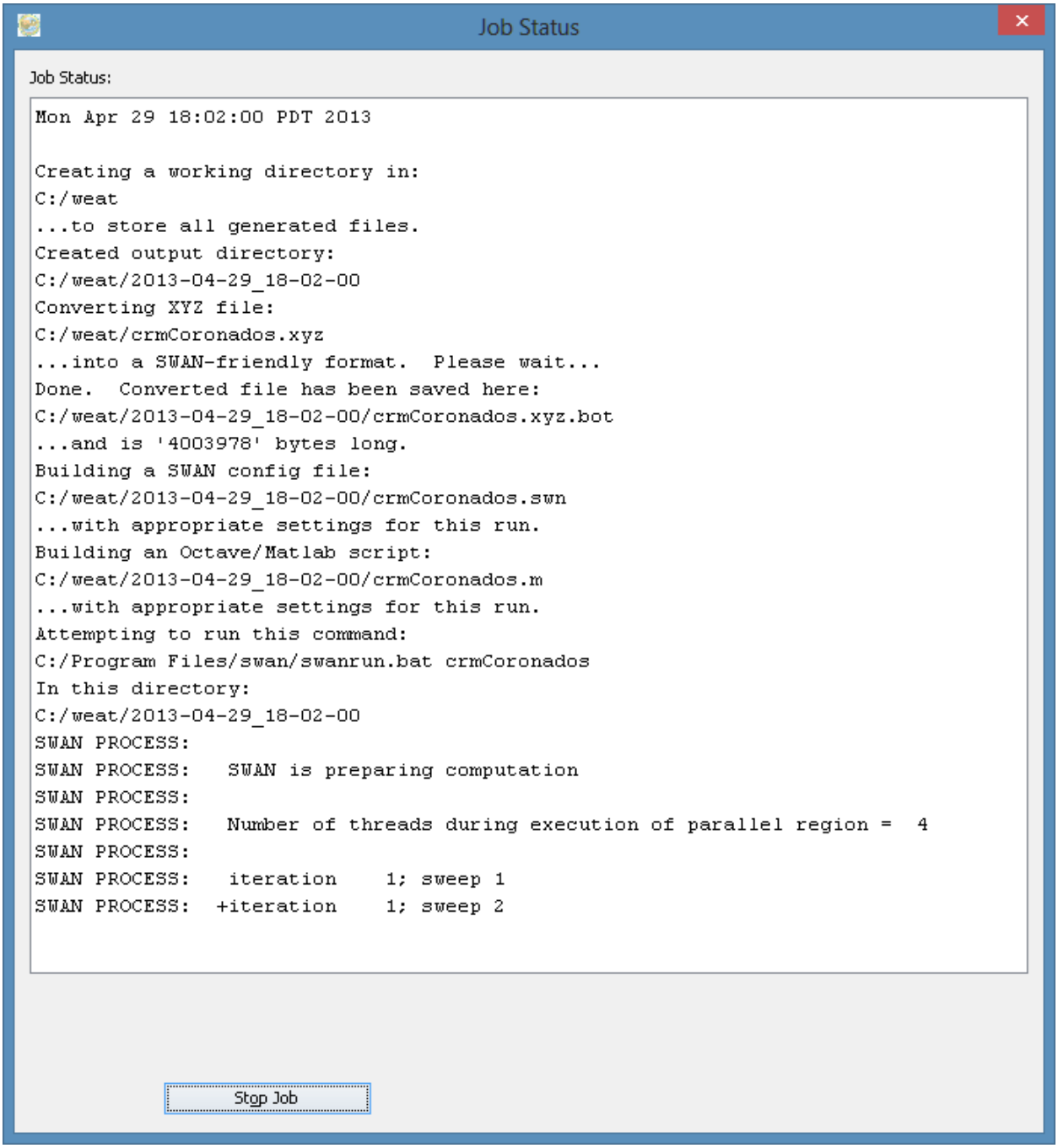

Figure A5: The Job Status dialog

The *SWAN* process can take a long time to complete if the data set to process is large. Running this tool on smaller data sets will let *SWAN* complete more quickly. Try starting out with small data sets that are less than 1 km by 1 km to get the settings

correct or else you may have to wait a long time during each job iteration to find and correct configuration-related issues.

After *SWAN* has completed: The Job Status dialog will remain on top while the output from the *SWAN* process is plotted in a few other windows. Close the Job Status dialog in order to interact with the chart plots.

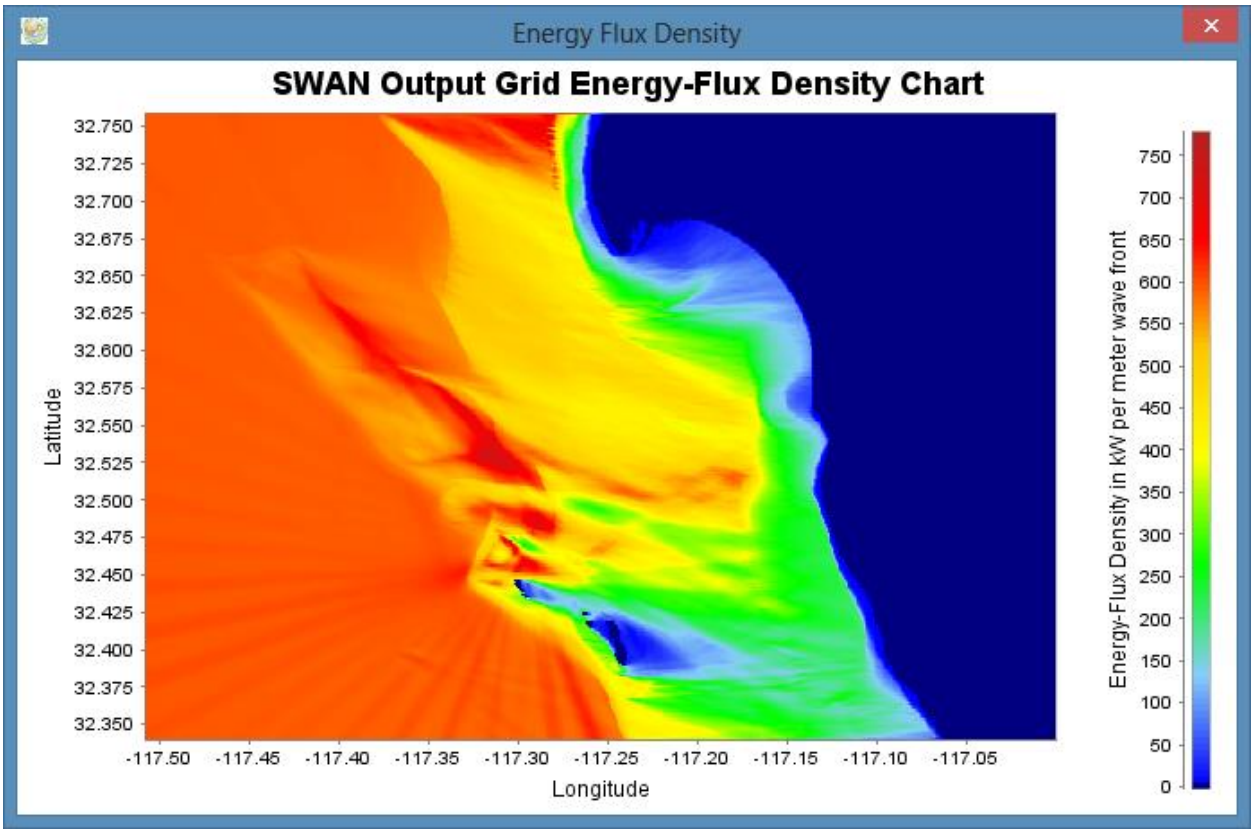

Figure A6: After *SWAN* completes - The resulting energy flux density chart

SWAN output chart maneuvering – Once *SWAN* completes, charts related to the run will then be displayed. The charts can be manipulated as follows:

Zooming: Scroll your mouse wheel to zoom in and out. Or, click and hold the left mouse button and drag from left-to-right in order to zoom in. Drag from right-to-left to zoom back to the default zoom level and to recenter a chart. You can also revert to the default zoom level and recenter the image by double or triple clicking a chart.

Panning: To pan a chart, hold down the Control (Ctrl) key (or the Alternate [Alt] key on Macs) and then click and hold the left mouse button and drag in order to override the zoom behavior. A variation of panning can be accomplished by zooming out and then back into a different location by moving the mouse pointer over different regions while you zoom in or out.

Right-click on the chart to display a menu containing all of these features and much more, including saving and printing of a chart. However, the mouse over the edge of the chart window to get these same instructions to display.

Hovering over a part of the chart will provide you with a value for that (X, Y) point on the chart in the form of a tooltip popup. Note that there currently are a few tooltip bugs that need to be resolved. If the tooltip does not display a value and instead displays the legend, shrink the chart window down to it's original size and try hovering again.

The main *WHEAT* window contains a "Plot Results" button which allows you to re-plot the charts from previous runs of the GUI. Click this button and browse for the *SWAN* output files that have the .blk file name extension which are normally located in the yyyy-mm-dd_hh-mm-ss directory that is created after each *SWAN* job completes.

You may also note that a file with a .m extension is created and stored in each yyyy-mm-dd_hh-mm-ss *SWAN* output directory. As a convenience to the user, this .m file is a script that can be used with other tools such as Octave or Matlab to display the the results in those tools as well.

Advanced *WHEAT*/*SWAN* Usage:

The default *WHEAT* configuration generates a simplistic *SWAN* configuration file that can provide baseline data for a region. To do more interesting computations, you may want to check the "Advanced Mode" checkbox in the main *WHEAT* window before starting a *SWAN* job. Then, start the job. The GUI will do some initial processing and then present you with a window that allows you to manually modify the generated configuration file that will be sent to *SWAN*.

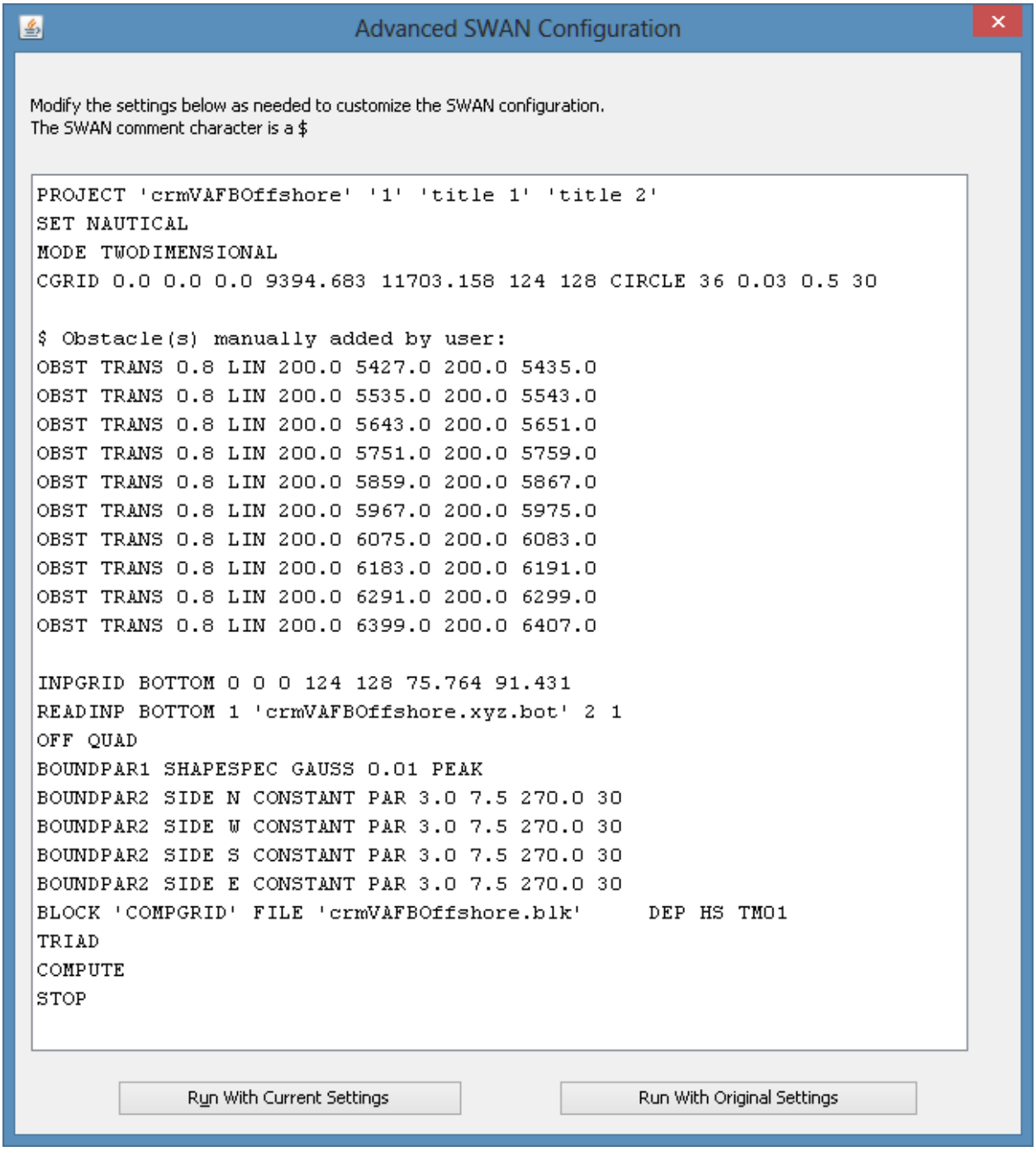

Figure A7: The advanced *SWAN* dialog showing the contents of a *SWAN* configuration file

The details about what you may want to add/change/delete in this dialog box are beyond the scope of this document.

SWAN Obstacles:

The *WHEAT* tool allows a user to manually enter *SWAN* obstacles in Advanced mode, but by checking the "Add Obstacles" check box before starting a job, you will be presented with a way to add obstacles in a less manual way. When checked, the Obstacles dialog is displayed and the user is given a chance to add obstacles in a more controlled manner than manually adding obstacles directly into the *SWAN* Advanced dialog box.

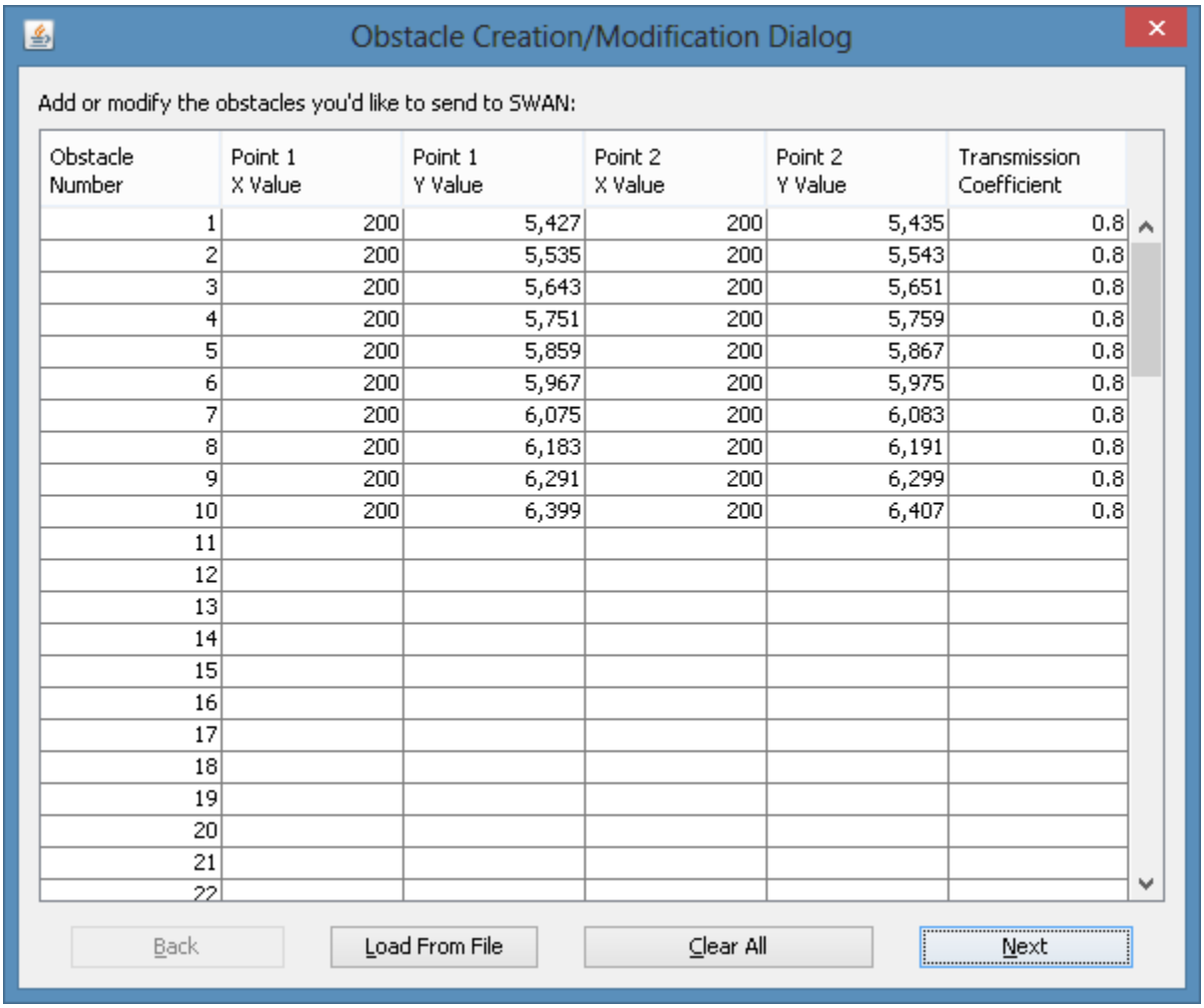

Obstacle Number	Point 1 X Value	Point 1 Y Value	Point 2 X Value	Point 2 Y Value	Transmission Coefficient
1	200	5,427	200	5,435	0.8
2	200	5,535	200	5,543	0.8
3	200	5,643	200	5,651	0.8
4	200	5,751	200	5,759	0.8
5	200	5,859	200	5,867	0.8
6	200	5,967	200	5,975	0.8
7	200	6,075	200	6,083	0.8
8	200	6,183	200	6,191	0.8
9	200	6,291	200	6,299	0.8
10	200	6,399	200	6,407	0.8
11					
12					
13					
14					
15					
16					
17					
18					
19					
20					
21					
22					

Figure A8: The Obstacles dialog showing a few obstacles

Any obstacles that you add are automatically saved in the current yyyy-mm-dd_hh-mm-ss *SWAN* working directory with an .obs file extension and can be reloaded for future runs, saving the user the trouble of having to re-enter the same obstacles over and over.

Checking both the "Add Obstacles" and "Advanced Mode" checkboxes allows you to add obstacles and then verify that they are added as you expected.

Future versions of *WHEAT* may provide more control of the advanced *SWAN* inputs, minimizing the manual effort needed in the Advanced Mode dialog box.

Other *WHEAT* screenshots:

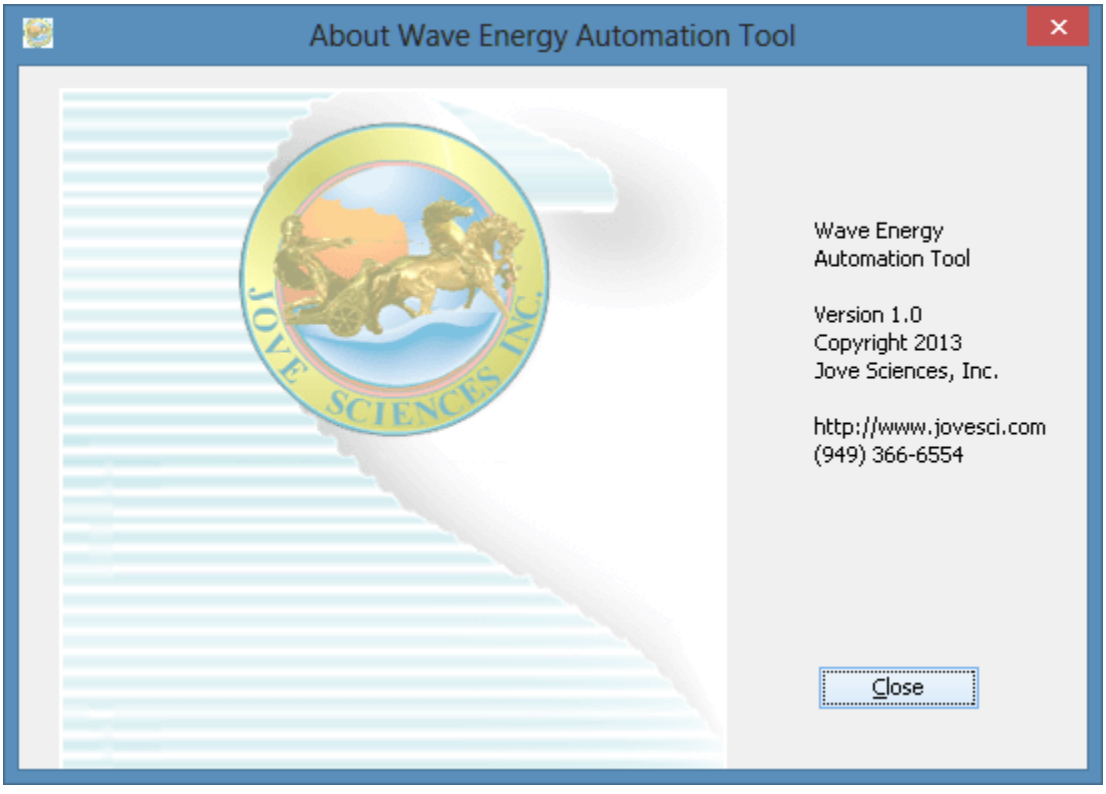

Figure A9: The About dialog

APPENDIX B:
SWAN Command File

```
PROJ 'a' 'a'
MODE NONST
COORD SPHE
CGRID -117.44 32.43 0 .34 .31 21 19 180 .04 1 34
INP BOT -117.441666666667 32.425 0 21 19 .01666666666667 &
 .016666666666667 EXC -9999
INP WIND -117.5 32.25 0 2 2 .25 .25 EXC -99 &
NONSTAT 20100107.060000 6 HR 20100113.060000
INP WLEV -117.44 32.43 0 &
1 1 .34 .31 EXC -9999 NONSTAT 20100107.060000 3 HR 20100113.060000
READ BOT 1 'bottom.dat' 1 0 FREE
READ WIND 1 SERIES 'wind02.dat' 3 0 FREE
READ WLEV 1 SERIES 'tide02.dat' 1 0 FREE
BOUN SIDE N CLOCKW VAR FILE .0716666666667 'swanspec021.dat'
BOUN SIDE S CLOCKW VAR FILE .255 'swanspec022.dat'
BOUN SIDE W CLOCKW VAR FILE .205 'swanspec023.dat'
INIT HOTS MULT 'htfle01.dat'
GEN3
BREA
FRIC
TRIAD
RAY 'ray' -117.44 32.43 -117.1 32.43 40 -117.44 32.74 -117.1 32.74
ISO 'out' 'ray' BOT 100 TAB 'out' NOHEAD 'HS02.dat' HS OUT &
20100107.060000 3 HR
TAB 'out' NOHEAD 'TRA02.dat' TRA OUT 20100107.060000 3 HR
GROUP 'Grid' 0 21 0 19
BLOCK 'Grid' NOHEAD 'hgrid02.dat' HS 1 OUT 20100107.060000 3 HR
BLOCK 'Grid' NOHEAD 'rtpgrid02.dat' RTP 1 OUT 20100107.060000 3 HR
BLOCK 'Grid' NOHEAD 'pdirgrid02.dat' PDIR 1 OUT 20100107.060000 3 HR
```

BLOCK 'Grid' NOHEAD 'tragrid02.dat' TRA 1 OUT 20100107.060000 3 HR

SPEC 'out' 'spray02.dat' OUT 20100107.060000 3 HR

TEST 1,0

COMP STAT 20100107.060000

COMP STAT 20100107.090000

COMP STAT 20100107.120000

COMP STAT 20100107.150000

COMP STAT 20100107.180000

COMP STAT 20100107.210000

COMP STAT 20100108.000000

COMP STAT 20100108.030000

COMP STAT 20100108.060000

COMP STAT 20100108.090000

COMP STAT 20100108.120000

COMP STAT 20100108.150000

COMP STAT 20100108.180000

COMP STAT 20100108.210000

COMP STAT 20100109.000000

COMP STAT 20100109.030000

COMP STAT 20100109.060000

COMP STAT 20100109.090000

COMP STAT 20100109.120000

COMP STAT 20100109.150000

COMP STAT 20100109.180000

COMP STAT 20100109.210000

COMP STAT 20100110.000000

COMP STAT 20100110.030000

COMP STAT 20100110.060000

COMP STAT 20100110.090000

COMP STAT 20100110.120000

COMP STAT 20100110.150000

COMP STAT 20100110.180000

COMP STAT 20100110.210000

```
 COMP STAT 20100111.000000
 COMP STAT 20100111.030000
 COMP STAT 20100111.060000
 COMP STAT 20100111.090000
 COMP STAT 20100111.120000
 COMP STAT 20100111.150000
 COMP STAT 20100111.180000
 COMP STAT 20100111.210000
 COMP STAT 20100112.000000
 COMP STAT 20100112.030000
 COMP STAT 20100112.060000
 COMP STAT 20100112.090000
 COMP STAT 20100112.120000
 COMP STAT 20100112.150000
 COMP STAT 20100112.180000
 COMP STAT 20100112.210000
 COMP STAT 20100113.000000
 COMP STAT 20100113.030000
 COMP STAT 20100113.060000
 COMP STAT 20100113.090000
HOTF 'htfle02.dat
 STOP
```

APPENDIX C:
COAWST Command File

B.1

Coupling File

```
NnodesATM =  0                ! atmospheric model
  NnodesWAV =  1                ! wave model
  NnodesOCN =  1                ! ocean model

! Time interval (seconds) between coupling of models.

 TI_ATM_WAV =     0.0d0           ! atmosphere-wave coupling interval
 TI_ATM_OCN =     0.0d0           ! atmosphere-ocean coupling interval
 TI_WAV_OCN =   3600.0d0            ! wave-ocean coupling interval

! Coupled model standard input file name.

   ATM_name = atmos.in                          ! atmospheric model, not used yet
   WAV_name = swan_small.in       ! wave model
!  For the larger swan grid, use inlet_test2.
!  WAV_name = Projects/Inlet_test/swan_inlet_test2.in
   OCN_name = ocean_small.in     ! ocean model
```

B.2

Ocean File

```
! Application title.

      TITLE = Small

! C-preprocessing Flag.

    MyAppCPP = THESIS
```

```
! Input variable information file name.  This file needs to be processed
! first so all information arrays can be initialized properly.

     VARNAME = varinfo.dat

! Grid dimension parameters. See notes below in the Glossary for how to set
! these parameters correctly.

        Lm == 30          ! Number of I-direction INTERIOR RHO-points
        Mm == 56          ! Number of J-direction INTERIOR RHO-points
         N == 30          ! Number of vertical levels

      Nbed =  10          ! Number of sediment bed layers

       NAT =  2           ! Number of active tracers (usually, 2)
       NPT =  0           ! Number of inactive passive tracers
       NCS =  0           ! Number of cohesive (mud) sediment tracers
       NNS =  2           ! Number of non-cohesive (sand) sediment tracers

! Domain decomposition parameters for serial, distributed-memory or
! shared-memory configurations used to determine tile horizontal range
! indices (Istr,Iend) and (Jstr,Jend), [1:Ngrids].

     NtileI == 1                  ! I-direction partition
     NtileJ == 1                  ! J-direction partition

! Time-Stepping parameters.

     NTIMES == 16704
        DT == 150.0d0
    NDTFAST == 35

! Model iteration loops parameters.
```

```
      ERstr =  1
      ERend =  1
     Nouter =  1
     Ninner =  50
  Nintervals =  1

! Number of eigenvalues (NEV) and eigenvectors (NCV) to compute for the
! Lanczos/Arnoldi problem in the Generalized Stability Theory (GST)
! analysis. NCV must be greater than NEV (see documentation below).

       NEV =  2                    ! Number of eigenvalues
       NCV =  10                   ! Number of eigenvectors

! Input/Output parameters.

     NRREC == 0
  LcycleRST == T
      NRST == 40
      NSTA == 1
      NFLT == 1
     NINFO == 1

! Output history, average, diagnostic files parameters.

    LDEFOUT == T
      NHIS == 40
   NDEFHIS == 0
    NTSAVG == 1
      NAVG == 40
   NDEFAVG == 0
    NTSDIA == 1
      NDIA == 40
   NDEFDIA == 0
```

```
! Output tangent linear and adjoint models parameters.

   LcycleTLM == F
      NTLM == 40
    NDEFTLM == 0
   LcycleADJ == F
      NADJ == 40
    NDEFADJ == 0

! Output check pointing GST restart parameters.

     LrstGST =  F                    ! GST restart switch
  MaxIterGST =  500                      ! maximun number of iterations
       NGST =  10                     ! check pointing interval

! Relative accuracy of the Ritz values computed in the GST analysis.

    Ritz_tol =  1.0d-15

! Harmonic/biharmonic horizontal diffusion of tracer: [1:NAT+NPT,Ngrids].

       TNU2 == 4.0d0 4.0d0              ! m2/s
       TNU4 == 0.0d0 0.0d0              ! m4/s

     ad_TNU2 == 4.0d0 4.0d0               ! m2/s
     ad_TNU4 == 0.0d0 0.0d0               ! m4/s

! Harmononic/biharmonic, horizontal viscosity coefficient: [Ngrids].

       VISC2 == 4.0d0                  ! m2/s
       VISC4 == 0.0d0                   ! m4/s

! Vertical mixing coefficients for active tracers: [1:NAT+NPT,Ngrids]
```

```
!    AKT_BAK == 1.0d-5 1.0d-5              ! m2/s
     AKT_BAK == 1.0d-5 1.0d-5              ! m2/s

! Vertical mixing coefficient for momentum: [Ngrids].

!    AKV_BAK == 1.0d-5                     ! m2/s
     AKV_BAK == 1.0d-5                     ! m2/s

! Turbulent closure parameters.

     AKK_BAK == 5.0d-6                     ! m2/s
     AKP_BAK == 5.0d-6                     ! m2/s
      TKENU2 == 0.0d0                      ! m2/s
      TKENU4 == 0.0d0                      ! m4/s

Generic length-scale turbulence closure parameters.

       GLS_P == -1.0d0                     ! K-omega
       GLS_M == 0.5d0
       GLS_N == -1.0d0
    GLS_Kmin == 7.6d-6
    GLS_Pmin == 1.0d-12

   GLS_CMU0 == 0.5477d0
     GLS_C1 == 0.555d0
     GLS_C2 == 0.833d0
    GLS_C3M == -0.6d0
    GLS_C3P == 1.0d0
   GLS_SIGK == 2.0d0
   GLS_SIGP == 2.0d0

! Constants used in surface turbulent kinetic energy flux computation.
```

```
 CHARNOK_ALPHA == 1400.0d0         ! Charnok surface roughness
ZOS_HSIG_ALPHA == 0.5d0            ! roughness from wave amplitude
     SZ_ALPHA == 0.25d0            ! roughness from wave dissipation
    CRGBAN_CW == 100.0d0           ! Craig and Banner wave breaking

! Constants used in momentum stress computation.

      RDRG == 3.0d-04                ! m/s
     RDRG2 == 2.5d-03                ! nondimensional
       Zob == 0.02d0                 ! m
       Zos == 0.02d0                 ! m

! Height (m) of atmospheric measurements for Bulk fluxes parameterization.

    BLK_ZQ ==  2.0d0                 ! air humidity
    BLK_ZT ==  0.01d0                ! air temperature
    BLK_ZW == 10.0d0                 ! winds

! Minimum depth for wetting and drying.

     DCRIT == 1.0001d0               ! m

! Various parameters.

      WTYPE == 1
    LEVSFRC == 30
    LEVBFRC == 1


! Vertical S-coordinates parameters, [1:Ngrids].

    THETA_S == 5.0d0                 ! 0 < THETA_S < 20
    THETA_B == 0.4d0                 ! 0 < THETA_B < 1
```

```
     TCLINE == 20.0d0                  ! m

!! Set vertical, terrain-following coordinates transformation equation and
! stretching function (see below for details), [1:Ngrids].

  Vtransform == 2                    ! transformation equation
 Vstretching == 3                    ! stretching function

! Mean Density and Brunt-Vaisala frequency.

       RHO0 =  1025.0d0              ! kg/m3
     BVF_BAK =  1.0d-5               ! 1/s2

! Time-stamp assigned for model initialization, reference time
! origin for tidal forcing, and model reference time for output
! NetCDF units attribute.

     DSTART =  15107d0               ! days
  TIDE_START =  15107.0d0                  ! days
    TIME_REF =  -2.0d0                ! yyyymmdd.dd

! Nudging/relaxation time scales, inverse scales will be computed
! internally, [1:Ngrids].

      TNUDG == 360.0d0  360.0d0        ! days
      ZNUDG == 360.0d0                ! days
     M2NUDG == 360.0d0                ! days
     M3NUDG == 360.0d0                ! days

! Factor between passive (outflow) and active (inflow) open boundary
! conditions, [1:Ngrids]. If OBCFAC > 1, nudging on inflow is stronger
! than on outflow (recommended).
```

```
      OBCFAC == 360.0d0                ! nondimensional

! Linear equation of State parameters:

         R0 == 1028.0d0                ! kg/m3
         T0 == 5.0d0                  ! Celsius
         S0 == 35.0d0                 ! nondimensional
       TCOEF == 1.0d-4                 ! 1/Celsius
       SCOEF == 7.6d-4                 ! nondimensional

! Slipperiness parameter: 1.0 (free slip) or -1.0 (no slip)

      GAMMA2 == 1.0d0

! Logical switches (TRUE/FALSE) to specify which variables to process for
! tracers climatology: [1:NAT+NPT,Ngrids]. See glossary below for details.

  LtracerCLM == T T                    ! temperature, salinity, inert

! Logical switches (TRUE/FALSE) to specify which variables to consider on
! tracers point Sources/Sinks (like river runoff): [1:NAT+NPT,Ngrids].
! See glossary below for details.

  LtracerSrc == T T                    ! temperature, salinity, inert

! Starting (DstrS) and ending (DendS) day for adjoint sensitivity forcing.
! DstrS must be less or equal to DendS. If both values are zero, their
! values are reset internally to the full range of the adjoint integration.

       DstrS == 0.0d0                 ! starting day
       DendS == 0.0d0                  ! ending day

! Starting and ending vertical levels of the 3D adjoint state variables
```

```
! whose sensitivity is required.

      KstrS ==  1                    ! starting level
      KendS == 30                      ! ending level

! Logical switches (TRUE/FALSE) to specify the adjoint state variables
! whose sensitivity is required.

Lstate(isFsur) == F                  ! free-surface
Lstate(isUbar) == F                   ! 2D U-momentum
Lstate(isVbar) == F                   ! 2D V-momentum
Lstate(isUvel) == F                   ! 3D U-momentum
Lstate(isVvel) == F                   ! 3D V-momentum

! Logical switches (TRUE/FALSE) to specify the adjoint state tracer
! variables whose sensitivity is required (NT values are expected).

Lstate(isTvar) == F F                  ! tracers

! Stochastic optimals time decorrelation scale (days) assumed for
! red noise processes.

   SO_decay == 2.0d0                    ! days

! Logical switches (TRUE/FALSE) to specify the state surface forcing
! variable whose stochastic optimals is required.

SOstate(isUstr) == T                   ! surface u-stress
SOstate(isVstr) == T                   ! surface v-stress

! Logical switches (TRUE/FALSE) to specify the surface tracer forcing
! variable whose stochastic optimals is required (NT values are expected).
```

```
SOstate(isTsur) == F F                  ! surface tracer flux

! Stochastic optimals surface forcing standard deviation for
! dimensionalization.

SO_sdev(isUstr) == 1.0d0                ! surface u-stress
SO_sdev(isVstr) == 1.0d0                ! surface v-stress
SO_sdev(isTsur) == 1.0d0 1.0d0          ! NT surface tracer flux

! Logical switches (TRUE/FALSE) to activate writing of fields into
! HISTORY output file.

Hout(idUvel) == T                       ! 3D U-velocity
Hout(idVvel) == T                       ! 3D V-velocity
Hout(idWvel) == T                       ! 3D W-velocity
Hout(idOvel) == T                       ! omega vertical velocity
Hout(idUbar) == T                       ! 2D U-velocity
Hout(idVbar) == T                       ! 2D V-velocity
Hout(idFsur) == T                       ! free-surface
Hout(idBath) == T                       ! time-dependent bathymetry

Hout(idTvar) == T T                     ! temperature and salinity

Hout(idUsms) == F                       ! surface U-stress
Hout(idVsms) == F                       ! surface V-stress
Hout(idUbms) == T                       ! bottom U-stress
Hout(idVbms) == T                       ! bottom V-stress

Hout(idUbrs) == T                       ! bottom U-current stress
Hout(idVbrs) == T                       ! bottom V-current stress
Hout(idUbws) == T                       ! bottom U-wave stress
Hout(idVbws) == T                       ! bottom V-wave stress
Hout(idUbcs) == T                       ! bottom max wave-current U-stress
```

```
Hout(idVbcs) == T                ! bottom max wave-current V-stress

Hout(idUbot) == T                ! bed wave orbital U-velocity
Hout(idVbot) == T                ! bed wave orbital V-velocity
Hout(idUbur) == T                ! bottom U-velocity above bed
Hout(idVbvr) == T                ! bottom V-velocity above bed

Hout(idW2xx) == F                 ! 2D radiation stress, Sxx component
Hout(idW2xy) == F                 ! 2D radiation stress, Sxy component
Hout(idW2yy) == F                 ! 2D radiation stress, Syy component
Hout(idU2rs) == F                ! 2D radiation U-stress
Hout(idV2rs) == F                ! 2D radiation V-stress
Hout(idU2Sd) == F                 ! 2D U-Stokes velocity
Hout(idV2Sd) == F                 ! 2D V-Stokes velocity

Hout(idW3xx) == F                 ! 3D radiation stress, Sxx component
Hout(idW3xy) == F                 ! 3D radiation stress, Sxy component
Hout(idW3yy) == F                 ! 3D radiation stress, Syy component
Hout(idW3zx) == F                 ! 3D radiation stress, Szx component
Hout(idW3zy) == F                 ! 3D radiation stress, Szy component
Hout(idU3rs) == T                ! 3D U-radiation stress
Hout(idV3rs) == T                ! 3D V-radiation stress
Hout(idU3Sd) == T                 ! 3D U-Stokes velocity
Hout(idV3Sd) == T                 ! 3D V-Stokes velocity

Hout(idWamp) == T                  ! wave height
Hout(idWlen) == T                 ! wave length
Hout(idWdir) == T                 ! wave direction

Hout(idTsur) == F F               ! surface net heat and salt flux
Hout(idLhea) == F                ! latent heat flux
Hout(idShea) == F                ! sensible heat flux
Hout(idLrad) == F                ! longwave radiation flux
```

```
Hout(idSrad) == F                    ! shortwave radiation flux
Hout(idevap) == F                    ! evaporation rate
Hout(idrain) == F                    ! precipitation rate

Hout(idDano) == F                    ! density anomaly
Hout(idVvis) == F                    ! vertical viscosity
Hout(idTdif) == F                    ! vertical T-diffusion
Hout(idSdif) == F                    ! vertical Salinity diffusion
Hout(idHsbl) == F                    ! depth of surface boundary layer
Hout(idHbbl) == F                    ! depth of bottom boundary layer
Hout(idMtke) == F                    ! turbulent kinetic energy
Hout(idMtls) == F                    ! turbulent length scale

! Logical switches (TRUE/FALSE) to activate writing of extra inert passive
! tracers other than biological and sediment tracers. An inert passive tracer
! is one that it is only advected and diffused. Other processes are ignored.
! These tracers include, for example, dyes, pollutants, oil spills, etc.
! NPT values are expected. However, these switches can be activated using
! compact parameter specification.

 Hout(inert) == F                    ! inert passive tracers

! Logical switches (TRUE/FALSE) to activate writing of exposed sediment
! layer properties into HISTORY output file.  Currently, MBOTP(model
! bottom properties) properties
! are expected for the bottom boundary layer and/or sediment models:
!
!   Hout(idBott(isd50)),  isd50 = 1       ! mean grain diameter
!   Hout(idBott(idens)),  idens = 2       ! mean grain density
!   Hout(idBott(iwsed)),  iwsed = 3       ! mean settling velocity
!   Hout(idBott(itauc)),  itauc = 4       ! critical erosion stress
!   Hout(idBott(irlen)),  irlen = 5       ! ripple length
!   Hout(idBott(irhgt)),  irhgt = 6       ! ripple height
```

```
!   Hout(idBott(ibwav)),  ibwav = 7        ! wave excursion amplitude
!   Hout(idBott(izdef)),  izdef = 8        ! default bottom roughness
!   Hout(idBott(izapp)),  izapp = 9        ! apparent bottom roughness
!   Hout(idBott(izNik)),  izNik = 10       ! Nikuradse bottom roughness
!   Hout(idBott(izbio)),  izbio = 11       ! biological bottom roughness
!   Hout(idBott(izbfm)),  izbfm = 12       ! bed form bottom roughness
!   Hout(idBott(izbld)),  izbld = 13       ! bed load bottom roughness
!   Hout(idBott(izwbl)),  izwbl = 14       ! wave bottom roughness
!   Hout(idBott(iactv)),  iactv = 15       ! active layer thickness
!   Hout(idBott(ishgt)),  ishgt = 16       ! saltation height
!
!                           1 1 1 1 1 1 1
!             1 2 3 4 5 6 7 8 9 0 1 2 3 4 5 6

Hout(idBott) == T T T T T T T T T F F F F F F F

! Generic User parameters, [1:NUSER].

      NUSER =  0
       USER =  0.d0

! Input NetCDF file names, [1:Ngrids].

    GRDNAME == small-grid.nc
    ININAME == small_ini.nc
    ITLNAME == scb20_itl.nc
    IRPNAME == scb20_irp.nc
    IADNAME == scb20_iad.nc
    CLMNAME == small_clm.nc
    BRYNAME == small_bdy.nc
    FWDNAME == scb20_fwd.nc
    ADSNAME == scb20_ads.nc
```

```
! Input forcing NetCDF file name(s).  The USER has the option to enter
! several files names per each nested grid.  For example, the USER may
! have a different files for wind products, heat fluxes, rivers, tides,
! etc.  The model will scan the file list and will read the needed data
! from the first file in the list containing the forcing field. Therefore,
! the order of the file names is very important.  If multiple forcing
! files per grid, enter first all the file names for grid 1, then grid 2,
! and so on.  Use a single line per entry with a continuation (\) symbol
! at the each entry, except the last one.

    NFFILES ==   9                  ! number of forcing files

    FRCNAME == Data/lwrad10.nc \
Data/swrad10.nc \
Data/SST10.nc \
Data/rain10.nc \
Data/Pair10.nc \
Data/Tair10.nc \
Data/Qair10.nc \
Data/tides.nc \
Data/wind10.nc      ! forcing file 1, grid 1

! Output NetCDF file names, [1:Ngrids].

    GSTNAME == scb20_gst.nc
    RSTNAME == small_rst.nc
    HISNAME == small_his.nc
    TLMNAME == scb20_tlm.nc
    TLFNAME == scb20_tlf.nc
    ADJNAME == scb20_adj.nc
    AVGNAME == scb20_avg.nc
    DIANAME == scb20_dia.nc
    STANAME == scb20_sta.nc
```

FLTNAME == scb20_flt.nc

! Input ASCII parameter filenames.

APARNAM = *ROMS*/External/s4dvar.in
SPOSNAM = *ROMS*/External/stations.in
FPOSNAM = *ROMS*/External/floats.in
BPARNAM = *ROMS*/External/bioFasham.in
SPARNAM = sediment_small.in
USRNAME = *ROMS*/External/MyFile.dat

B.3

***SWAN* file**

```
PROJECT 'THESIS' ''
'ocean_test_head test case to drive ROMS'
''
''

MODE NONSTATIONARY TWODIMENSIONAL
SET  INRHOG 0
COORDINATES SPHERICAL

CGRID CURVILINEAR 31 57 EXC 9.999000e+003 9.999000e+003 &
     CIRCLE 180 0.04 1.0 34
READGRID COORDINATES 1 'swan_coord.grd' 4 0 0 FREE

INPGRID BOTTOM CURVILINEAR 0 0 31 57 EXC 9.999000e+003
READINP BOTTOM 1 'swan_bathy.bot' 4 0 FREE

INPGRID WIND REG -117.8128369411765 32.627913350430134 &
0 2 2 0.312499588235312 0.312228801177 &
EXC 9999 NONSTAT 20091002.0000 &
1 HR 20091031.0000
```

```
READINP WIND 1 'swan_wind.wnd' 3 0 FREE

INPGRID CURRENT CURVILINEAR 0 0 31 57 EXC 9.999000e+003 &
     NONSTATIONARY 20091002.0000 10 DAY 20091031.0000
 INPGRID WLEV CURVILINEAR 0 0 31 57 EXC 9.999000e+003  &
     NONSTATIONARY 20091002.0000 10 DAY 20091031.0000
INPGRID FRIC CURVILINEAR 0 0 31 57 EXC 9.999000e+003  &
     NONSTATIONARY 20091002.0000 10 DAY 20091031.0000

BOUN SEG IJ 31 0 0 0 0 57 VAR FILE 0.145144149469386 'spec1a.dat'
BOUN SEG IJ 31 57 0 57 0 0 VAR FILE 0.097432373540324 'spec2a.dat'

!POINTS 'nest' FILE 'points.dat'
!SPECOUT 'nest' 'specout.dat' OUT 20091002.000000 1 HR
POINTS 'output' -117.3617 33.0774 -117.3567 33.0793 -117.3517 33.0812 &
-117.3467 33.0831 -117.3417 33.0850 -117.3367 33.0868 -117.3317 &
33.0887 -117.3267 33.0906 -117.3216 33.0925 -117.3166 33.0944
SPECOUT 'output' 'output.dat' OUT 20091002.000000 1 HR


& Restart name **********************************
&INIT HOTSTART 'swan_restart.dat'

& PHYSICS  ***************************************
BREAKING CONSTANT 1.0 0.73
FRICTION MADSEN 0.05
&OFF QUAD
GEN3
TRIAD
PROP BSBT

COMPUTE NONSTAT 20091002.000000 1 HR 20091031.0000
```

STOP

B.4

Sediment File

```
!-----------------------------------------------------------------------
!  Sediment model control switch.
!-----------------------------------------------------------------------

! Switch is used to control sediment model computation within nested and/or
! multiple connected grids, [1:Ngrids].

   Lsediment == T T

!-----------------------------------------------------------------------
!  General sediment bed model controls.
!-----------------------------------------------------------------------

! Depositional bed layer thickness criteria to create a new layer (m). If
! deposition exceeds this value, then a new layer is created, [1:Ngrids].

    NEWLAYER_THICK == 0.15d0 0.01d0

! Bed load transport rate coefficient. [1:Ngrids].

    BEDLOAD_COEFF == 1.0d0 1.0d0

!-----------------------------------------------------------------------
! Suspended Cohesive Sediment Parameters, [1:NCS,1:Ngrids] values expected.
!-----------------------------------------------------------------------

! Median sediment grain diameter (mm).

    MUD_SD50 == 0.1d0  0.06d0  0.10d0 \
```

```
            0.1d0  0.06d0  0.10d0

! Sediment concentration (kg/m3).

   MUD_CSED == 0.0d0  0.0d0  0.0d0 \
            0.0d0  0.0d0  0.0d0

! Sediment grain density (kg/m3).

   MUD_SRHO == 2650.0d0  2650.0d0  2650.0d0 \
            2650.0d0  2650.0d0  2650.0d0

! Particle settling velocity (mm/s).

   MUD_WSED == 10.0d0  1.0d0  2.0d0 \
            10.0d0  1.0d0  2.0d0

! Surface erosion rate (kg/m2/s).

  MUD_ERATE == 5.0d-3  5.0d-5  5.0d-5 \
            5.0d-3  5.0d-5  5.0d-5

! Critical shear for erosion and deposition (N/m2).

 MUD_TAU_CE == 0.1d0  0.05d0  0.05d0 \
            0.1d0  0.05d0  0.05d0
 MUD_TAU_CD == 0.01d0 0.01d0  0.01d0 \
            0.01d0 0.01d0  0.01d0

! Porosity (nondimensional: 0.0-1.0):  Vwater/(Vwater+Vsed).

  MUD_POROS == 0.0d0  0.0d0  0.0d0 \
            0.0d0  0.0d0  0.0d0
```

```
! Lateral, harmonic and biharmonic, constant, diffusion coefficient.

   MUD_TNU2 == 0.0d0  0.0d0  0.0d0 \
               0.0d0  0.0d0  0.0d0            ! m2/s
   MUD_TNU4 == 0.0d0  0.0d0  0.0d0 \
               0.0d0  0.0d0  0.0d0            ! m4/s

! Vertical diffusion coefficients.

 MUD_AKT_BAK == 5.0d-6  5.0d-6  5.0d-6 \
               5.0d-6  5.0d-6  5.0d-6         ! m2/s

! Nudging/relaxation time scales, inverse scales will be computed
! internally.

   MUD_TNUDG == 0.0d0 0.0d0 0.0d0 \
               0.0d0 0.0d0 0.0d0              ! days

! Morphological time scale factor (greater than or equal to 1.0). A
! value of 1.0 has no scale effect.

   MUD_MORPH_FAC == 10.0d0 1.0d0 1.0d0 \
                    10.0d0 1.0d0 1.0d0         ! nondimensional

! Logical switches (TRUE/FALSE) to specify which variables to consider on
! tracers point Sources/Sinks (like river runoff). See glossary below for
! details.

 MUD_Ltracer == F F

! Logical switch (TRUE/FALSE) to activate writing of cohesive sediment
! into HISTORY output file.
```

```
Hout(idmud)  == T T                    ! suspended concentration
Hout(iMfrac) == T T                    ! bed layer fraction
Hout(iMmass) == T T                    ! bed layer mass
Hout(iMUbld) == T T                    ! bed load at U-points
Hout(iMVbld) == T T                    ! bed load at V-points

!-----------------------------------------------------------------------
! Non-cohesive Sediment Parameters, [1:NNS,1:Ngrids] values expected.
!-----------------------------------------------------------------------

! Median sediment grain diameter (mm).

   SAND_SD50 == 0.024d0 0.125d0 0.250d0 0.1250d0 0.06250d0 0.031250d0 \
                1.0d0 0.50d0 0.250d0 0.1250d0 0.06250d0 0.031250d0

! Sediment concentration (kg/m3).

   SAND_CSED == 0.00d-2 0.00d-2 0.0d0 0.0d0 0.0d0 0.0d0 \
                0.0d0 0.0d0 0.0d0 0.0d0 0.0d0 0.0d0

! Sediment grain density (kg/m3).

   SAND_SRHO == 2650.0d0 2650.0d0 2650.00d0 2650.0d0 2650.0d0 2650.0d0 \
                2650.0d0 2650.0d0 2650.00d0 2650.0d0 2650.0d0 2650.0d0

! Particle settling velocity (mm/s).

   SAND_WSED == 0.40d0 9.40d0 27.0d0 8.70d0 2.40d0 0.620d0 \
                140.0d0 57.0d0 27.0d0 8.70d0 2.40d0 0.620d0

! Surface erosion rate (kg/m2/s).

  SAND_ERATE == 1.0d-4 2.5d-3 1.0d-4 1.0d-4 1.0d-4 1.0d-4 \
```

```
            1.0d-4 1.0d-4 1.0d-4 1.0d-4 1.0d-4 1.0d-4

! Critical shear for erosion and deposition (N/m2).

 SAND_TAU_CE == 0.075d0 0.15d0 0.19d0 0.19d0 0.19d0 0.19d0 \
            0.19d0 0.19d0 0.19d0 0.19d0 0.19d0 0.19d0
 SAND_TAU_CD == 0.02d0 0.02d0 0.02d0 0.02d0 0.02d0 0.02d0 \
            0.02d0 0.02d0 0.02d0 0.02d0 0.02d0 0.02d0

! Porosity (nondimensional: 0.0-1.0):  Vwater/(Vwater+Vsed).

  SAND_POROS == 0.4d0 0.40d0 0.7d0 0.7d0 0.7d0 0.7d0 \
            0.7d0 0.7d0 0.7d0 0.7d0 0.7d0 0.7d0

! Lateral, harmonic and biharmonic, constant, diffusion coefficient.

   SAND_TNU2 == 0.0d0 0.0d0 0.0d0 0.0d0 0.0d0 0.0d0 \
            0.0d0 0.0d0 0.0d0 0.0d0 0.0d0 0.0d0            ! m2/s
   SAND_TNU4 == 0.0d0 0.0d0 0.0d0 0.0d0 0.0d0 0.0d0 \
            0.0d0 0.0d0 0.0d0 0.0d0 0.0d0 0.0d0            ! m4/s

! Vertical diffusion coefficients.

SAND_AKT_BAK == 5.0d-6 5.0d-6 5.0d-6 5.0d-6 5.0d-6 5.0d-6 \
            5.0d-6 5.0d-6 5.0d-6 5.0d-6 5.0d-6 5.0d-6      ! m2/s

! Nudging/relaxation time scales, inverse scales will be computed
! internally.

  SAND_TNUDG == 0.0d0 0.0d0 0.0d0 0.0d0 0.0d0 0.0d0 \
            0.0d0 0.0d0 0.0d0 0.0d0 0.0d0 0.0d0            ! days

! Morphological time scale factor (greater than or equal to 1.0). A
```

```
! value of 1.0 has no scale effect.

SAND_MORPH_FAC == 1.0d0 1.0d0 1.0d0 1.0d0 1.0d0 1.0d0 \
                  1.0d0 1.0d0 1.0d0 1.0d0 1.0d0 1.0d0         ! nondimensional

! Logical switches (TRUE/FALSE) to specify which variables to consider on
! tracers point Sources/Sinks (like river runoff). See glossary below for
! details.

SAND_Ltracer == T T
SAND_Ltracer == T T

! Logical switches (TRUE/FALSE) to activate writing of non-cohesive
! sediment into HISTORY output file.

Hout(idsand) == TT                    ! suspended concentration
Hout(iSfrac) == TT                    ! bed layer fraction
Hout(iSmass) == TT                     ! bed layer mass
Hout(iSUbld) == TT                     ! bed load at U-points
Hout(iSVbld) == TT                     ! bed load at V-points

!------------------------------------------------------------------------------
! Bed layer and bottom sediment parameters, [1:Ngrids] values expected.
!------------------------------------------------------------------------------

 Hout(ithck) == T T                    ! sediment layer thickness
 Hout(iaged) == T T                     ! sediment layer age
 Hout(iporo) == T T                     ! sediment layer porosity
 Hout(idiff) == F F                    ! biodiffusivity
```

APPENDIX D:
Related Publications

Journal Publications

- Beyene, A., Wilson, J., California Wave Resource Study, California Energy Commission, 2003
- Beyene A., Wilson J., Wave Energy Conversion: Prospects and Challenges, Sea Technology, Vol. 49, No. 5, page 43-46, May 2008
- Beyene A., Wilson J., Digital Mapping of California Wave Energy Resource, International Journal of Energy Research, Vol. 31, page 1156-1168, 2007
- Wilson H. J., Beyene A., California Wave Energy Resource Evaluation, Journal of Coastal Research, Vol. 23, No. 3, page 679-690, May 2007
- Beyene, A., Wilson H. J., Comparison of Wave Energy Flux for Northern, Central, and Southern Coast of California Based on Long Term Statistical Wave Data, *Energy: the International Journal*, Elsevier, 2006, Vol. 31, p. 1520-1533.
- Beyene A., Wilson H. J., Parameter Variation and Part-load Efficiencies of Wave Energy Conversion, American Society of Civil Engineers (ASCE*), Journal of Energy Engineering*, April 2006, Vol. 132: 1, p. 15
- Beyene, A., Wilson H. J., Wave Energy Capacity and Part-load Operation, *Sea Technology*, pp 45-48, July 2005

Articles in Refereed Proceedings

- Stiber B., Beyene A., Towards Integrating Desalination and Wave Energy Conversion Technologies, Proceedings of ECOS, 24rd International Conference on Efficiency, Cost, Optimization, Simulation and Environmental Impact of Energy Systems, July 16 – 19, 2013, Guilin, China
- Beyene A., MacPhee D., Integrating Wind and Wave Energy Conversion, 2nd International Conference on Electrical and Control Engineering, Sep 16-18, 2011, Yichang, China
- Peffley J., Beyene, A., A Morphing Blade for Wave and Wind Energy Conversion, OCEANS '07, IEEE Conference, Aberdeen, June 18-21, 2007.
- Beyene A., Wilson J., Digital Mapping of California Wave Energy Resource, International Green Energy Conference, Oshawa, Canada, June 24-29, 2006
- Beyene A., Wilson J., Wave Energy Conversion in a Strongly Variable Sea State, EnergyOcean 2006, San Diego, June 21 – 24, 2006
- Beyene A., Wilson J., Matching wave energy capacity and efficiency at part-load, Combined *OCEANS'04 MTS/IEEE/TECHNO-OCEAN'04* annual conference Kobe, Japan, November, 2004
- Beyene A., Wilson J., Comparison of California's Wave Energy Density North and South of Point Conception Based on Long-term Statistical Wave Data, Palm Beach, Florida, 2004